LIGAND EFFECTS IN THE CHEMISTRY OF GAS PHASE METAL IONS

By

Richard Martin Stepnowski

A DISSERTATION

Submitted to
Michigan State University
in partial fulfillment of the requirements
for the degree of

DOCTOR OF PHILOSOPHY

Department of Chemistry

1988

ABSTRACT

LIGAND EFFECTS IN THE CHEMISTRY OF GAS PHASE METAL IONS

By

Richard Martin Stepnowski

The gas phase chemistry of transition metal ions with organic molecules has been extensively studied in recent years. The study of the interactions between metals and molecules can give insight to basic questions of organometallic chemistry.

For small compounds such as alkyl halides (RX), reaction products appear to be formed via three steps: metal ion insertion/ ß-H / competitive ligand loss step.

This study involves the reactions of Ni^+, $NiCO^+$, $NiPF_3^+$, and $NiCp^+$ with phenyl, benzyl, and aromatic carbonyl compounds. Reaction products and pathways were determined by Ion Cyclotron Resonance (ICR) Mass Spectrometry, using a frequency scanned detector (FSD).

The phenyl group in some aspects behaves chemically intermediate to the methyl and ethyl groups. H transfer from the phenyl group is a high energy process; nonetheless, reactions such as:

$$Ni^+ + C_6H_5X \rightarrow NiC_6H_4^+ + HX$$

are observed. When other pathways are open, such as the elimination of a molecule from the functional group, these pathways

are preferred.

A major effect of the phenyl group is its inductive effect. The weak $C_6H_5CH_2$-X bond plays an important role in in reactions of substituted benzyl compounds. Charge transfer to $C_6H_5CH_2^{\cdot}$ following insertion into this bond can occur, due to the low ionization potential of the benzyl radical.

Much of the chemistry of the NiL^+ ions can be explained by the formation of intermediates with low steric interactions. The NiL^+ ions insert into bonds where steric interactions will be minimized. By size, Cp > PF_3 > CO. This is also the same order as for the metal-ligand bond energies; the reactivity of the ligated metal ions may be related to both these factors. The reactions of $NiPF_3^+$ follow closely the reactions of $NiCO^+$, with slightly lower reactivity observed for the $NiPF_3^+$ ion. The slightly lower reactivity of $NiPF_3^+$ reflects the steric crowding for insertion produced by this larger ligand. The reactivity of $NiCp^+$ indicate that the Cp ligand affects the metal ion differently than either CO or PF_3, more reactive than the other NiL^+ species in the case of the halobenzenes. For aromatic carbonyls, the steric hindrance of the bulky Cp group appears to prohibit insertion.

ACKNOWLEDGEMENTS

It is difficult to acknowledge all the people who have helped so much in my time here at MSU; their help has been enormous. Let me start by thanking Mark Bishop, who represents the best of teachers. His T'ai Chi classes always gave a pleasant and bizarre contrast to the world of chemistry. John Wronka gets a special thanks for building and installing the FSD, which helped so much. The group always made the lab a fun place to be; thanks, Mike, Mac, Barb, Pinky, Tony, d.B., Spike, Dan, Karen, Paul, Mark, Jeff, Gary, and Mary. A toast to the waitresses of the Boom Boom Room and the Peanut Barrel; there exists no finer place to raise a glass! A round of applause to the MSU hockey team!

The assistance of John Allison has been immeasureable; he deserves thanks for giving me the opportunity to work for him, for his long and patient guidance, and for his sense of humor, which would always make things look not so bad, just when I thought things couldn't get worse.

Finally, Mom and Dad, thanks for everything. Let's hope you don't get too many phone calls like: "Send laywers, guns, and money; Dad, get me out of this."

Each of us knows one small fraction of the overall plan at any given moment-his own assingment-and no one is allowed to disclose his function to another. It's a precaution against the maniac finding out the plan. If each man properly brings off his own part, then the whole scheme will be brought to a successful conclusion. In the meantime, the plan can't be either carelessly disclosed or given up under duress or threat. Each one can only account for a tiny fragment which would have no meaning to the maniac should he gain access to it.

Woody Allen
from Death {A Play}

TABLE OF CONTENTS

LIST OF TABLES

LIST OF FIGURES

LIST OF SCHEMES

Chapter 1

Introduction

In recent years the reactions in the gas phase of transition metal ions with organic molecules have been extensively studied.[1] Besides the fundamental interest in this area, it is hoped that the study of interactions between metals and molecules can provide an understanding concerning the question of how catalysts function.

Transition metal ions, M^+, especially Fe^+, Ni^+, and Co^+, have been observed to react by the following mechanism[2] (Scheme 1-1):

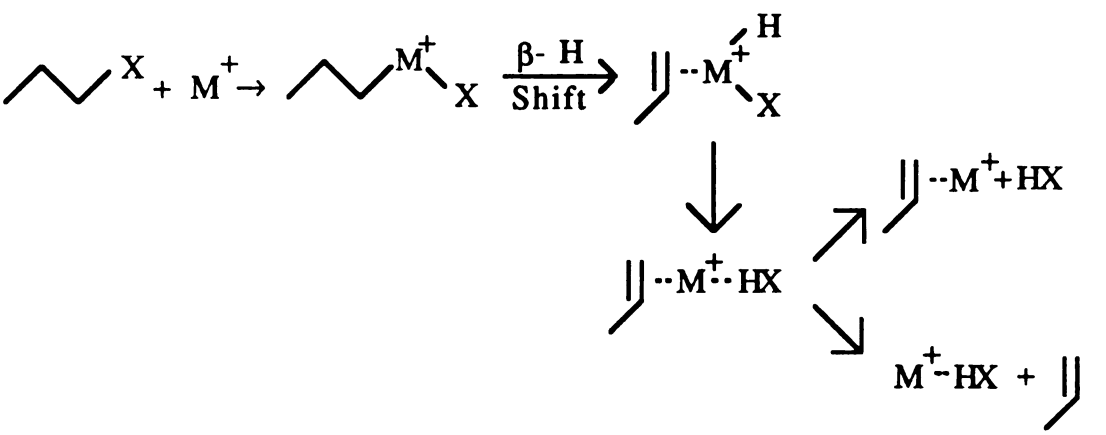

Scheme 1-1

The reaction has been proposed to proceed by four distinct steps[3]. First, complexation occurs as the metal ion and the molecule form an

initial ion/molecule complex. This step can be followed by insertion of the metal ion into a bond of the molecule. The third step involves a ß-H shift to produce two adducts on the metal ion. Finally, by competitive ligand loss, a neutral molecule is lost, usually the molecule with the lower proton affinity. This reaction mechanism has been used to explain the reaction products of metal ions with many classes of compounds,[1] including alkanes,[4] alcohols,[2] and alkyl halides.[2]

Why is it that the transition metal ions have received so much attention? One reason is the phenomenal reactivity that is observed in the gas phase. What causes this unusual reactivity? It has been observed that the reactivity of the first row transition metals with alkanes follows the trend $Fe^+ > Co^+ > Ni^+$, with Cr^+ and Mn^+ being unreactive[5]. This order also is the same as the order for the promotional energy of the the ions, that is, the energy required to achieve an electronic state in which two electrons are not in d orbitals[5]. With two electrons promoted out of d orbitals into s or p orbitals, the metal ion is capable of forming the two bonds necessary for bond insertion. Cr^+ with a $3d^5$ configuration and Mn^+ with $3d^54s^1$ configuration both have high promotional energies, requiring the excitation of electrons out of a stable half filled d shell. These ions are correspondingly less reactive than Fe^+, Ni^+, and Co^+.

Other concepts have been used to explain the relative reactivity of metal ions. Recently, Schilling and Beauchamp[6] have reported the reactions of Pr^+, Eu^+, and Gd^+ with alkanes and alkenes. Their intent was to determine the role of f-orbitals in the reactivity of metal ions. They found that Pr^+ and Eu^+ were quite unreactive. Their proposed explanation for this unreactive behavior lies in the first step of the reaction, complexation. A loose collision complex is formed by the interaction of the ion with a permanent dipole or an

ion-induced dipole. The energy gained from this ion/molecule association allows many ion/molecule reactions to proceed with no appreciable barrier. This is illustrated in Figure 1-1, taken from reference 6:

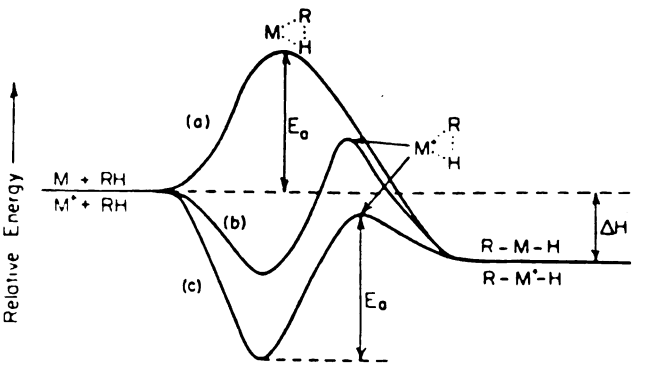

Figure 1-1 Interaction of metal ions and alkanes

Curve a shows the hypothetical interaction between a neutral metal and a neutral molecule, with an activation barrier E_a for the insertion process. Curve c shows the same insertion process for a metal ion. Here the "chemical activation" lowers the effective barrier, allowing the reaction to occur as if there were no barrier. They hypothesize that, due to the large size of the Pr^+ and Eu^+, ions the ion-neutral separation would be greater. This would reduce the energy of association, which results from electrostatic interactions. Such a case is shown in curve b, where the energy lowering is not enough to compensate for the energy barrier, which must occur for the reaction to proceed. For C-H insertion to occur, the sum of the M^+-C and M^+-H bond strengths must be larger than the C-H bond being broken.

Since almost all of the low-lying electronic states of Pr^+ and Eu^+ have either a $4f^{n-1}6s^1$ or $4f^{n-1}5d^1$ valance electronic configuration, one of the metal σ bonds must be made with a 4f orbital. They cited several drawbacks to bonding to f orbitals. First, the 4f orbitals are small and spatially compact relative to the 5d and 6s orbitals, making access to these orbitals difficult. Second, the shape of the f orbitals produces lower electron density along a potential bond axis. This is similar to the situation with the first row transition metals. The 3d orbitals are smaller than the 4s orbitals, so it is necessary to the promote electrons out of the 3d orbitals.

In contrast, Gd^+ was observed to be quite reactive. Its ground state $4f^75d^16s^1$ has two electrons in non-f orbitals, and is thus able to insert, forming 2 σ bonds without utilizing f electrons.

In another report, Schilling and Beauchamp[7] have compared the reactivity of Cr^+ ($3d^5$ ground state) to Mo^+ ($4d^5$ ground state). As stated before, Cr^+ is unreactive with alkanes, while Mo^+ reacts with all alkanes, except methane, by dehydrogenation (with a small reaction cross section). From theoretical considerations, they concluded that Cr^+ forms very weak σ bonds, causing insertion into C-H bonds to be endothermic. The larger size of the d orbitals of Mo^+ and the resultant decrease in d-d exchange energy lost on the formation of σ bonds results in stronger bonds to Mo^+, just strong enough to activate the C-H bonds of alkanes. Thus exchange energy loss in the metal that results from bond formation can have an important role in the insertion process.

An important consideration is whether the reactant ions are formed in the ground state. Halle, Armentrout, and Beauchamp[8] have reported that excited state Cr^+ is reactive with alkanes while, again, the ground state is not. More recently, Schultz, Elkind, and Armentrout[9] have reported that the ^6D ground state of Fe^+ is much

less reactive in endothermic reactions with small alkanes than the first excited state ^4F, even though the ground state is less than 0.25 eV lower in energy. These examples confirm the importance of electronic structure in metal ion reactions.

In addition to studies of bare metal ions, many reactions of ligated metal ions have been studied. Historically, these reactions were studied because of the method of producing metal ions. Electron ionization (EI) of volatile organometallic species such as $Fe(CO)_5$ produced large amounts of Fe^+, and also the ions $Fe(CO)_x^+$, x =1-5, which have been studied.[10] These ions also undergo interesting reactions. Using Fourier Transform Mass Spectrometry (FTMS), ions can be manipulated to undergo multiple reactions. Using this method, exotic ML^+ species have been produced by other workers, with L= H, OH, S, and even other metals.[11,12] These ligands are presumably bonded to the metal ion by covalent bonds. Studies of these species show that the ligand plays a direct role in reactions. For example CoD^+ reacts with propene to yield four products:[13]

$$CoD^+ + C_3H_6 \rightarrow CoCH_3^+ + C_2H_3D \ (6\%) \quad (1)$$
$$\rightarrow CoCH_2D^+ + C_2H_4 \ (4\%) \quad (2)$$
$$\rightarrow CoC_3H_5^+ + HD \ (36\%) \quad (3)$$
$$\rightarrow CoC_3H_4D^+ + H_2 \ (54\%) \quad (4)$$

With species such as MCO^+, the ligand does not play such an active role in the reaction. Recent theoretical studies of MCO^+ ions show that the bonding of the ligand in these species is primarily electrostatic in nature.[14] The reactions of MCO^+ resemble that of M^+ to a large extent, for no change in the electronic structure of M^+

occurs upon complexation with the CO ligand.

Obviously, an important consideration in the study of ion/molecule reactions is the choice of the neutral organic molecule for the ion to react with. Many different classes of organic compounds have been used in these studies. Interestingly, small molecules tend to be unreactive, except for ligand substitution reactions, where an neutral molecule displaces a ligand on the ion. For example, acetonitrile and acetaldehyde are unreactive with Co^+.[15,16] However, reactions such as

$$CoCO^+ + CH_3CN \rightarrow CoCH_3CN^+ + CO \quad (5)$$

occur.

The early experiments in this field suggested that all polar compounds reacted in the same way, that is by metal ion insertion into the polar bond, followed by a ß-H shift. This is illustrated in scheme 1. Reactions of this type were observed for ethyl iodide, ethanol, diethyl ether, and other compounds.[2,17] Amines were an exception to this trend.[18] It was proposed that the M^+-NH_2 bond strength was unusually low, so the overall process would be thermodynamically unfavored. Thus, the functional group can be influential in the reaction products formed.

When the functional group is more complex, such as a carboxylic acid[19] or nitro group,[20] insertion into bonds within the functional group is a common pathway, in addition to insertion into the carbon-functional group bond.

Several studies have examined the question of how bifunctional organic molecules react with metal ions.[21,22] Tsarbopoulos has studied the reactions of a series of chloroalcohols and bromoalcohols.[22] He concluded that, when two functional groups were present, the product distribution could not be predicted,

based on the known chemistry of each functional group. For the various bifunctional compounds studied, the reaction products were unique to the combination of functional groups and length of the alkyl chain between the two functional groups.

Tsarbopoulos and Allison also have reported on the reactions of molecules with long straight alkyl chain attached to the functional groups.[23] These included chloro- and bromo- alkanes and alcohols, with two to eight carbons in the alkyl chain. Based on the reactions of Co with ethanol, insertion into the C-OH bond should be the only process predicted:

$$Co^+ + C_2H_5OH \rightarrow CoC_2H_4^+ + H_2O\ (87\%) \quad (6)$$

$$\rightarrow CoH_2O^+ + C_2H_4\ (13\%) \quad (7)$$

However, C-OH insertion does not occur in the reaction of heptanol:

$$Co^+ + C_7H_{15}OH \rightarrow CoC_2H_5OH^+ + C_5H_{10}\ (3\%) \quad (8)$$

$$\rightarrow CoC_4H_8^+ + C_3H_7OH\ (24\%) \quad (9)$$

$$\rightarrow CoC_3H_7OH^+ + C_4H_8\ (7\%) \quad (10)$$

$$\rightarrow CoC_3H_5OH^+ + C_4H_{10}\ (4\%) \quad (11)$$

$$\rightarrow CoC_4H_6^+ + C_3H_7OH + H_2\ (14\%) \quad (12)$$

$$\rightarrow CoC_3H_6^+ + C_4H_9OH\ (14\%) \quad (13)$$

$$\rightarrow CoC_4H_9OH^+ + C_3H_6\ (1\%) \quad (14)$$

$$\rightarrow CoC_4H_7OH^+ + C_3H_8\ (12\%) \quad (15)$$

$$\rightarrow CoC_7H_{15}OH^+\ (21\%) \quad (16)$$

As the chain length increases, insertion into internal C-C bonds becomes preferred over insertion into the C-X bond. A mechanism was proposed in which the metal ion interacts with carbon atoms remote from the functional group by the formation of cyclic intermediates, shown in Figure 1-2.

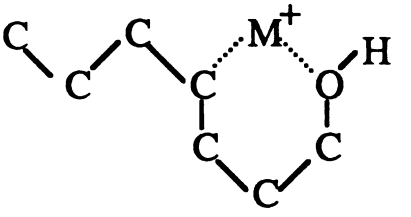

Figure 1-2 Cyclic intermediates allow carbon atoms remote from the functional group to interact with the metal ion.

After initial complexation, the alkyl chain can wrap around to bring remote carbon atoms into close proximity with the metal ion. This suggests that the initial attraction between the metal ion and the molecule is a dynamic system. Electrostatic modeling can suggest that some sites in the molecule are more attractive to the ion than other sites.[3]

Branching sites on the alkyl chain can influence where bond insertion will occur . Ni^+ does not insert into the C-CN bond of n-propyl cyanide, nor does it into insert into the C-CN bond of any of the n-alkyl cyanides studied.[15] However, the following reactions were observed:

$$Co^+ + i\text{-}C_3H_7CN \rightarrow CoHCN^+ + C_3H_6 \quad (18)$$

$$\rightarrow CoC_3H_6^+ + HCN \quad (19)$$

In this case, the lower bond strength of the C-CN bond for the

secondary cyano group may allow insertion at this point.

Another example of how the alkyl group allow the metal to insert into a normally inaccessible bond is seen with allylamine.[21] Reactions of Co^+ with primary and secondary amines showed that insertion into C-NH_2 did not occur.[18] However, allylamine was observed to react as follows:

$$Co^+ + C_3H_5NH_2 \rightarrow CoC_3H_4NH^+ + H_2 \quad (20)$$

$$\rightarrow CoC_3H_4^+ + NH_3 \quad (21)$$

$$\rightarrow CoC_3H_5^+ + \cdot NH_2 \quad (22)$$

The strong Co^+-allyl bond allowed insertion to occur even though the Co^+-NH_2 bond is thought to be unusually weak. One must consider the strength of the bonds formed as well as the strength of the bonds broken when proposing why insertion processes occur when they are not expected.

The study of gas phase metal ion chemistry has progressed rapidly in the last decade. Our understanding of the factors that control the reactivity of metal ions has grown. In addition to the factors that the metal ion have on the reaction, we have seen that polar molecules themselves can react in many different ways, ways that perhaps would not have been predicted. These factors include alkyl chain size and chain branching, as well as the obvious factors involved with the functional group.

In the projects described in this dissertation, a major goal was to understand better the role of ligands in the reactions of metal ions. In the primary project, $Ni(CO)_4$, $Ni(PF_3)_4$, and NiCpNO were chosen as the organometallic sources of the mono-ligated metal ions. Large amounts of $NiCO^+$, $NiPF_3^+$, and $NiCp^+$ are formed on the electron ionization of these compounds. Reactions of these species would allow a comparison of the effect of different ligands on reactivity.

Aromatic compounds were chosen to react with the metal ions. There are several reasons why aromatic compounds make a good set of test compounds. The size of the molecules provides a large cross section for reaction. The aromatic ring for the most part does not participate in the reaction. Complications that occur with alkyl compounds, such as the chain length effect or chain branching, will not be present. The chemistry is simpler, with usually only one product being formed. In addition to these practical considerations, the chemistry of aromatic compounds in these reactions had been largely unexplored, except for a few isolated experiments.

The experiments described in chapter 5 give information on ligand effects on metal reactivity. At the same time we would find how the aromatic group influences reactions, in contrast to alkyl groups, which have previously been studied by many other workers.

In the process of doing these experiments, it was noticed that the Ni^+ ions created from the three different organometallic compounds had, in some cases, different reactivity. This raises the question of whether the metal ions produced by EI are formed in different electronic states.

Two other projects will be reported in this dissertation. The first, in chapter 3, concerns the reactions of aldehydes with Ni^+ and Co^+. Unfortunately, some of the data of these experiments were unambiguous, due to the resolution of our instrument. Still, some conclusions about the chain length effect in the reactions of aldehydes can be made.

A third project, presented in chapter 4, concerned the reactions of Co^+ with straight chain alkyl nitriles. (Nitriles are the same as cyano compounds, except that there is a difference in nomenclature. For example, hexyl cyanide is the same molecule as heptanitrile.) In addition to the reactions of Co^+, the reactions of hexyl cyanide were studied with a variety of other metal ions. A few preliminary

experiments of metal- nitrile complexes were also carried out on a triple quadrupole instrument. The results of these experiments will be presented in chapter 4, also.

References

1. Allison, J. *Prog. Inorg. Chem.* **1986,** *34,* 627.
2. Allison, J.; Ridge, D. P. *J. Am. Chem. Soc.* **1979,** *101,* 4998.
3. Hankinson, D. J.; Allison, J. *J. Phys. Chem.* **1987,** *91,* 5307.
4. Radecki, B. D.; Allison, J. *Organometallics* **1986,** *5,* 411.
5. Babinec, S. J.; Allison, J. *J. Am. Chem. Soc.* **1984,** *106,* 7718.
6. Schilling, J. B.; Beauchamp, J. L. *J. Am. Chem. Soc.* **1988,** *110,*15.
7. Schilling, J. B.; Beauchamp, J. L. *Organometallics* **1988,** *7,* 194.
8. Halle, L. F.; Armentrout, P. B.; Beauchamp, J. L. *J. Am. Chem. Soc.*1981, *103,* 962.
9. Schultz, R. H.; Elkind, J. L.; Armentrout, P. B. *J. Am. Chem. Soc.* **1988,** *110,* 411.
10. Foster, M. S.; Beauchamp, J. L. *J. Am. Chem. Soc.* **1975,** *97,* 4808.
11. Jackson, T. C.; Carlin, T. J.; Freiser, B. S. *Int. J. Mass Spec. Ion Proc.*1986,*72*,169.
12. Jacobson, D. B.; Freiser, B. S. *J. Am. Chem. Soc.*1985,*107*,1581.
13. Jacobson, D. B.; Freiser, B. S. *J. Am. Chem. Soc.* **1984,** *106*,3891.
14. Allison, J.; Mavridis, A.; Harrison, J. F. *Polyhedron,* in press.
15. Stepnowski, R. M.; Allison, J. *Organometallics,* in press.
16. this work, chapter 3
17. Huang, S. K.; Allison, J. *Organometallics* **1983,** *2,* 883.
18. Radecki, B. D.; Allison, J. *J. Am. Chem. Soc.* **1984,** *106,* 946.
19. Lombarski, M.; Allison, J. *Int. J. Mass Spec. Ion Proc.*1985, *65*,31.
20. Cassidy, C. J.; Freiser, B.S.; McElvany, S. W.; Allison, J.; *J. Am. Chem. Soc.* **1984,** *106,* 6125.
21. Lombarski, M.; Allison, J. *Int. J. Mass Spec. Ion Phys.* **1983,***49,* 281.
22. Tsarbopoulos, A.; Allison, J. *Organometallics* **1984,** *3,* 86.
23. Tsarboploulos, A.; Allison, J. *J. Am. Chem. Soc.* **1985,** *107,* 5085.

Chapter 2

Experimental

Ion cyclotron resonance (ICR) spectrometry is particularly well suited for the study of ion/molecule reactions. This relatively new technique (less than three decades old) detects ions non-destructively by measuring the frequency of the ion motion in a magnetic field. The ICR experiment allows ion/molecule reactions to occur because of the long residence times of the ions; ions are typically contained in the reaction region for several milliseconds. It also allows the user to determine if an ion is the product of an ion/molecule reaction and what reactant ion led to the formation of the product ion. ICR has been extensively reviewed in the literature.[1,2] An overview of the technique will be presented here. An "operating manual" will be presented in Appendix A, that will give details of the operating procedures used.

The ICR experiment takes place within a cell shown Figure 2-1,

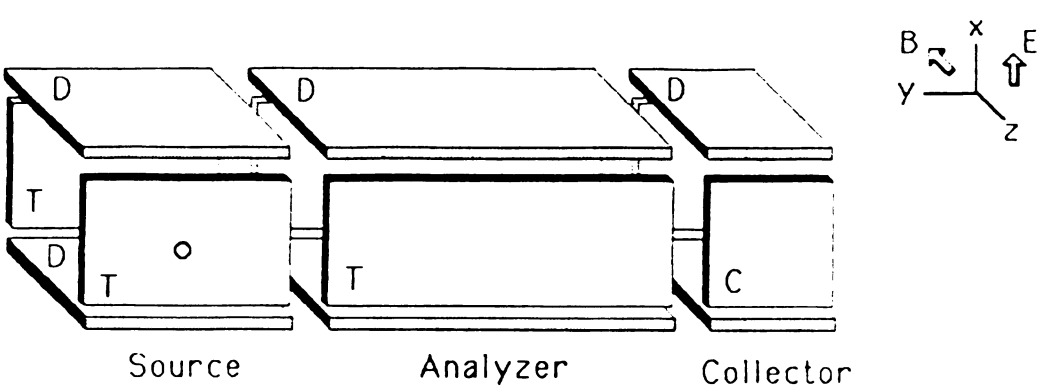

Figure 2-1 The ICR cell

which is contained in a high vacuum chamber. This is placed between the pole caps of an electromagnet. The cell is divided into three regions: source, analyzer, and collector. A small positive potential (~0.5 V) is applied across the trapping plates of the cell to contain positive ions in the center of the cell. A potential difference is applied across the drift plates of the source and analyzer regions. An electric field (E) applied between the plates is perpendicular to the magnetic field (B). As a result, a force (F) is exerted on the ions, given by the following equation[2]:

$$F = qE + q(v \times B) \qquad (1)$$

where v is the velocity of the ions and q is the charge. This force causes the ions to move in a direction perpendicular to both the magnetic and electric field, through the ICR cell with a velocity (v_d) given by:

$$v_d = E / B \qquad (2)$$

Given the typical length of an ICR cell, ~ 8 cm, and the typical voltages used on the drift plates, ~ 0.5 volts, it can be calculated from the drift velocity that the ions will remain in the cell for several milliseconds.

Ions thus contained in the cell will precess with a frequency given by f=qB/m, the cyclotron frequency. The frequency of precession is proportional to the strength of the magnetic field and inversely proportional to the mass of the ion, m. If radiofrequency radiation is applied to the drift plates, at a frequency close to that of the cyclotron frequency of the ion, the ions gain kinetic energy.

On gaining energy, the ions move into orbits with larger radii (Figure 2-2).

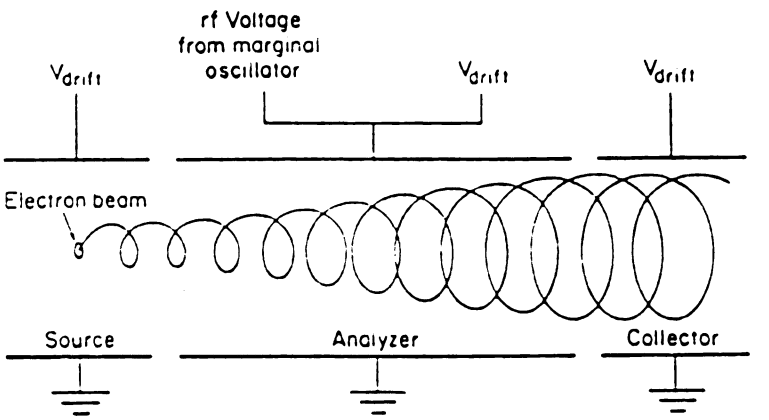

Figure 2-2. Ion motion in the ICR cell

Three modes of detection have been used to detect ions: fixed frequency detection with magnetic field scanning; scanned frequency detection with fixed magnetic field; and simultaneous detection of all frequencies and interpretation of the complex signal via Fourier transformation.

The detection technique used in the first commercially available ICR instrument was to scan the magnetic field, B, bringing ions into resonance with a fixed frequency oscillator. The parallel drift plates serve as the capacitive element of an LC tank circuit of a marginal oscillator. When the magnetic field is scanned such that the frequency of the ion matches the frequency of the marginal

oscillator, the ion is said to be in resonance and will absorb power from the rf field produced by the marginal oscillator. It is convenient to operate the marginal oscillator at a frequency of 153 kHz. At this frequency, a change in 100 gauss corresponds to a 1 u change in mass. By scanning the magnetic field, a plot of power absorption versus B is obtained.

To improve the signal-to-noise ratio, signal modulation is used. One of the trapping plates is pulsed to a negative voltage , and so sweeps all the ions out of the cell, at a rate of 20 Hz. The modulated signal is then analyzed with a lock-in amplifier. Because of the modulation, slow scan times are necessary, requiring about 20 minutes to record a spectrum. A block diagram of the experimental setup is shown in Figure 2-3.

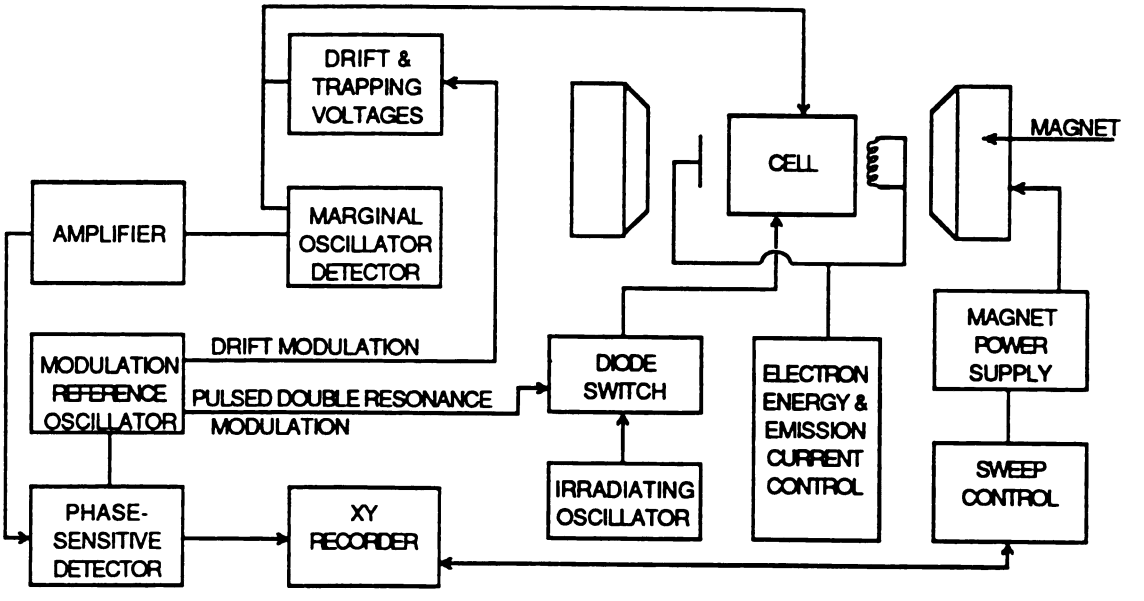

Figure 2-3. Block diagram for ion detection using a Marginal Oscillator Detector

We performed experiments with this type of instrument in the following way. An organometallic compound, such as $Co(CO)_3NO$ is admitted into the ICR cell, at a pressure of about $3x10^{-6}$ torr. This gas is ionized by 70 eV electron ionization, and a mass spectrum obtained. In a similar manner, the spectrum of an organic molecule, such as propyl chloride, is obtained. If the two gases were admitted to the cell at the same time, peaks would appear in the spectrum, if the total pressure was sufficiently high, that are neither in the spectrum of $Co(CO)_3NO$ nor propyl chloride. One such product ion is $CoHCl^+$ at m/z 95. How is this ion formed?

To investigate this product, a "double resonance" experiment can be performed. In this technique, the intensity of a product ion is constantly monitored. A second radiofrequency signal is then applied to the ICR cell. This signal, which is of sufficient strength to eject ions from the cell, is scanned to irradiate all the possible precursor ions of the monitored ion. When an ion which is a precursor to the monitored ion is ejected from the cell, the intensity of the monitored ion decreases. In the above example, the intensity of the $CoHCl^+$ ion decreases when Co^+ is ejected. This confirms that $CoHCl^+$ is formed in the reaction:

$$Co^+ + C_3H_7Cl \rightarrow CoHCl^+ + C_3H_6 \qquad (3)$$

In this way, a double resonance spectrum is obtained, which links ionic reactants to products. This experiment reveals much information about ion chemistry, but is time consuming. Each double resonance experiment takes about ten minutes to perform, and in a complex system, many possible products could be formed. The data for aldehydes and nitriles presented in this dissertation were collected using a marginal oscillator detector.

Because of the long time required to complete an experiment, a second detection method, frequency scanned detection, is desirable. Frequency scanned detection (FSD) had been used by Wobschall as early as 1963, and holds several advantages over marginal oscillator (MO) detection.[3] A spectrum can be taken much faster - in less than a second. Also, an alternate double resonance scheme can be used, in which all of the products of a reactant ion are identified. This is a simpler experiment. For example, if the only information desired was how one particular ion reacted, the information could be obtained in one double resonance experiment, rather than the many experiments it would take by identifying all precursors for all products, the necessary procedure when using the marginal oscillator.

The FSD used in our laboratory was designed, built, and installed by Dr. John Wronka, and his design considerations have been published.[3] This FSD was used to collect the data presented in Chapter 5, the reactions of metal ions with aromatic compounds. A block diagram of the circuitry is shown in Figure 2-4. Figure 2-5 shows the block diagram for the complete experimental setup for using the FSD.

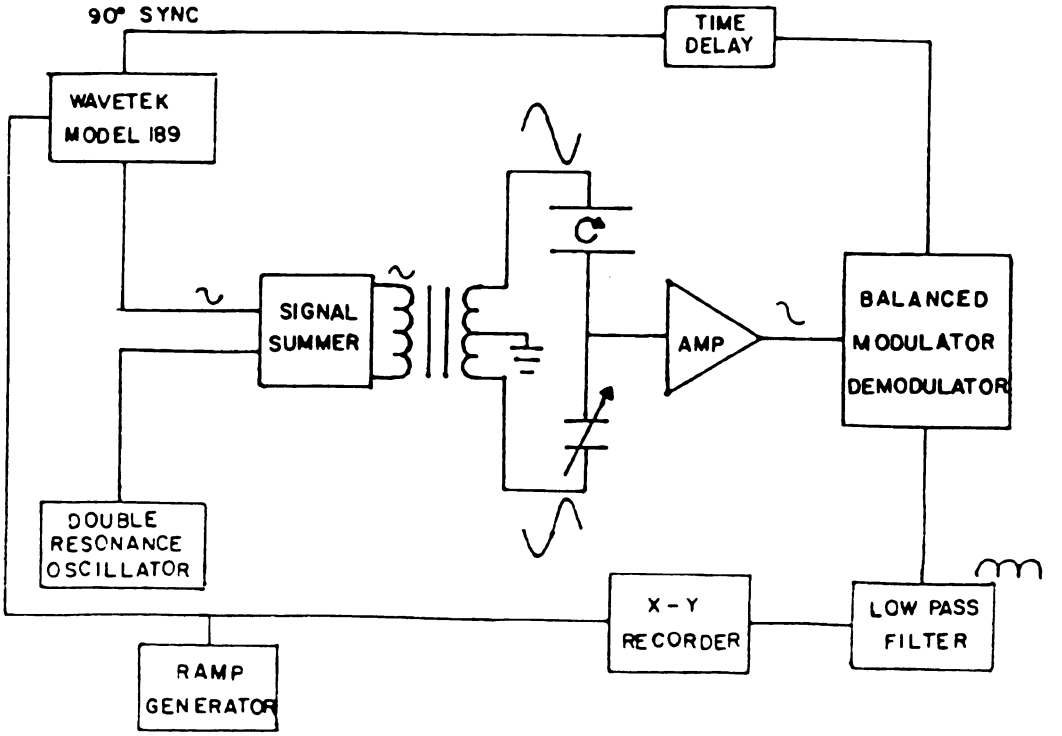

Figure 2-4 Circuitry diagram for the Frequency Scanned Detector

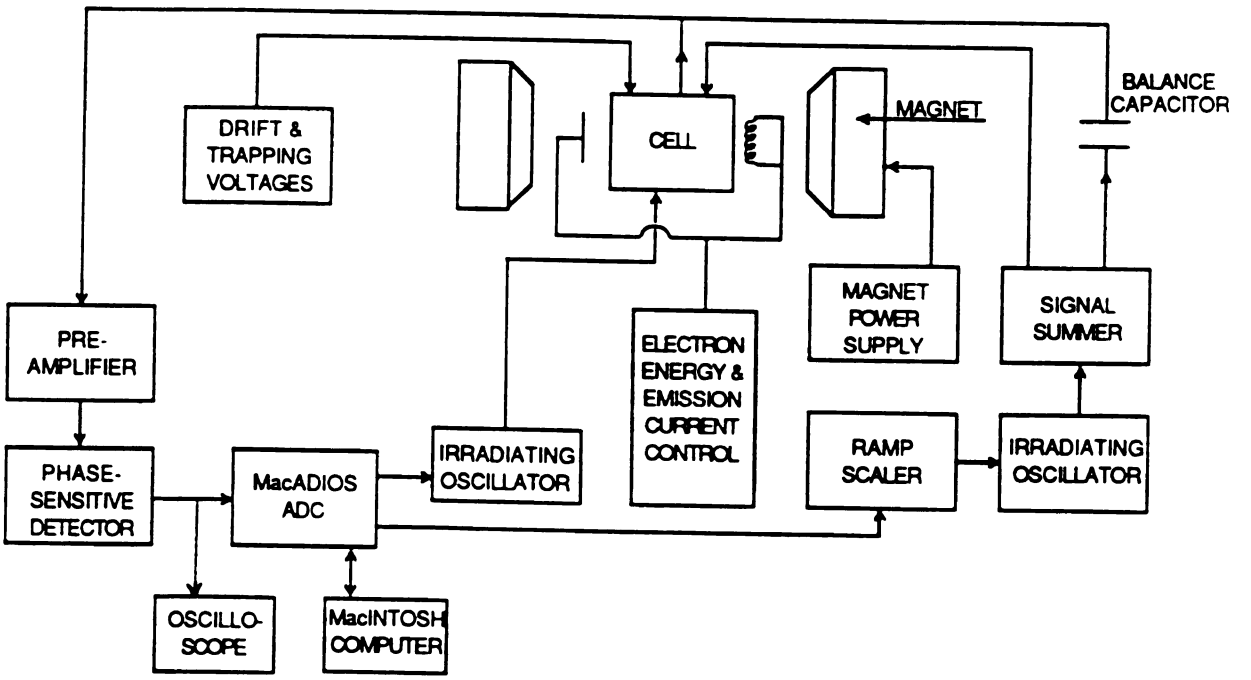

Figure 2-5. Block diagram for ion detection using a Frequency Scanned Detector

The following circuit description is excerpted from the Frequency Scanned Detector Model #3 Instruction Manual:[4] (p15-16, "circuit theory")

> "In the basic configuration developed by Wobschall a broadband transformer is driven by a voltage controlled oscillator (VCG) to provide two complementary radio frequency (rf) signals. These two signals are sent to the ICR cell and a balance capacitor connected to form a capacitance bridge. The rf signal sent to the excitation plate of the ICR cell provides an excitation source for the ions. The complementary rf signal and the balance capacitor function to provide a null point at the receiver plate. At the cyclotron frequency, ions will disturb the balance of the bridge and a voltage at the cyclotron frequency will be developed at the null point.
>
> The motion of the ions is a current in a parallel plate capacitor (the ICR cell). Since current and voltage in a capacitor are 90^{o} out of phase the voltage developed at the null point is phase shifted by 90^{o} from the excitation voltage.
>
> Phase sensitive detection with a reference signal of the same frequency as the excitation source but phase shifted by 90^{o} may be used to rectify the power absorption signal...
>
> Frequency scanned operation of the bridge detector can be greatly simplified if the excitation source already provides a 90^{o} reference. Fortunately, many commercially available function generators provide this feature due to their basic design.
>
> This assumes that there is no phase shift in the devices

used in construction of the bridge detector. Every amplifier has some phase shift with frequency. In fact even the upper and lower frequency limits of an amplifier imply phase shift.

With proper attention to impedance matching and the proper choice of components it is possible to build a system where the phase shift is corrected with a delay line."

After the FSD had been installed, it was necessary to determine the optimum operating parameters for its use. The most important parameter which affects the ion signal is the amplitude of the irradiating voltage. The effect of irradiating voltage on spectra can be seen in Figure 2-6a-e.

The amplitude of the irradiating voltage was varied and spectra were recorded. Figure 2-6 shows two peaks, at m/z 105 and 107, from the spectrum of methylbenzyl alcohol. It is clear that the peak intensity increases with irradiating voltage until a maximum is reached with an irradiating voltage of ~120 mV. With higher irradiating voltage, ions absorb too much energy and collide with the cell walls. Thus the signal decreases. The noise level stays constant with irradiating voltage.

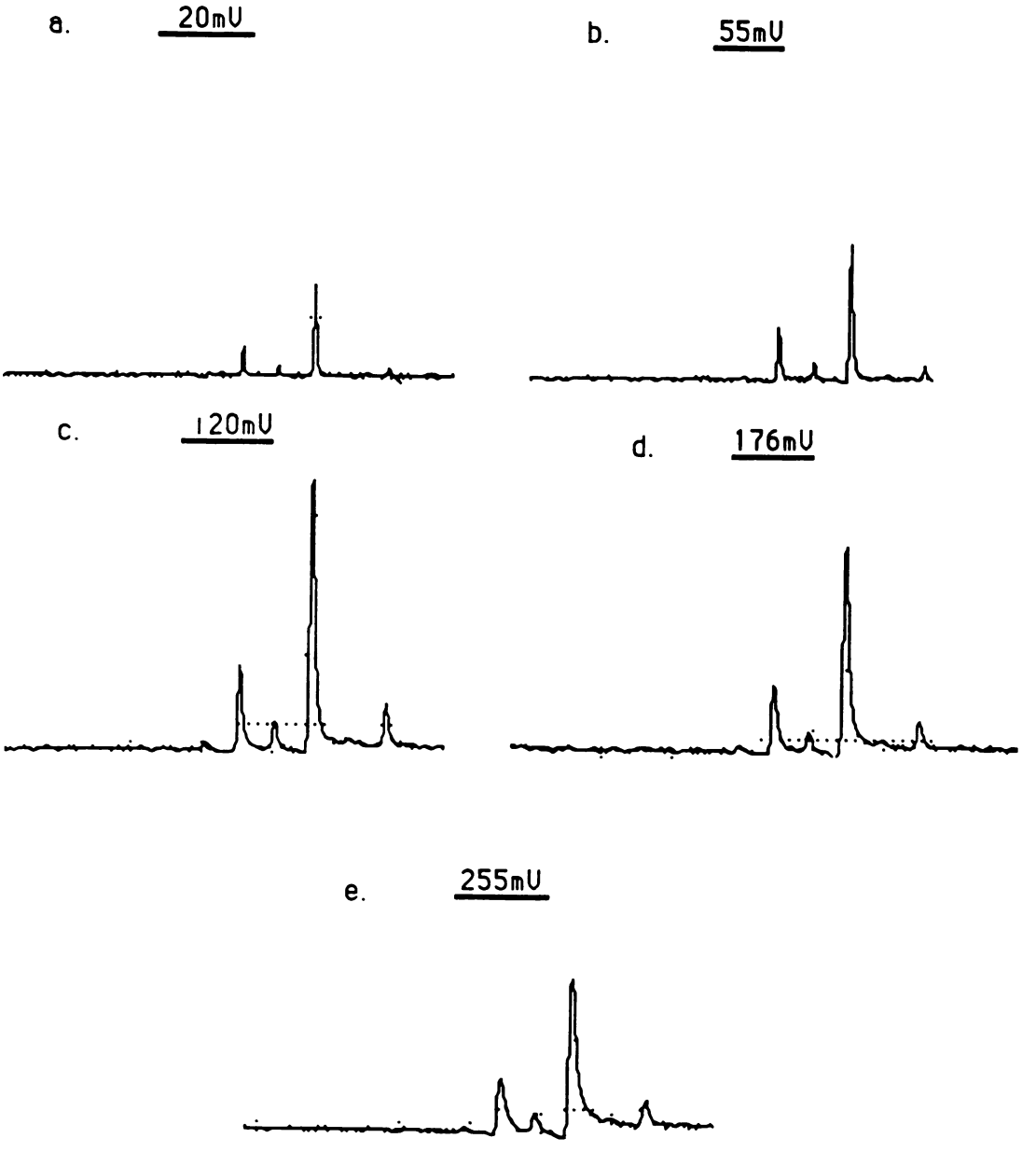

Figure 2-6 Effect of irradiating voltage on peak intensity

Another effect of the irradiating voltage is on the baseline. Because the capacitance of the balance cell does not match *exactly* the capacitance of the ICR cell, the baseline of the spectrum will not be flat and level. A large irradiating signal will cause this effect to be more noticeable. This can be observed in Figure 2-7a-f. These figures show the baseline obtained for different levels of rf voltage with no ions in the cell. The y- axis represents the dc voltage level. The scan is from 100 kHz to 440 kHz, a typical range. As the magnitude of the rf voltage increases, the dc level of the baseline increases, and also the slope increases, rising towards the high frequency (low mass) end of the scan.

A parameter of great importance is the amount of double resonance radiation to use to selectively eject ions from the cell. The effect of changing the double resonance irradiating voltage on a selected ion can be seen in Figure 2-8a-f. These spectra show the m/z 58, 60, and 62 isotopes of Ni^+. The magnetic field was set at 16 kG and the double resonance oscillator set to 424 kHz. At low irradiating voltages, the mass 58 ion is partially ejected. At 220 mV irradiating voltage, the ion is almost completely ejected. Note that the abundance of the mass 60 ion, at 410 kHz, is totally unaffected by the double resonance irradiation. The fact that the isotope is unaffected can be of great use in some experiments. In these spectra, a spike appears at the exact frequency that the oscillator is tuned to. This spike increases with the voltage level but causes no problem. Occasionally an overtone of the irradiating frequency can be seen at exactly three times the irradiating frequency as a small spike, but this is easily recognized. An important consideration in performing double resonance experiments is that an ion, in the process of being ejected from the cell, absorbs power and gains higher translational velocity. Reactions that would not normally occur may be seen because of the

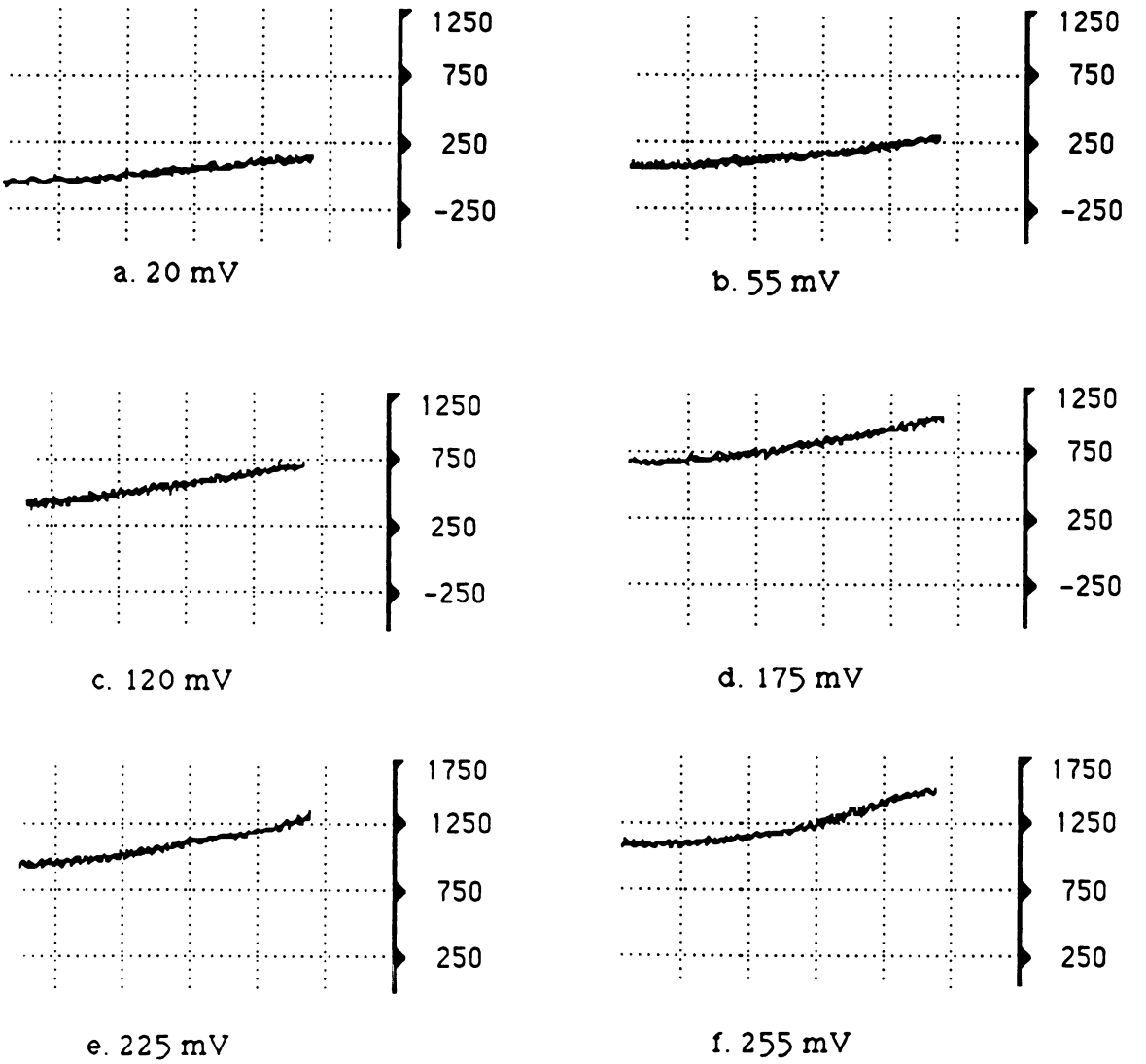

Figure 2-7 Effect of irradiating voltage on spectrum baseline

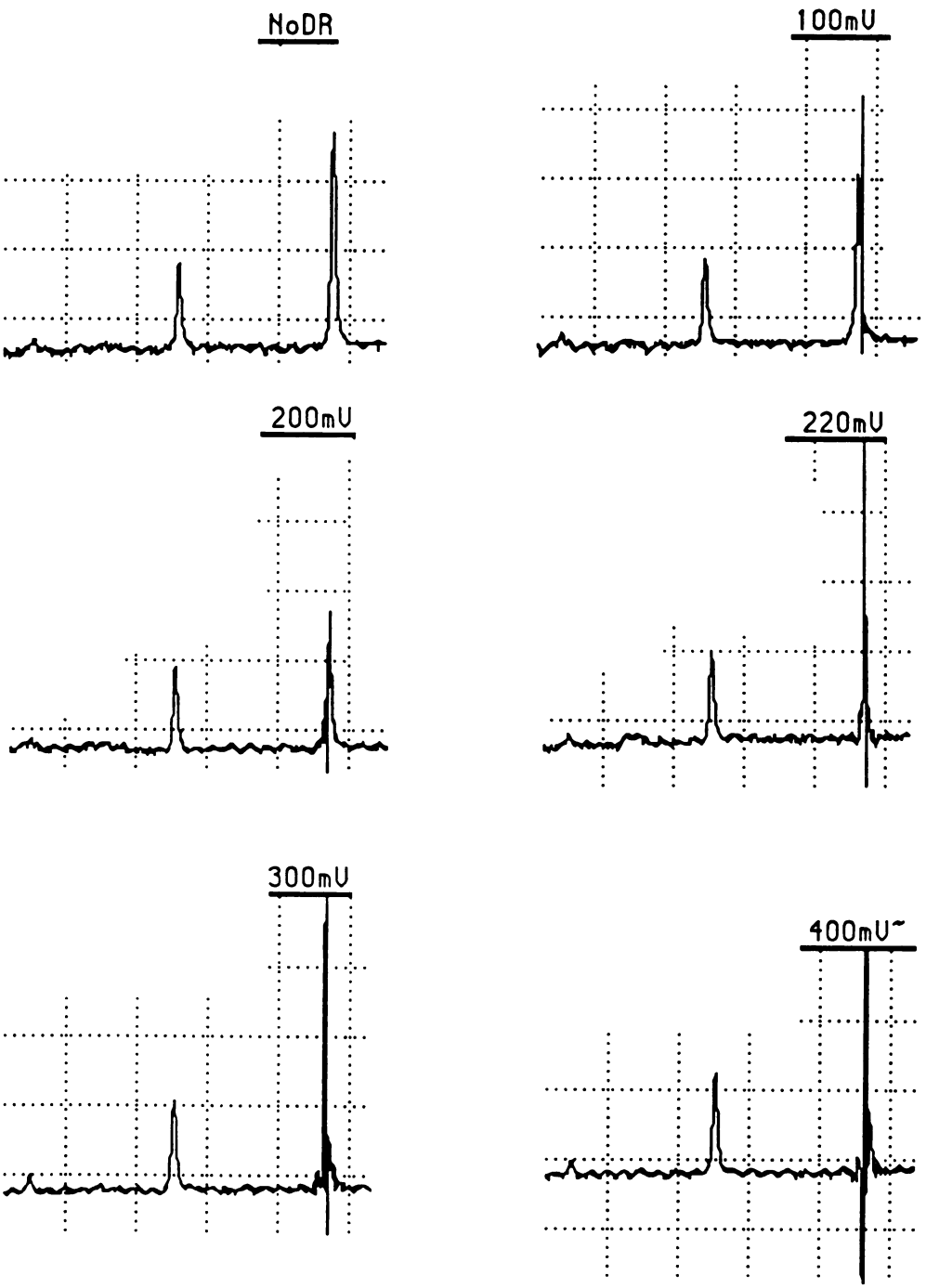

Figure 2-8 Effect of double resonance voltage on a selected ion

higher energy of the reactant ion. To minimize this problem, the lowest irradiating power that causes sufficient ion ejection is used. A rf level of 220 mV works well.

In order to improve the signal-to-noise ratio and to simplify instrument operation, a MacADIOS (Macintosh Analog/Digital Input/ Output System) data acquisition system, coupled to a Macintosh Plus computer, is used for signal averaging. The MacADIOS is multi-purpose system that allows input or output of analog waveforms at rates of up to 20 kHz. Digital input and output is also allowed. Communication of acquired data to the Macintosh Plus is via a 500k bits per second serial interface to the modem port. Software is provided to allow the user to develop experiments to collect, manipulate, analyze, and view data. Programming can be done in three different languages: "MacADIOS Manager"; BASIC; and Aztec C. MacADIOS Manager is a simple language developed to work with the MacADIOS. Although the language is easy to use, it has certain limitations that prohibit the user from performing certain types of procedures. In these cases, BASIC or C, being more flexible, may allow the user to perform the experiment. For example, while a program in MacADIOS Manager allows the user to perform a nested loop, it does not allow performing successive loops. However, this type of program is very simple to write in BASIC.

The program has since been translated from BASIC into MacADIOS Manager language and performs just as well, though it is not as flexible.

A BASIC program, Scanner, (listed in Appendix A) was used to collect the data presented in Chapter 5. The basic experiment consists of first stepping the analog output of the MacADIOS to provide a -5 to +10 volt ramp in 3150 discrete steps of 4.88 mV/step. This ramp then passes through a potentiometer serving as a voltage divider. The magnitude of the ramp is here reduced to

about -0.5 to +1 volts, and then fed into the voltage controlled frequency (VCF) input of a Tektronix FG 504 function generator. The function generator, on receiving a negative voltage, will produce a lower frequency than the dial is set for. Conversely, a positive voltage will cause a higher frequency; in this way a frequency scan in the range 100 kHz to 500 kHz can be produced. Any appropriate frequency sweep can be produced. The frequency range scanned will depend on the masses of the ions to be examined. The frequency output is then attenuated and sent to the signal summer module. At each step of the voltage ramp the output of the detector is amplified, low pass filtered, and digitized. Twelve data points are taken, with 2.5 msec between each point. This makes the sampling period long compared to the time of a 60 Hz wave period. Line frequency, 60 Hertz, is a common source of periodic noise, and this periodic noise can be hard to remove.

After digitization, the data points are added together and stored. The ramp is then stepped to the next value. A plot of detector response versus step number is then produced. By knowing the starting and stopping frequency, and also the magnetic field strength, the step number can be converted to m/z. In order to perform the double resonance experiment the procedure is repeated, with one important difference. A gate signal is sent to a Wavetek model 144 HF sweep function generator that is tuned to the frequency of the ion that is to be ejected. The experiment then takes place as usual, except that one ion will not be present in the cell, i.e., the selected ion will be constantly ejected from the cell upon formation. Consequentially, any ions produced by reactions of that ion will not be present, either. When the spectrum with irradiation on is subtracted from the normal spectrum, a subtraction spectrum is produced. The subtraction spectrum should be flat and featureless, except at the points where the irradiated ion and its products were.

At these points, negative dips appear. This is illustrated in Figure 2-9a-c.

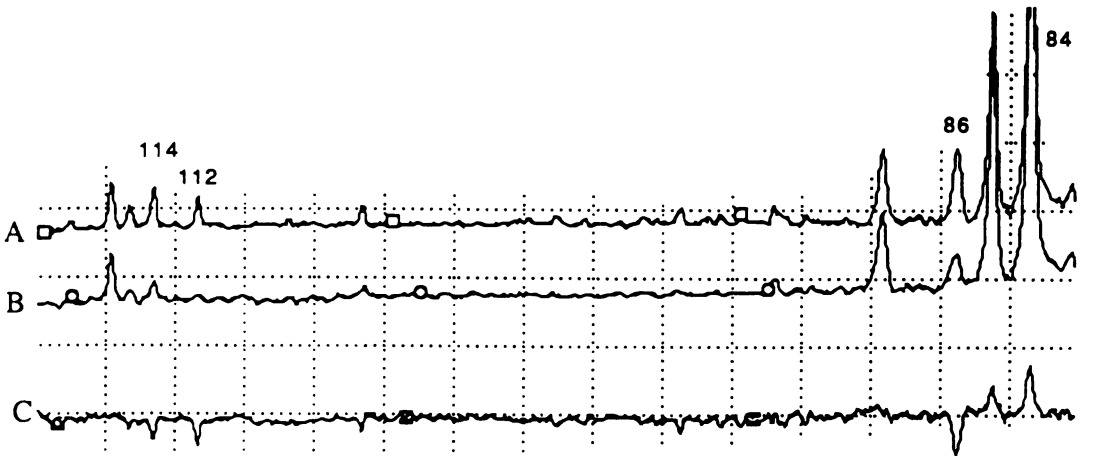

Figure 2-9 Double resonance spectra

Spectrum A show part of the spectrum the 1:1 mixture of $Ni(PF_3)_4$ and cyclopentanone at a total pressure of $6x10^{-6}$ torr. The mass range is from 118 to 83 amu. The parent ion of cyclopentanone occurs at m/z 84 and is off scale. Product ions that do not occur in the spectrum of $Ni(PF_3)_4$ or cyclopentanone are observed at m/z 86, 112 and 114. In spectrum B, m/z 58, Ni^+, has been ejected from the cell (see Figure 2-8). Notice that the intensities of the products at m/z 86, 112, and 114 has decreased. Spectrum C shows the subtraction of spectrum B from C. Negative peaks at m/z 86, 112, and 114 can be assigned as the products $NiCO^+$, $NiC_4H_6^+$, and $NiC_4H_8^+$. There is a slight positive peak at m/z 84 and 85 in this

spectrum. During the course of the experiment, the pressure of cyclopentanone increased slightly, causing the peaks here to increase from spectrum A to B.

To acquire data in this way, several programs were evaluated, but did not produce adequate results. The program tried used the fast scanning ability of the FSD. The irradiating frequency generator was triggered to produce a 0.2 sec spectrum and 2000 data points were accumulated at a 10 kHz digitization rate. This program had the advantage of gathering data very quickly; however, it was difficult to discriminate against high frequency noise. The bandpass of the peaks was narrow and did not allow filtering.

A second attempt used a slower ramp and a 400 Hz digitization rate. The slower scanning speed allowed filtering to reduce noise. A drawback to this program was that the scan times produced by the function generator were not exactly constant. As a result, the position of the peaks in the irradiated spectrum and the nonirradiated spectrum would shift relative to each other. When the two spectra were subtracted from each other, the results could be very erratic. If the peaks in the spectra mismatched by just a few data points, the subtraction would produce a signal that looked like a first derivative of a peak. Figure 2-10 illustrates this effect. When spectrum A is subtracted from spectrum B, the result is line C.

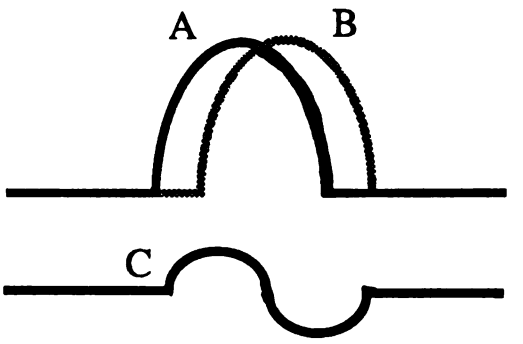

Figure 2-10 Effect of mismatched peaks

The program used for these experiments, Scanner, overcomes the problems in these unsuccessful programs. It uses a 4 minute scan speed that allows low pass filtering. Controlling the frequency of the function generator with the MacADIOS produces a very reproducible frequency scan which minimizes problems caused by mismatching peaks. A disadvantage is that the slow scan time causes the experiment to take a long time, over eight minutes. A concern on taking the data was that the detector may not stabilize sufficiently before the data is taken. This program utilized time spent in calculations as delay time, allowing the detector response to stabilize as much as possible. Care was used that the two spectra, irradiated and nonirradiated, were gathered in exactly the same way, except for the gating of the double resonance oscillator. The presence of the double resonance voltage does not appear to affect the spectrum in any adverse way.

Several other features are used in collecting data. Adding data points will increase the signal-to-noise ratio (S/N) by increasing the signal more than the noise. Subtracting spectra has the result of adding nothing to the signal but increasing the noise, not a desirable effect. To avoid from increasing the noise by the mathematical subtraction, a "moving window" convolution is performed on both spectra. The spectra are convoluted with a step function. This digital filtering removes much of the noise of the collected spectrum, but also has the deleterious effect of decreasing peak intensity. Using more points in the step function will reduce the noise more, so a compromise must be reached between the noise reduction and signal reduction. A three point step function works well.

To decrease noise before digitization, a passive filter with a 0.1 msec time constant is placed before the MacADIOS. This reduces

much of the high frequency noise produced in the amplification stage of the phase sensitive detection module.

The ICR cell was changed in several ways in order to improve its performance when used with the FSD. The filament had previously been located in the center of the source region, but was moved to 1/2 inch from the top of the source. This gives the ions a longer residence time in the source region, and a greater chance to react. Another modification was to reduced the distance between the drift plates from 3/4 to 1/2 inch, changing from a "square cell" cross section geometry to a "flat cell". This reduced the occurrence of "trapping", a condition in which the ions remain in the cell for long periods of time, up to many seconds. The ideal condition is when the ions drift through the cell in several milliseconds, under single collision conditions. In trapping, the ions may undergo multiple collisions and make interpretation difficult. Spectra cannot be recorded when trapping occurs. Reducing the distance between the drift plates increased the field felt by the ions and forced them to drift through the cell. A greater distance between the drift plates results in poorer control over the ion movement.[2]

The chemicals used in these experiments were all commercially available. They were degassed by multiple freeze-pump-thaw cycles and used without further purification. Any impurities present would be evident in the spectrum of the compound.

The necessary low pressure in the instrument is produced by a 4 inch diffusion pump with a liquid nitrogen cold trap, and a Ultek 20 l/s ion pump. Samples are admitted from a triple inlet (individually pumped by a 2 inch diffusion pump and liquid nitrogen cold trap) through Varian 951-5106 precision leak valves. Approximate pressures are measured with a Veeco RG1000 ionization gauge. Pressure can also be measured by the Ultek ion pump.

References

1. Budzikiewicz, H. *Mass Spectrometry Reviews* **1987,** *6,* 329.
2. Lehmann, T. A.; Bursey, M. M. *" Ion Cyclotron Resonance Spectrometry" Wiley* : New York **1976**
3. Wronka, J; Ridge, D. P. *Rev Sci. Instrum.* **1982,** *53,* 491.
4. Wronka, J; Frequency Scanned Detector Model #3 Instruction Manual

Chapter 3

Reactions of aldehydes with metal ions

This chapter will discuss the reactions of aldehydes with Co^+, Fe^+, and Ni^+. Aldehydes are an interesting class of compounds for study because of the presence of the carbonyl functional group. Aldehydes and ketones can serve as ligands in transition metal complexes, in the liquid phase. Numerous transition metal catalyzed-reactions involve aldehydes and ketones as starting products or intermediates.[1] Study of the how the metal reacts with the carbonyl group may give insight how the metal is influenced by having CO as a ligand. Aldehydes represent one of the first class of compounds systematically studied by metal ion/molecule reactions.

In one of the first studies, Corderman and Beauchamp[2] observed, for seven aldehydes, the following decarbonylation reactions:

$$NiCp^+ + RCHO \rightarrow NiCpCO^+ + RH \quad (1)$$

$$\rightarrow NiCpRH^+ + CO \quad (2)$$

Decarbonylation reactions were not seen for formaldehyde, trifluoro-acetaldehyde, acetyl chloride, acetyl bromide, acetone, and methyl acetate. They concluded that decarbonylation reactions of $NiCp^+$ were specific for aldehydes, since this reaction did not occur for the acetone or methyl acetate. Unfortunately, they did not report the results of Ni^+ reacting with these compounds. The experiment was performed in a conventional ICR mass spectrometer, with $NiCp^+$ generated by 20 eV EI. This also produces Ni^+, and its reactions

should have been observed occurring simultaneously with the reactions of $NiCp^+$.

Halle, Crowe, Armentrout, and Beauchamp[3] performed the next study of aldehydes using cobalt ions in an ion beam apparatus. In this experiment the reaction products are formed with the cobalt ions at a well defined kinetic energy. At low energy the only reaction observed for formaldehyde and acetaldehyde was:

$$Co^+ + RCHO \rightarrow CoCO^+ + RH \qquad (3)$$

More recently, I.K. Gregor[4] has reported the reactions of $Cr(CO)_3^-$ and $Cr(CO)_4^-$ with the straight chain aldehydes, formaldehyde through heptanal, and also isopropanal and isobutanal. All the aldehydes studied reacted to give alkane elimination. Loss of CO was also observed, but reactions of ^{13}C labeled acetaldehyde indicated that the CO lost was a metal bonded ligand rather than from the decarbonylation reaction. For propanal and larger aldehydes, loss of H_2, as well as loss of CO, occurs.

$$RCHO + Cr(CO)_3^- \rightarrow (alkene)Cr(CO)_3^- + H_2 + CO \qquad (4)$$

The compounds larger than butanal can further dehydrogenate:

$$(alkene)Cr(CO)_3^- \rightarrow (alkadiene)Cr(CO)_3^- + H_2 \qquad (5)$$

The results indicate that when a sufficiently long alkyl chain is present, the chain may wrap around to interact with the metal center, resulting in H_2 loss.

The reactions between the 70 eV EI fragments of $Ni(PF_3)_4$ and $Co(CO)_3NO$ with the straight chain aldehydes propanal through heptanal will be presented in this chapter. The reactions of hexanal and heptanal with $Fe(CO)_5$ will also be presented. In addition, reactions of benzaldehyde with Ni^+ and Co^+ will be presented. The results of these reactions are summarized in Table 3-1.

A basic question is whether the metal ion inserts into the R-(CO)H bond, intermediate I, followed by a α-H shift to the metal ion, or whether the initial insertion is into the R(CO)-H bond, intermediate II, followed by a α-R group shift.

I II

Thermodynamic estimates of the bond strengths indicate that the R-CO bond is slightly weaker than the H-CO bond (82.5 kcal vs. 86 kcal).[3] Insertion into C-CO bonds is a major pathway in the reactions of ketones;[3,5] however, the cross section for the reaction between Co^+ and formaldehyde is very small.[3] This result indicates that insertion into the CO-H bond is not a favored pathway. Insertion into the R-CO bond would result in an intermediate in which the metal ion would be bonded to the polarizable R group, producing a stabilizing effect.

The results in Table 3-1 are, in some cases, unfortunately ambiguous. For example, it is impossible to determine the difference between the loss of C_2H_4 and CO, both with a nominal mass of 28 u. The products listed in the table are believed to be the most reasonable according to known mechanisms. While some of the

products may be ambiguous, many of the products can be explained. For example, consider the reactions of Ni^+. With propanal, butanal, and benzaldehyde, all of the products can be explained by initial insertion into the R-CHO bond. For example,

$$Ni^+ + C_3H_7CHO \rightarrow NiCO^+ + C_3H_8 \ (17\ \%) \quad (6)$$

$$\rightarrow NiC_3H_8^+ + CO \ (38\ \%) \quad (7)$$

For hexanal and heptanal, most of the reactions observed <u>cannot</u> be explained by insertion into the R-CHO bond.

$$Ni^+ + C_6H_{13}CHO \rightarrow NiC_3H_6O^+ + C_4H_8 \ (44\ \%) \quad (8)$$

$$\rightarrow NiC_4H_6O^+ + C_3H_8 \ (22\ \%) \quad (9)$$

A different mechanism must be used to explain why insertion is favored at the middle of the alkyl chain rather than at the functional group. If the alkyl chain wraps around to interact with the metal ion, after the initial complexation with the functional group, as shown in intermediate III, then insertion at this location can be explained.

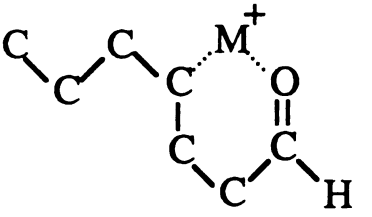

III

The preferred sites of insertion for the metal ions with hexanal and heptanal are shown in Figure 3-1. For comparison, the preferred insertion sites for Co^+ into hexanol[6] is also shown. The C-C bonds are labeled with numbers in this figure. The bonds that the metal ion insert into are listed in order of occurrence. For example, in the reaction of Ni^+ with hexanal, most of the products are formed by insertion into bond C, with a smaller amount of product formed by insertion into bond D.

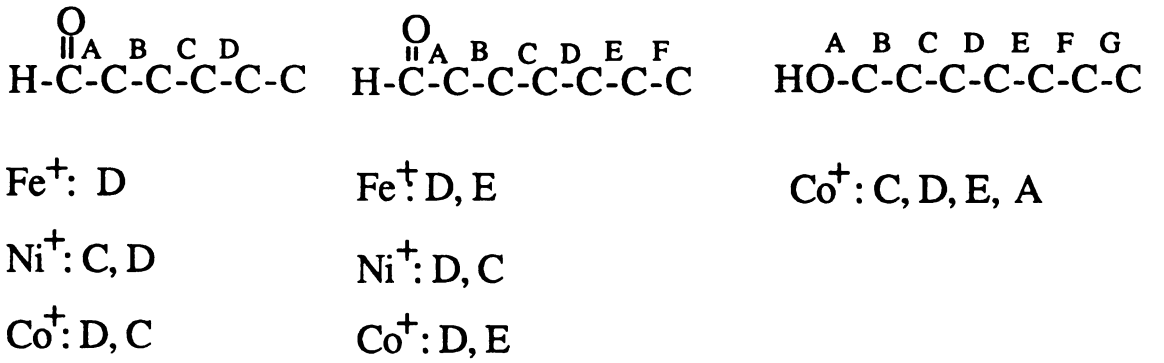

Figure 3-1 Bond insertion preferences of the different metal ions into hexanal and heptanal.

The preferred site of insertion for aldehydes smaller than hexanal appears to be adjacent to the carbonyl. Several general trends are seen in these reactions. The number of products formed is less than in the reactions of alcohols with similar chain length. This may reflect that the aldehydes are more specific in the bonds attacked. The presence of the double bond in the carbonyl may

make the intermediate more rigid, making fewer of the C-C bonds in the alkyl chain susceptible to attack.

Differences in the reactivity of the different metals can also be seen. Nickel forms more products than cobalt. This is unusual; for in the nitriles and most other compounds, cobalt is more reactive than nickel. In general, cobalt is more reactive than nickel, the former having a lower promotional energy.[7]

The *types* of products formed from all the metal ions with the aldehydes are similar. An exception is that Fe^+ here does act specifically to eliminate H_2 from the large aldehydes. Also, the formation of butadiene is specific for Fe^+.

Ni^+ also inserts into bonds closer to the functional group than either Co^+ or Fe^+. Ni^+ and Co^+ also are more specific for attacking bonds, both inserting into only two bonds, while Fe^+ inserts into three bonds. In contrast, these trends are not observed in the nitriles. For hexyl cyanide, Ni^+ inserts into one bond, Fe^+ inserts into two bonds, and Co^+ inserts into three bonds. Co^+ prefers to insert one bond closer than the most preferred insertion site for both Fe^+ or Ni^+. Clearly, conclusions about the reactivity of the different metal ions are difficult to make, based only these three examples.

Because many of the products could not be unambiguously identified, further work on aldehydes was not pursued. The use of isotope labeled aldehydes would be of great use to identify these products.

Table 3-1

Reactions of aldehydes with M^+ and ML^+

Reactant	P= CH_3CH_2CHO	$CH_3(CH_2)_2CHO$	$CH_3(CH_2)_3CHO$
Co^+	$CoCO^+ + C_2H_6$ (.83)	$CoCO^+ + C_3H_8$ (.16)	$CoC_3H_6O^+ + C_2H_4$(.56)
	$CoC_3H_4O^+ + H_2$ (.17)	$CoC_3H_8^+ + CO$ (.57)	$CoC_5H_8O^+ + H_2$ (.44)
		CoP^+ (.26)	
$CoCO^+$	$CoP^+ + CO$ (.83)	$CoC_3H_8^+ + 2\ CO$ (.18)	$CoC_5H_8O^+ + H_2 + CO$(.31)
	$CoCOP^+$ (.17)	$CoP^+ + CO$ (.56)	$CoP^+ + CO$ (.69)
		$CoCOP^+$ (.26)	
$CoNO^+$	$CoP^+ + NO$	N. R.	N. R.
Ni^+	$NiCO^+ + C_2H_6$ (.41)	$NiCO^+ + C_3H_8$ (.17)	$NiC_2H_4^+ + C_3H_6O$ (.19)
	$NiC_3H_4O^+ + H_2$ (.11)	$NiC_3H_5^+ + CHO$ (.18)	or $NiCO^+ + C_4H_{10}$
	NiP^+ (.43)	$NiC_3H_6^+ + CO + H_2$ (.12)	$NiC_3H_4O^+ + C_2H_6$ (.13)
	? (m/z =144) (.04)	$NiC_3H_8^+ + CO$ (.38)	or $NiC_4H_8O^+ + CO + H_2$
		NiP^+ (.15)	$NiC_4H_{10}^+ + CO$ (.68)
			or $NiC_3H_6O^+ + C_2H_4$
$Ni(PF_3)^+$	$Ni(PF_3)P^+$	$NiP^+ + PF_3$	$NiP^+ + PF_3$

N. R. = No Reaction

Table 3-1, continued

	$CH_3(CH_2)_4CHO$	$CH_3(CH_2)_5CHO$	C_6H_5CHO
Co^+	$CoC_3H_6O^+ + C_3H_6$ (.32)	$CoC_4H_6O^+ + C_3H_8$ (.44)	$CoC_6H_6^+$ (.68)
	$CoC_4H_6O^+ + C_2H_6$ (.30)	$CoC_4H_8O^+ + C_3H_6$ (.29)	CoP^+ (.31)
	$CoC_4H_8O^+ + C_2H_4$ (.18)	$CoC_5H_8O^+ + C_2H_6$ (.27)	
	CoP^+ (.20)		
$CoCO^+$	$CoC_3H_6O^+ + CO + C_3H_6$ (.14)	$CoC_4H_8O^+ + C_3H_6 + CO$ (.42)	$CoP^+ + CO$
	$CoC_4H_6O^+ + CO + C_2H_6$ (.25)	$CoP^+ + CO$ (.40)	
	$CoC_4H_8O^+ + CO + C_2H_4$ (.17)	$CoCOP^+$ (.18)	
	$CoC_6H_{10}O^+ + CO + H_2$ (.12)		
	$CoP^+ + CO$ (.25)		
	$CoCOP^+$ (.08)		
$CoNO^+$	N. R.	N. R.	$CoP^+ + NO$
Ni^+	$NiC_3H_6^+ + C_3H_6O$ (.11)	$NiC_3H_8^+ + C_4H_6O$ (.36)	$NiC_6H_6^+ + CO$
	$NiC_3H_8^+ + C_3H_4O$ (.15)	$NiC_3H_6O^+ + C_4H_8$ (.42)	
	$NiC_3H_6O^+ + C_3H_6$ (.29)	$NiC_4H_6O^+ + C_3H_8$ (.22)	
	$NiC_4H_8O^+ + C_2H_4$ (.22)		
	NiP^+ (.23)		
$NiPF_3^+$	$NiP^+ + PF_3$	$NiC_4H_6O^+ + C_3H_8 + PF_3$ (.34)	$NiP^+ + PF_3$
		NiP^+ (.66)	

Table 3-1, continued

	P= $CH_3(CH_2)_4CHO$	$CH_3(CH_2)_5CHO$
Fe^+	$FeC_3H_6^+ + C_3H_6O$ (.13)	$FeC_4H_6^+ + C_3H_6O + H_2$ (.38)
	$FeC_4H_6^+ + C_2H_4O + H_2$ (.41)	$FeC_4H_4O^+ + C_3H_8 + H_2$ (.20)
	$FeC_4H_6O^+ + C_2H_6$ (.06)	$FeC_4H_6O^+ + C_3H_8$ (.15)
	$FeC_4H_8O^+ + C_2H_4$ (.09)	$FeC_4H_8O^+ + C_3H_6$ (.07)
	$FeC_6H_{10}O^+ + H_2$ (.23)	$FeC_5H_8O^+ + C_2H_6$ (.13)
	FeP^+ (.06)	FeP^+ (.06)
$Fe(CO)^+$	$FeC_4H_6O^+ + C_2H_6 + CO$ (.04)	$FeC_4H_6O^+ + C_3H_8 + CO$ (.09)
	$FeC_4H_8O^+ + C_2H_4 + CO$ (.17)	$FeC_4H_8O^+ + C_3H_6 + CO$ (.14)
	$FeC_6H_{10}O^+ + H_2 + CO$ (.56)	$FeC_5H_8O^+ + C_2H_6 + CO$ (.07)
	$FeP^+ + CO$ (.22)	$FeC_7H_{12}O^+ + H_2 + CO$ (.44)
		$FeP^+ + CO$ (.26)

References

1. Huang, Y-H.; Gladysz, J. A. *J. Chem. Ed.* **1988,** *65*,298.
2. Corderman, R. R.; Beauchamp, J. L. *J. Am. Chem. Soc.* **1976,** *98*,5700.
3. Halle, L. F.; Crowe, W. E.; Armentrout, P. B.; Beauchamp, J. L. *Organometallics.* **1984,** *3,* 1694.
4. Gregor, I. K. *Org. Mass Spectrom.* **1987,** *22*,644.
5. Burnier, R. C.; Byrd, G. D.; Freiser, B.S.; *J. Am. Chem. Soc.***1981,** *103*,4360.
6. Tsarboploulos, A.; Allison, J. *J. Am. Chem. Soc.* **1985,** *107,* 5085
7. Babinec, S. J.; Allison, J. *J. Am. Chem. Soc.* **1984,** *106,* 7718.

Chapter 4

Reactions of Co^+ with nitriles

The gas phase chemistry of nitriles with Co^+ is discussed in this chapter. This work was performed in 1984-85. As the results were being prepared for publication, Helmut Schwarz at the Institut für Organische Chemie, Technische Universitat Berlin, published several reports on the reactions of Fe^+ with nitriles.[8] Ions formed by EI on $Fe(CO)_5$ were allowed to react with nitriles in the source of a ZAB-HF-3HF triple sector mass spectrometer. The ion corresponding to $Fe(RCN)^+$ was selected and collided with neutral argon at high energy, 8 keV. Based on the ions produced by the collision ("daughter ions"), they concluded that Fe^+ inserted into only C-H bonds of alkyl nitriles, because no loss of alkane occurred. In later papers, they did report alkane loss for large nitriles. In comparing the reactions of Fe^+, Co^+, and Ni^+, they reported that, based solely on the percent of alkene loss, a different mechanism must be operating for the reactions of Fe^+ than for Co^+ and Ni^+.

In our data we see no evidence for different mechanisms for the reactions of the different metals. It is true that the different metals do have different product distributions (see Table 4-3). However, we feel that the products can be explained by the chain length mechanism which was proposed to explain the reactions of alcohols and chloroalkanes. This mechanism allows for both C-H and C-C bond insertion at sites remote from the functional group. Tendencies for insertion into C-H or C-C may be dependent on the metal, but not to the extent to indicate that two separate mechanisms are operative.

Our study of the reactions of metal ions with nitriles follows this introduction, in the form of a preprint of a paper which has been accepted for publication in *Organometallics*. It includes a discussion of our results and also comments on the recent work of Schwarz. Again, his results are not directly comparable to ours, due to the different experimental technique. His collisional activation results do parallel our results, however.

One of Schwarz's claims is that the iron ion adducts that are formed in the source of his mass spectrometer are only in the form $Fe(RCN)^+$. Alternatively, the $FeRCN^+$ ion could be in a form such as:

$$C_3H_6\cdots Fe^+\cdots\cdots C_3H_7CN$$

To investigate the structure of some of the products formed in the reactions of Co^+ and alkyl nitriles, collisionally activated dissociation (CAD) experiments were performed on an Extrel Triple Quadrupole instrument. In these experiments, selected ions collide with an inert collision gas at low energies, only several eV. If the ion existed as the adduct $M(RCN)^+$ then a collision might produce only the M^+ ion with loss of the nitrile ligand. However, if the nitrile rearranged, existing as two ligands bonded to the metal, then a collision might show more products, such as one of the ligands bonded to the metal.

$Co(CO)_3NO$ and a nitrile of interest were introduced into the chemical ionization (CI) source of the instrument and ionized by 70 eV EI. The metal ions formed react with neutral nitrile as expected. The "adduct ion" CoP^+ (P = parent) was mass selected with the first quadrupole, and sent into the second quadrupole, the collision region. The collision chamber was filled with argon at low pressure, $1x10^{-5}$ torr. About 50% of the selected ion dissociated at this pressure. Ionic products were then mass selected with the third set of quadrupoles. Higher pressure in the collision chamber resulted in a

greater percentage of the ions dissociating, but also resulted in sequential reactions due to multiple collisions. The ion energy was set at 2 eV. At higher energy, such as 10 eV, the main reaction observed was $CoP^+ \rightarrow Co^+ + P$. The product of some of these reactions are listed in Table 4-1. The table lists the normalized data of the reactions. A branching ratio (B. R.) for only the reactions which resulted in the breaking of a carbon-carbon bond is listed.

The products resulting from 2 eV collisions with argon are very similar to those seen in the ICR experiment. For example, consider the CAD spectrum of CoP^+ produced by the reaction of hexyl cyanide and Co^+. Five products are formed; in the ICR experiment, four of these five products are formed by bimolecular reaction. This suggests that the mechanism for product formation is the same for both techniques. The energy gained on collision is may be enough to cause rearrangement and dissociation of a neutral molecule. Alternatively, if the CoP^+ ion is in a form such as:

$$C_3H_6 \cdots Co^+ \cdots C_3H_7CN$$

prior to the collision, the collision may act to break the bond to the ligand which is held more weakly. In these experiments, it would be difficult to say whether the products were formed by rearrangement, simple dissociation, or a combination of both of these processes. However, the large amount of Co^+ produced on collision indicates that at least some of the ions exist as the simple adduct with no rearrangement. Collision of a rearranged molecule should not produce the Co^+ ion, unless both ligands are simultaneously lost, or through multiple collision.

In addition to the CAD spectrum of the CoP^+ ion, other products formed in the source could be studied. Table 4-1 lists the CAD spectrum of m/z 142 and 128 formed ion the Co^+/heptyl cyanide

system (by loss of ethylene and propylene, respectively).

The CAD spectrum of m/z 128 show that ethylene loss and ethyl cyanide loss to be the only important reactions. In the ICR experiment, ethylene loss is the major product in the reaction of Co^+ and propyl cyanide. The CAD spectrum of m/z 142 gives branching ratios similar to those found by the ICR reaction of Co^+ and butyl cyanide. The results produced in the ICR experiment are:

$$Co^+ + C_4H_9CN \rightarrow CoC_4H_9CN^+ \ (26\ \%) \quad (1)$$

$$\rightarrow CoC_4H_7CN^+ + H_2 \ (41\ \%) \quad (2)$$

$$\rightarrow CoC_2H_3CN^+ + C_2H_6 \ (11\%) \quad (3)$$

$$\rightarrow CoCH_3CN^+ + C_3H_6 \ (21\ \%) \quad (4)$$

The products from the CAD reaction of the ion at m/z 142, presumed to be the reaction product $CoC_4H_9CN^+$ (neglecting the Co^+ product) are:

$$CoC_4H_9CN^+ \rightarrow CoC_4H_9CN^+ \ (67\ \%) \quad (5)$$

$$\rightarrow CoC_4H_7CN^+ + H_2 \ (13\ \%) \quad (6)$$

$$\rightarrow CoCH_3CN^+ + C_3H_6 \ (20\ \%) \quad (7)$$

These results indicate that the the products of the initial reaction between hexyl cyanide and Co^+ have the structure of simple adducts.

Experiments were attempted in which acetonitrile was used as the collision gas instead of argon. It was hoped that acetonitrile would react with the selected ion via ligand substitution reactions. For example, when Co^+ reacts with hexyl cyanide to form the product at m/z 170, some of the product may be in the form $(C_4H_8)Co^+(C_2H_5CN)$. We hoped that reactions such as:

$$(C_4H_8)Co^+(C_2H_5CN) + CH_3CN \rightarrow (CH_3CN)Co^+(C_2H_5CN) + C_4H_8 \quad (8)$$

and

$$(C_4H_8)Co^+(C_2H_5CN) + 2\ CH_3CN \rightarrow (CH_3CN)_2Co^+ + C_2H_5CN + C_4H_8 \quad (9)$$

would be observed. These reactions would give products at m/z 156 and 141, respectively. Reactions of this type were not observed. The results between using argon and acetonitrile as collision gases were very similar.

When comparing the results of the two different experimental techniques, one should realize exactly what factors can influence the data. In the triple quadrupole experiment, the number and type of products seen and their relative intensities are dependent on many parameters, including collision energy and collision chamber pressure. Conditions in the triple quadrupole must be set so that enough ions dissociate, but these conditions also tend to increase the amount of multiple collisions. The multiple collisions make data interpretation difficult. Because of the many variables involved, it is difficult to obtain a consistent set of data for these reactions. The similarities in the results between the two techniques is interesting, and in many cases CAD spectra could provide complementary data to the ICR data.

Table 4-1

CAD reactions of Co^+-(Nitrile) adducts

CAD of hexyl cyanide·Co^+, m/z 156, at $1x10^{-5}$ and $8x10^{-5}$ torr collision chamber pressure

	$1x10^{-5}$ torr[a]		$8x10^{-5}$ torr		
m/z	Per cent	B.R[b]	Per cent	B.R.	Neutral loss
156	100.0		30.3		
154	6.6	.35	43.5	.25	H_2
128	11.1	.60	94.6	.54	C_2H_4
100	.9	.05	37.3	.21	$2\,C_2H_4$
59	17.7		100.0		$C_5H_{11}CN$

CAD of heptyl cyanide·Co^+, m/z 170 at $1x10^{-5}$ torr collision chamber pressure

m/z	Per cent	B.R	ICR B.R.	Neutral loss
170	80.3			
168	5.0	.17	.11	H_2
142	10.3	.36	.17	C_2H_4
140	1.5	.05	.07	C_2H_6
128	8.7	.31	.34	C_3H_6
112	2.8	.11	.00	C_4H_{10}
59	17.7			$C_6H_{13}CN$

a: pressure of collision gas b: B. R. = Branching Ratio

Table 4-1, continued

CAD of m/z 142, ($C_4H_9CN{\cdot}Co^+$) from heptyl cyanide·Co^+ at $1x10^{-5}$ torr, 2eV collision

m/z	Per cent	B.R	ICR B.R. of butyl-CN	Neutral loss
142	100.0	.67	.26	
140	20.0	.13	.41	H_2
112	0.0	.00	.11	C_2H_6
100	30.0	.20	.21	C_3H_6
59	62.0			C_4H_9CN

CAD of m/z 128, ($C_3H_6CN{\cdot}Co^+$) from hexyl cyanide·Co^+ at $1x10^{-5}$ torr, 2eV collision

m/z	Per cent	B.R	ICR B.R. of propyl-CN	Neutral loss
128	100.0	.77	.35	
100	30.0	.23	.61	C_2H_4
87	0.0		.04	CH_3CN
59	72.0			C_3H_7CN

The Gas Phase Chemistry of First Row Transition Metal- and Metal-Containing Ions With Alkyl Nitriles

ABSTRACT

The gas phase ion/molecule reactions of first row transition metal ions with a series of alkyl nitriles is discussed, with the focus on the chemistry of Co^+. As the length of the alkyl chain of the nitrile increases, cleavage of C-C bonds far from the functional group is observed, which supports an initial "end-on" interaction with the -CN group. When a single ligand is attached to the metal, the resulting chemistry appears to be very different from that observed for the bare metal ion. The steric nature of the ligand effects is discussed. The observed ion/molecule reactions yield similar results to those suggested by collisional activation studies of transition metal ion/alkyl nitrile complexes.

I. Introduction

For almost fifteen years, reports have appeared in the literature concerning the rich chemistry that transition metal ions exhibit with organic molecules in the gas phase.[1] Such studies are begining to provide fundamental insights into the structure/function relationships of organometallic chemistry. For the prototypical reaction[2]

$$Co^+ + C_3H_7Cl \rightarrow CoC_3H_6^+ + HCl \qquad (1)$$

the proposed mechanism for formation of the observed products[2] involves a sequence of events. A metal insertion into the C-Cl bond is followed by a β-H shift to form the $(C_3H_6)Co^+(HCl)$ intermediate. This then dissociates in a competitive ligand loss step,[3-5] to yield the observed products.

As larger molecules were studied, an additional mechanistic step received attention - the complexation step in which the metal ion and the molecule form an adduct before the "chemistry" (bond cleavage and bond formation) begins. If this initial complex is sufficiently long lived, preferred geometries of the complex may be an important factor in determining the final product distributions - by determining which bonds in the molecule the metal ion can access.

We have discussed the chainlength effects in the reactions of Co^+ with alcohols and alkyl halides.[6] It appears that, if Co^+ first complexes with the polar group, and the chain is sufficiently long, parts of the molecule that are "remote" to the functional group can come into close proximity with the metal ion via 5- and 6-membered rings. These geometries allow for the attack of C-C and C-H bonds far

from the functional group. This approach has also been successful in explaining the collisional activation (CA) spectra of $Fe^+(A)$ complexes, where A is an alkyne[7] or nitrile,[8a-d] and may even explain the preference with which transition metal ions appear to attack skeletal bonds in saturated hydrocarbons.[9]

Consider this first step of reaction (1) in which Co^+ and propyl chloride form a complex. One might envisage two extremes concerning the interactions that would dominate in determining which geometries would be most favored. One extreme is an electrostatic interaction. If the Co^+/C_3H_7Cl interaction is dominated by electrostatics, characteristics of the molecule such as its dipole moment, charge distribution, and polarizability would control the situation. The other extreme would require a quantum-mechanical description of the complex. This would be the case if dative interactions ($Co^+ \Leftarrow :ClR$) were dominant. We have recently reported that the metal-ligand bonding in ionic species such as $ScCO^+$ and $CrCO^+$ is predominantly electrostatic in nature.[10] This has also been suggested[11,12] for $NiCO^+$ and $CuCO^+$. One would certainly expect a Dewar-Chatt type bonding scheme in these systems, and it does appear to occur in species such as Ni^oCO.[11] However, when the metal is charged, the total bond energy is dominated by the ion-dipole, ion-quadrupole, ion-octopole and ion-induced dipole interactions. Because of this, we are pursuing electrostatic models for these initially-formed metal ion/organic molecule complexes.[9,13]

In light of the chain length effects observed for the reactions of metal ions (M^+) with alcohols, alkyl halides and alkanes,[6] one might expect other functional groups to behave differently in their "directing ability" to parts of the molecule far from the functional group. One group of interest is the cyano group, -CN. This work is

the first report on bimolecular ion/molecule reactions of transition metal ions with alkyl nitriles; however, Schwarz et al. have reported a number of experiments in which collisional activation (CA) was performed on complexes generated from ion/molecule reactions involving transition metal-containing ions and alkyl nitriles[8a-d]. In their first report[8a], a mixture of $Fe(CO)_5$ and a nitrile, $C_nH_{2n+1}CN$ (n = 1-6) was introduced into the ion source of a mass spectrometer and subjected to electron impact. In their instrument (of "BEB" design), ions with the composition $[FeC_nH_{2n+1}CN]^+$ were selected for the collisional activation study. Such ions are formed by ligand-displacement reactions such as

$$Fe(CO)_m^+ + C_nH_{2n+1}CN \rightarrow FeC_nH_{2n+1}CN^+ + m\,CO$$

(where m = 0,1). These ions undergo 8 kV collisions with helium, and a mass spectrum of the fragment ions thus formed is obtained. Their discussion focussed on two dominant processes, in which the selected ion (M^+), once collisionally-activated, forms two species, $(M-H_2)^+$, and $(M-C_2H_4)^+$. In addition to loss of H_2 and ethylene, loss of other species (e.g., C_2H_5) occurred to yield minor CA products. It was proposed that the ions under study were complexes of Fe^+ with the intact nitrile, and that the metal ion initially complexes with the functional group in an "end-on" fashion. Since labelling studies suggested that H_2 and C_2H_4 elimination occurs from the same part of the alkyl chain, it was proposed that the losses of these two neutrals occur as competing processes, through a common intermediate of the type:

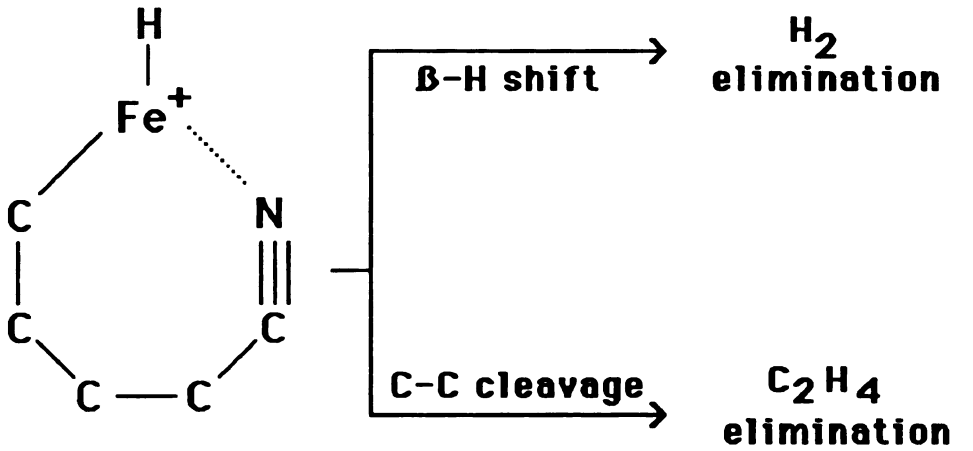

A second paper,[8b] which highlights the use of fast atom bombardment (FAB) to generate ions such as Fe^+ from an $FeSO_4$ target, showed that CA of analogous ions from larger nitriles leads to the loss of $C_{3,4}$ -containing neutrals to a greater extent than loss of ethylene. This was discussed in a subsequent paper, [8c] in which loss of H_2, alkenes and alkanes for larger nitriles is noted. For larger nitriles, loss of ethylene and hydrogen could not be considered as occurring via a common intermediate, since their origins appear to be different parts of the alkyl chain. Analogous experiments with other metal ions suggest that Co^+ has a "shorter reach", as reflected in alkane and alkene losses - the results for Co^+ were more consistent with a conventional metal insertion into C-C bonds / ß-H shift mechanism, while insertion into C-H bonds was presented as the first step in the chemistry of Fe^+.

Two possible explanations were cited regarding the "shorter reach" observation for Co^+ chemistry (relative to Fe^+). One possibility is that the M^+-NCR bond length is shorter for M = Co^+, than for M =

Fe^+. This would affect the intermediate ring sizes that would be accessible. (This explanation correlates with our results[10] on MCO^+ ions. The bond length order $r(Fe^+\text{-}CO) > r(Co^+\text{-}CO)$ reflects the fact that the ligand can get closer to Co^+ because it is smaller than Fe^+. In general, first row transition metal ions such as Co^+, Ni^+ and Cr^+ can get closer to a ligand than can Fe^+, because the former have only 3d-electrons in their valence shell, while Fe^+ has a 4s electron. The 4s orbital is more spatially extended than the 3d orbitals, resulting is size differences as a function of electronic configuration.) A second possibility may be related to back-bonding, which would affect the rigidity/geometry about the C-C-N···M^+ portion of the initially-formed intermediate. The role of the metal's donor/acceptor ability was pursued further.[8d] The possible distortion of the N-C-C bond to angles less than 180° due to a change in hybridization that would follow $d_\pi\text{-}\pi^*$ back-bonding was suggested. Results with a third transition metal ion, Ni^+, were similar to those presented for Co^+, leading to the proposal that back-bonding is least important for Fe^+ of the three metals studied. The back-bonding aspect may be related to metal-ligand bond lengths; those metals that can approach the molecule more closely may provide a situation in which improved orbital overlap for back-bonding occurs.

We present here the products of bimolecular ion/molecule reactions for a variety of transition metal ions with a series of nitriles. Reactions for several ligated metal ions are also reported. These results provide additional insights into the chemistry of metal centers with polar organic molecules containing one of the more complex ligands of organic chemistry.

II. Experimental Section

All experiments were performed on an ion cyclotron resonance (ICR) mass spectrometer that has been described elsewhere.[14] The instrument is of conventional design, and was used in the "drift mode". All samples were degassed by multiple freeze-pump-thaw cycles and were used without further purification.

Metal ions were made by electron impact on the corresponding metal carbonyls. $Co(CO)_3NO$ was used to form Co^+ and $CoCO^+$. $Ni(PF_3)_4$ was used to generate $NiPF_3^+$. The data presented here were derived from ICR spectra obtained using 1:1 mixtures (metal-compound:organic) at pressures up to 1.0×10^{-5} torr. From these, ion/molecule reaction products were identified, and their precursors determined using ion cyclotron double resonance methods. It should be noted that there are ion/molecule reaction products for which unique elemental compositions cannot be assigned. However, we believe that the reactions as listed in Tables 4-2 and 4-3 represent the chemistry that is occurring; they are self-consistent. Future plans of labeling experiments should provide further information on these complex systems.

Table 4-2

Reactions of Co^+ and $CoCO^+$ with Alkyl Nitriles

	n =	1	2	3	(3i)	4	5	6	7	8
$Co^+ + C_nH_{2n+1}CN \rightarrow$	$CoHCN^+ + C_3H_6$				.20					
	$CoC_3H_6^+ + HCN$				.07					
	$CoC_nH_{2n+1}CN^+$		1.0	.35	.73	.26	.18	.21	.22	.09
	$CoC_nH_{2n-1}CN^+ + H_2$					.41	.32	.11	.14	.04
	$CoC_{n-1}H_{2n-1}CN^+ + CH_2$							.10		
	$CoC_{n-1}H_{2n-3}CN^+ + CH_4$									.02
	$CoC_{n-2}H_{2n-3}CN^+ + C_2H_4$			.60		.11	.38	.17	.06	.05
	$CoC_{n-2}H_{2n-5}CN^+ + C_2H_6$							.07	.10	.12
	$CoC_{n-3}H_{2n-5}CN^+ + C_3H_6$					.22		.34	.21	.14
	$CoC_{n-3}H_{2n-7}CN^+ + C_3H_8$								.14	.18
	$CoC_{n-4}H_{2n-7}CN^+ + C_4H_8$						.12		.13	.24
	$CoC_{n-5}H_{2n-9}CN^+ + C_5H_{10}$									.12
	$CoC_{n-1}H_{2n-2}^+ + CH_3CN$			.05						
$CoCO^+ + C_nH_{2n+1}CN \rightarrow$	$CoCOC_nH_{2n+1}CN^+$	.24	.43	.85	.19	.12		.13	.10	
	$CoC_nH_{2n+1}CN^+ + CO$	.76	.57	.15	.81	.88	1.0	.64	.68	.43
	$CoC_nH_{2n-1}CN^+ + CO + H_2$							.18	.22	.23
	$CoC_{n-1}H_{2n-3}CN^+ + CO + CH_4$									.07
	$CoC_{n-2}H_{2n-3}CN^+ + CO + C_2H_4$									.16
	$CoC_{n-2}H_{2n-5}CN^+ + CO + C_2H_6$							.05		.11

Table 4-3

Reactions of M^+ and ML^+ with $C_6H_{13}CN$

$M^+ + C_6H_{13}CN \longrightarrow$	$M^+ =$	Fe^+	Co^+	Ni^+	Mn^+	Cr^+
$MC_6H_{13}CN^+$		.08	.21	.10	.80	1.0
$MC_6H_{11}CN^+ + H_2$		.21	.11	.15	.20	
$MC_6H_9CN^+ + 2H_2$		.11				
$MC_5H_{11}CN^+ + CH_2$			.10			
$MC_4H_9CN^+ + C_2H_4$		.38	.17	.29		
$MC_4H_7CN^+ + C_2H_6$			.07	.19		
$MC_3H_7CN^+ + C_3H_6$		.11	.34	.27		
$MC_5H_8^+ + CH_3CN + H_2$ and/or $MC_3H_6CN^+ + C_3H_7$		.11				

Reactions of ML^+ with $C_6H_{13}CN$

$ML^+ + C_6H_{13}CN \longrightarrow$	$ML^+ =$	$FeCO^+$	$CoCO^+$	$NiCO^+$	$NiPF_3^+$	$MnCO^+$	$CrCO^+$
$MLC_6H_{13}CN^+$			.13				
$MC_6H_{13}CN^+ + L$		.35	.64	.33	1.0	1.0	1.0
$MC_6H_{11}CN^+ + H_2 + L$		.65	.18	.15			
$MC_4H_9CN^+ + C_2H_4 + L$				.39			
$MC_4H_7CN^+ + C_2H_6 + L$			.05				
$MC_3H_7CN^+ + C_3H_6 + L$				.13			

III. Results and Discussion

Table 4-2 shows the ion/molecule reaction products observed from bimolecular reactions of Co^+ with $C_nH_{2n+1}CN$, for n = 1-8, and with 2-cyanopropane. Branching ratios indicating the product distributions are shown. A number of observations can be made on these data:

1. Co^+ apparently does not insert into the R-CN bond, except in the case of 2-cyanopropane. It is not suprising that this bond would <u>not</u> be attacked as easily as C-OH and C-Cl bonds, since it is the strongest of these bonds.[15] Also, more energy is required to eliminate HCN from RCN than is required to eliminate, e.g., HCl from RCl, as suggested in Table 4-4. Insertion into the C-CN bond in the branched nitrile may be favored since, in contrast to its straight chain analog, the branched compound should have a slightly lower C-CN bond energy.[16] Also, the insertion intermediate is expected to be somewhat more stable when the C_3H_7- on the metal is a secondary propyl group.

Table 4-4

Some Thermochemical Considerations (kcal/mol)

	X = Cl	OH	CN
D $(CH_3\text{-}X)$[15]	82	91	117
ΔH $(C_2H_5X \rightarrow C_2H_4 + HX)$[15]	17	11	33

Proton Affinities (PA) of Some Relevant Compounds[24]

L	PA(L), kcal/mol
H_2	101.3
CH_4	132.0
C_2H_4	162.6
CO	141.9
HCN	171.4
CH_3CN	188.4

2. In these reactions for $C_nH_{2n+1}CN$, the chemistry obviously changes as n increases. Dihydrogen elimination (following insertion into C-H bonds) does not occur for n<4; as n varies from 4 to 8, the importance of the H_2-elimination pathway decreases.

3. Attack of the terminal C-C bond is rarely observed, and is only a minor product for the largest nitrile studied here.

4. Many of the reaction products appear to be typical for mechanisms in which insertion into C-H and C-C bonds occurs. Insertion into various C-C bonds may lead to an intermediate of the type R'-Co^+-R"CN, where both R' and R"CN posess β-H atoms that can shift - thus elimination of ethylene or ethane, propene or propane, etc. is observed. We can interpret the data based on the metal insertion/β-H shift mechanism, however the chemistry could certainly be more complex. We cannot, for example, distinguish between loss of ethane and loss of {ethylene + H_2}. The patterns of losses of C_nH_{2n} vs. C_nH_{2n+2} we believe are consistent with a simple mechanism in which the C_nH_{2n+2} may be lost as an intact alkane. This has been proposed by Schwarz[8c] for the chemistry involving Co^+, while loss of C_nH_{2n+2} from Fe^+ reactions may in fact be {C_nH_{2n} + H_2} loss.

5. The reactions as listed follow the proton affinity rule,[3] consistent with retention of the more strongly bound ligand(s). Proton affinities for molecules representative of those types of species involved in the reactions are given in Table 4-4.

Table 4-3 shows, for contrast, the reaction products for a number of other metal ions with a selected nitrile, $C_6H_{13}CN$. As is typically observed, the Fe^+, Co^+ and Ni^+ ions each form a variety of products, many of which are common to all three metals. In terms of

attack of the skeletal bonds, it is interesting to note that ethylene loss dominates for Fe^+, propene loss dominates for Co^+, and the two processes occur with approximately equal probabilities for Ni^+. In contrast to these three metals, Mn^+ and Cr^+ are much less reactive, and do not appear to attack C-C bonds.

The M^+(RCN) Complex: The reactions reported here are best put into perspective by comparison with those observed for other polar organic compounds. First, a few comments are in order on the initial interaction between a transition metal ion and an alkyl nitrile. Schwarz et al.[8a] have discussed the side-on (**I**) and end-on coordination (**II**) possibilities for the -CN group, and suggest that the chemistry is consistent with an end-on

I **II**

description of the complex. (A similar geometry has been proposed for protonated molecules such as protonated HCN[17].) This same conclusion is reached if one considers the M^+-RCN complex to be electrostatically bound. If the molecular polarizability is described by the approximate bond-polarizability model, the C=N bond is more than twice as polarizable **along** the bond axis, as it is perpendicular to the internuclear axis.[18] Thus, a greater ion/induced dipole interaction energy would result in the end-on configuration. The charge distribution in an RCN molecule would also favor an end-on complex,[19] since the dipole moments of nitriles are large[19] (e.g., dipole moment of CH_3CN = 3.92 Debyes), with the nitrogen at the negative end of the dipole. Thus, it appears that the most stable

configuration of a transition metal ion/alkyl nitrile complex would posess a linear geometry about the C-C-N-M^+ atoms (based on consideration of features **of the functional group alone.**) This suggests another factor that prevents M^+ insertion into the C-CN bond - inaccessibility due to geometric restrictions.

For small nitriles such as acetonitrile, one may expect the end-on geometry (**II**) to dominate.

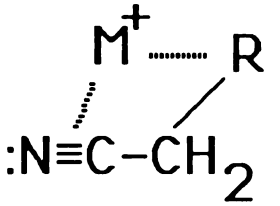

III

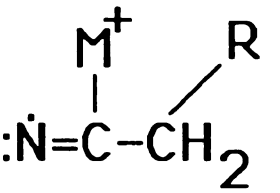

IV

However, for larger alkyl groups, the substantial polarizability of R- may make the geometry shown in **III** favored, bringing the metal ion to a position where it can form smaller ringed intermediates, not unlike those proposed for saturated polar compounds.[6,13]

A second possibility is that, upon complexation, sufficient energy is released to essentially promote the nitrile to a triplet state - converting the triple bond to a double bond, with the concurrent formation of an M-C or M-N σ-bond yielding a structure such as **IV**, again drastically changing the geometric relationship of the metal to the rest of the molecule. We note that, for the HCN molecule, the first triplet state ($^3A''$) is 4 eV above the ground state.[20] If this is typical for alkyl nitriles, the singlet-triplet gap may be prohibitively large for this mechanism to be operative.

The Chemistry of M^+: To discuss the implications of the possible interaction geometries about the nitrile group, it is useful to consider the skeletal bonds that are attacked, and the order of preference for which insertion appears to occur, based on the final product distributions. We have presented previously the approach used to determine the order of preference for insertion,[6] which is shown here for the $C_8H_{17}X$ compounds (X = CN, OH, Cl) for the Co^+ ion. A bond labeled (1) is that bond which, upon insertion, leads to the largest fraction of the observed products. The bond whose cleavage leads to the next most significant fraction of the products is labeled (2), etc.

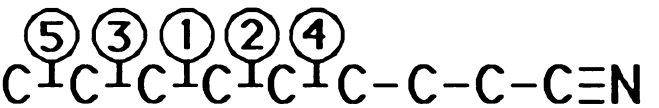

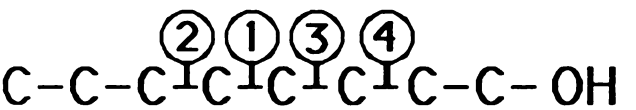

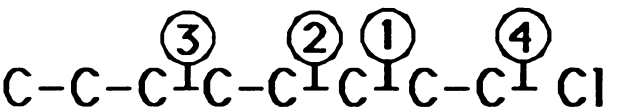

If one compares the products and their distributions for the nitriles and the corresponding alcohols and alkyl halides,[6] it is apparent that the skeletal bond which is cleaved to a greatest extent (labeled (1)) is farthest from the functional group in the nitrile cases, which would be expected from an end-on complexation model. Larger rings would be required to bring atoms of the alkyl group close to the metal. On the other hand, the effect is not that dramatic for the smaller nitriles. In fact, cleavage of many of the skeletal bonds would not be predicted if a fairly constrained end-on

complexation is maintained. There are some differences in reactivity unique to the nitriles when compared to other polar compounds, but not as dramatic as might be expected from the initial formation of the proposed end-on complex.

The data suggest that, while alkyl halides and alcohols may prefer to interact with parts of the alkyl group via 5- and 6-membered ring intermediates[6] such as (V) and (VI):

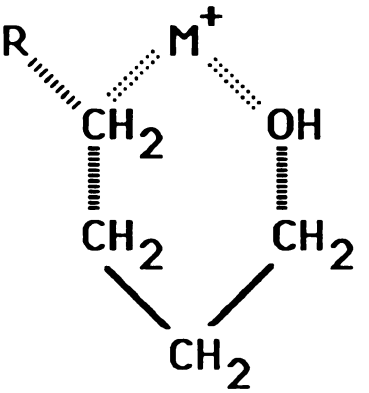

V

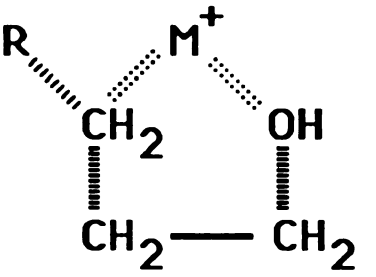

VI

Larger nitriles appear to preferentially utilize eight membered ring-intermediates. For example, the fact that H_2 elimination is observed only for nitriles with n=4 or larger may suggest that intermediate (VII) is important.

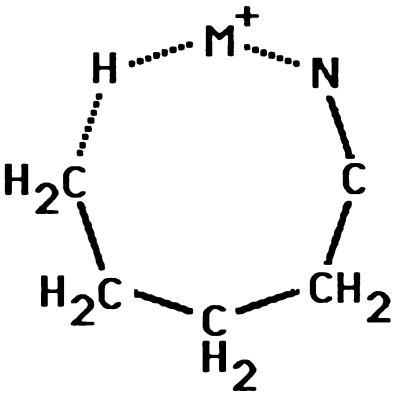

VII

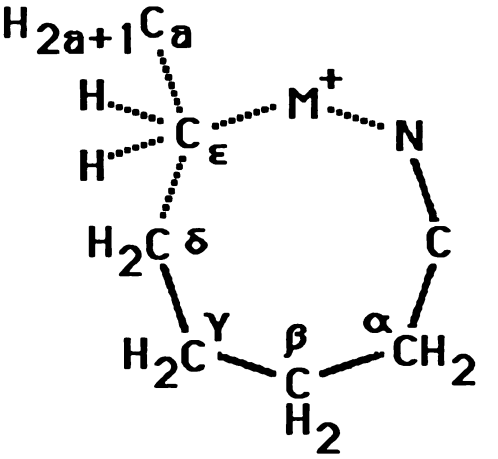

VIII

Intermediate **VIII** could explain why certain C-C and C-H bonds are most often cleaved. For example, structure **VIII** suggests that, via an 8-membered ring, the ε−C comes into close proximity to the metal, making the two C-C bonds that contain that ε−C candidates for insertion (as well as the ε-C-H bonds). Consider the data for $C_8H_{17}CN$ in Table I. Insertion via intermediate **VIII** into the C(δ)-C(ε) bond leads to loss of butene, which represents 24% of the total products; insertion into the C(ε)-C(ξ) bond leads to loss of propene and propane, which represent a total of 32% of the products formed. A similar analysis of the $C_7H_{15}CN$ data also suggests that intermediate **VIII** can account for a substantial fraction of the products formed (>50%). However, for the shorter chains, attack of C-C bonds closer to the functional group accounts for a substantial fraction of the products. Both (**VII**) and (**VIII**) involve eight membered rings. Thus, the end-on geometry is certainly influencing, but need not dominate the observed chemistry. Presumably a distribution of cyclic

intermediates of various ring sizes may be sampled by the metal, presenting a variety of "choices". Whether attack of a skeletal bond will follow or not depends on additional considerations, such as the subsequent thermodynamics of each insertion process.

Ligand Effects: Tables 4-2 and 4-3 show the effects of the addition of a carbonyl ligand to the metal center on the products formed, and their distributions. The effects are dramatic. What is typically considered to be a "ligand substitution" process

$$MCO^+ + RCN \rightarrow MRCN^+ + CO \qquad (2)$$

dominates. (For larger reactant molecules, the neutral loss corresponding to 28 u could also represent ethylene loss, with retention of the CO ligand - however the binding energy of ethylene to M^+ appears to be slightly larger than that for CO[4,21]) What is most obvious from Table I is that very little chemistry is **apparent** for $CoCO^+$ except with the largest nitriles. Attack of C-C bonds much farther out on the alkyl chain dominates when a CO is bound to the metal. The order in which skeletal bonds are preferred for insertion is dramatically altered. Only in the octyl nitrile is C-C cleavage evident - and then only involving the two skeletal bonds most distant from the functional group.

We propose two possible scenarios in which the CO could play a role leading to this dramatic change in product distributions for a metal center when this ligand is attached. Both are steric in nature. In the first case, the CO prevents the metal from getting close to the more interior C-C bonds, due to steric effects, shown schematically in **IX.**

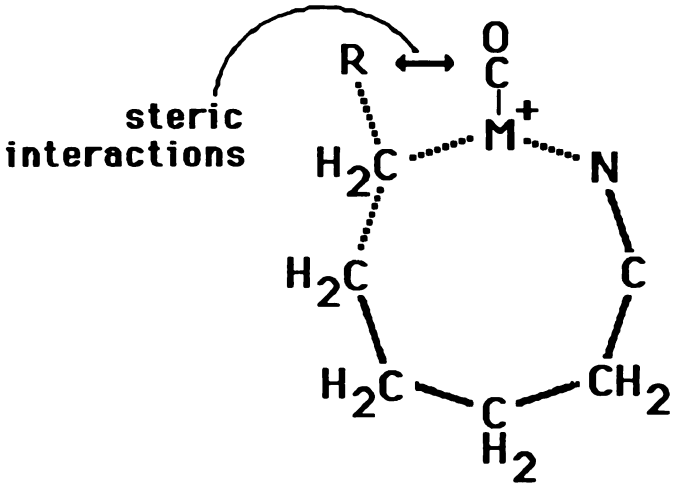

IX

In a second scenario, the CO does not interfere, allowing the metal to "sample" the same preferred complex geometries as it does when it is ligand-free. However, the relative stabilities of the insertion intermediates determine which bonds will actually be attacked. For example, in the case of hexyl cyanide, the Co^+ can apparently attack the central C-C bond to form the insertion intermediate:

$$C_3H_7 — Co^+ — C_3H_6CN$$

This intermediate must, then, be both geometrically and energetically accessible. However, when a CO is present, the analogous intermediate

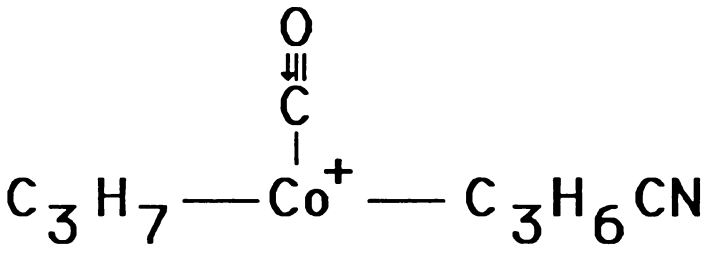

may be less stable due to interactions of the fairly large alkyl groups with the third ligand, CO. The most favored insertion intermediates might then become those in which one of the σ-bonded groups on the metal is relatively small (such as **H** or **CH3**), consistent with the reactions observed for $CoCO^+$ with octyl nitrile, and the data for the other MCO^+ ions in Table 4-3. Similar behavior has been observed in other systems. A dramatic example is in the chemistry of Ni^+, $NiCO^+$ and $NiPF_3^+$ with heptane.[22] Ni^+ inserts into a number of skeletal bonds in heptane, resulting in the elimination of C_2, C_3 and C_4-containing neutral molecules. Dihydrogen elimination is also observed. In contrast, $NiCO^+$ forms two products

$$NiCO^+ + n\text{-}C_7H_{16} \rightarrow NiC_7H_{16}^+ + CO \quad (3)$$

$$\rightarrow NiC_7H_{14}^+ + H_2 + CO \quad (4)$$

When the ligand is changed to PF_3, no chemistry at all is apparent, except for ligand substitution.

$$NiPF_3^+ + n\text{-}C_7H_{16} \rightarrow NiC_7H_{16}^+ + PF_3 \quad (5)$$

This would be the trend expected for the types of steric effects proposed, since the cone angle[23] for PF_3 , which reflects its relative size as a ligand, is larger than that for CO, suggesting that its steric effects would be more dramatic.

Relationship to Prior Work: Two points are to be made here. The first is that results presented here and elsewhere suggest that CA experiments may be difficult to interpret, and need not correlate with the analogous bimolecular ion/molecule reactions. The second point is that, while there need not be similarities between these very different experiments, they do provide similar results in the case of Co^+/RCN chemistry. Schwarz et al.[8a] suggest that these ions are formed by ion/molecule reactions of $FeCO^+$ and $Fe(CO)_2^+$, and the mechanism by which the ions are formed has "no implications for the chemistry of mass-selected $Fe(RCN)^+$ ions".[8a] The implication is that an apparent ligand substitution reaction is a literal ligand substitution, and that all of the chemistry occurs after the energetic collision with a neutral helium atom. Can it be assumed that reactions such as

$$FeCO^+ + A \rightarrow FeA^+ + CO \qquad (6)$$

leave A inteact? If not, what possible forms could FeA^+ have?

Such reactions cannot always be considered literally as ligand substitutions. The observation of such a reaction only indicates that all of the atoms of the neutral reactant are now associated with the metal ion. For small molecules such as methanol, it has been suggested[2] that such processes are not simple ligand displacements. Consider the following:

$$FeCO^+ + CH_3OH \rightarrow FeCH_3OH^+ + CO \qquad (7)$$

$$FeCH_3OH^+ + CH_3OH \rightarrow FeOHCH_3OH^+ + CH_3 \qquad (8)$$

This sequence of reactions has been interpreted as an indication that the product of reaction (7) has the form CH_3-Fe^+-OH, suggested by the subsequent reaction in which the CH_3 is displaced. Labeling experiments show that the methyl group lost in (8) originates exclusively from the ion, negating the occurrence of (8) through a symmetric intermediate involving two equivalent "methanol ligands" such as:

$$CH_3OH \text{ - - } Fe^+ \text{ - - } HOCH_3$$

Similar experiments[2] involving $MC_2H_5I^+$ ions formed by reaction of MCO^+ with ethyl iodide suggest that the ion exists, at least in part, as $M(C_2H_4)(HI)^+$. Thus, ligand substitution need not guarantee that the incoming molecule remains intact.

Ions of the type MCO^+ do react with organic molecules, and induce rearrangement to smaller molecules. This is known. Consider the molecule ABC, which can be converted into AC and B by a metal ion. If this also occurs for MCO^+, the complex that finally dissociates to yield the observed products is $M^+(CO)(AC)(B)$. The ligands that are lost are those with the lower metal-ligand binding energies. Frequently, the ligand lost is a small alkane - which would be expected since the alkane is a poorer base than the unsaturated molecule left behind, or CO. When MCO^+ reacts with an alkyl chloride, one may see loss of HCl with retention of CO, again consistent with the relative proton affinities of the molecules involved. However, it would also be appropriate in some cases for $M^+(CO)(AC)(B)$ to lose one ligand, CO. Thus, for larger ABC species, the ion current at an m/z corresponding to $MABC^+$ may contain a collection of structures such as $M^+(AC)(B)$.

Suppose MCO^+ reacts with a nitrile and inserts into a C-C bond forming the intermediate

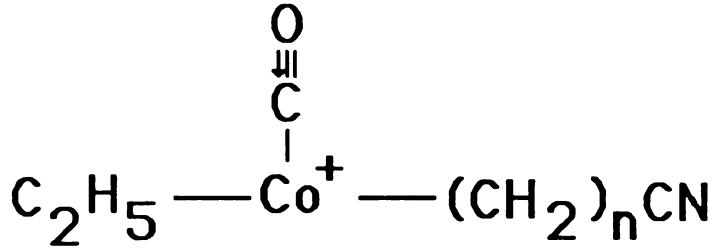

If $n \geq 2$, there are two groups from which a β-H may shift. These two possibilities yield two intermediates, $M^+(CO)(C_2H_4)(H(CH_2)_nCN)$ and $M^+(CO)(C_2H_6)(C_nH_{2n-1}CN)$. Based on proton affinities of these species, one might expect the former to lose ethylene or CO, while the latter would preferentially lose the alkane. Thus, the "ligand substitution" species $MC_{n+2}H_{2n+5}CN^+$ may take the form $M^+(C_2H_4)(H(CH_2)_nCN)$, but not $M^+(C_2H_6)(C_nH_{2n-1}CN)$. This may explain why collisional activation of some $[FeRCN]^+$ ions leads to loss of C_2H_4, but not loss of C_2H_6. The discussion of the Fe^+/CH_3OH system above may explain why CA spectra also show loss of C_2H_5. Thus, the question remains as to whether the energetic collision of a transition metal-containing ion such as $[MRCN]^+$ leads to a "collisional activation" or to a collision-induced dissociation. The collisional activation experiment need not directly parallel the reactivity of the bare metal ion with the neutral substrate, since the ion selected for study need not contain the intact organic molecule. This depends on the chemistry by which the selected ion is formed. If there are, indeed, ligand effects that alter the reactivity of MCO^+ relative to that for M^+, then the distribution of the various $MRCN^+$ geometries may not resemble the ion/molecule reaction products for M^+ with RCN. In fact, the combination of the ion/molecule reaction results and the CA data can provide interesting contrasts, and both are useful for understanding the observed chemistry. The minor

processes observed in the CA experiments (such as loss of C_2H_5) may provide more information than the dominant products, since such minor products are not formed in exothermic bimolecular processes.

While such possible complications should be expected, the results of CA^{8c} of $[CoRCN]^+$ ions are very similar to the chemistry presented here. There are, of course differences in product distributions, and in the observation of the least abundant products, however the correlations are substantial. For example, no reaction products were observed for Co^+ with CH_3CN and C_2H_5CN, and there was no evidence for chemistry between these species in the analogous CA experiments. In the case of C_3H_7CN, loss of C_2H_4 is observed in both experiments, however no loss of H_2 was observed in the ICR experiments. In the larger nitriles such as $C_6H_{13}CN$ and $C_7H_{15}CN$, it is interesting to note that loss of methane is reported from the CA experiments, but not in the ICR experiments. There are many reasons why this may occur. The ICR experiment may be less sensitive in detecting minor products. Also, the reaction may be slightly endothermic - but sufficient energy is available in the collisional-activation to allow it to occur. However, since the CA results parallel the ion/molecule reaction results presented here, ions of the type $[CoRCN]^+$ formed by ligand substitution processes are apparently simple adduct ions, with the RCN still intact to a great extent.

IV. Conclusions

The -CN group appears to have unique directing abilities in the reactions of transition metal ions with alkyl nitriles. An end-on geometry of the initially-formed complex appears to explain at least some of the reactivity that follows, in which atoms of the alkyl chain

far from the functional group are involved. When a CO is attached to the metal ion, the reactivity appears to change dramatically. This may be due to steric interactions at a number of points along the reaction coordinate. Before the "reactivity" of MCO^+ with alkyl nitriles can be evaluated, further work must be undertaken to determine the structure(s) of the various $MRCN^+$ product ions.

V. References

1. Allison, J. Prog. *Inorg. Chem.* **1986**, *34*, 627.
2. a) Allison,J.; D.P. Ridge, D.P. *J. Am. Chem. Soc.* **1976**, *98*, 7445; b) Allison, J.; Ridge, D.P. *J. Am. Chem. Soc.* **1979**, *101*, 4998.
3. Tsarbopoulos, A.; Allison, J. *Organometallics* **1984**, *3*, 86.
4. Weddle, G.H.; Allison, J.; Ridge, D.P. *J. Am. Chem. Soc.* **1977**, *99*, 105.
5. Foster, M.S.; Beauchamp, J.L. *J. Am. Chem. Soc.* **1975**, *97*, 4808.
6. Tsarbopoulos, A.; Allison, J. *J. Am. Chem. Soc.* **1985**, *107*, 5085.
7. Schulze, C.; Schwarz, H. *Chimia* **1987**, *41*, 29.
8. a) Lebrilla, C.B.; Schulze, C.; Schwarz, H. *J. Am. Chem. Soc.* **1987**, *109*, 98; b) Drewello, T.; Eckart, K.; Lebrilla, C.B.; Schwarz, H. *Int. J. Mass Spectrom. Ion Proc.* **1987**, *76*, R1 ; c) Lebrilla, C.B.; Drewello, T.; Schwarz, H. *J. Am. Chem. Soc.* **1987**, *109*, 5639; d) Lebrilla, C.B.; Drewello T.; Schwarz, H. *Int. J. Mass Spectrom. Ion Proc.* **1987**, *79*, 287.
9. Hankinson, D.J.; Allison, J. *J. Chem. Phys.* **1987**, *91*, 5307.
10. Allison, J.; Mavridis, A.; Harrison, J.F. *Polyhedron*, in press.
11. Bauschlicher, C.J., Jr. *J. Chem. Phys.* **1986**, *84*, 260.
12. Merchan, M.; Nebot-Gil, I.; Gonzalez-Luque, R.; Orti, E. J. *Chem. Phys.* **1987**, *87*, 1690.
13. Hankinson, D.J.; Hooper, E.J.; Allison, J. "Modeling the Electrostatic Interactions Between Transition Metal Ions and Polar Molecules"; Presented at the 35th ASMS Conference on Mass Spectrometry and Allied Topics, Denver, Colorado, May 24-29, 1987.
14. Radecki, B.D.; Allison, J. *J. Am. Chem. Soc.* **1984**, *106*, 946.
15. Thermodynamic information taken/derived from data in: a) Franklin, J.L.; Dillard, J.G.; Rosenstock, H.M.; Herron, J.T.; Draxl, K.;Field, F.H. Nat. Stand. Ref. Data Ser., Nat. Bur. Stand. **1969**, *26*.; b) Rosenstock, H.M.; Draxl, K.; Steiner, B.W.; Herron, J.T. J. Phys. Chem. Ref. Data **1977**, *6*, suppl.1.

16. Thermochemical data in ref. 15a shows this to be the general case, while the difference is not large. If

$$\Delta D = \{D(i\text{-}C_3H_7\text{--}X) - D(n\text{-}C_3H_7\text{ --}X)\},$$

the difference in C-X bond energies, typical values for Δ D are -2 kcal/mol for X = OH, -4.1 kcal/mol for X = NH_2, -3.8 kcal/mol for X = NO_2.

17. See, for example: a) DeFrees, D.J.; McLean, A.D. *J. Am.Chem. Soc.* **1985**, *107*, 4350; b) Pearson, P.K.; Schaefer, H.F., III *Astrophys. J.* **1974**, *192*, 33.
18. Denbigh, K.G. *Trans. Faraday Soc.* **1940**, *36*, 936.
19. Pople, J.A.; Gordon, M. *J. Am. Chem. Soc.* **1967**, *89*, 4253.
20. Ditchfield, R.; DelBene, J.; Pople, J.A. *J. Am. Chem. Soc.***1972**, *94*, 4806.
21. Hanratty, M.A.; Beauchamp, J.L.; Illies, A.J.; vanKoppen, P.; Bowers, M.T. *J. Am. Chem. Soc.* **1988**, *110*, 1.
22. a) Radecki, B.D. Ph.D. Thesis, Michigan State University, 1985; b) Radecki, B.D.; Allison, J. presented at the 33rd ASMS Conference on Mass Spectrometry and Allied Topics, San Diego, CA, May 26-31, 1985.
23. Tolman, C.A. *Chem. Rev.* **1977**, *77*, 313.
24. Lias, S.G.; Liebman, J.F.; Levin, R.D. J. Phys. Chem. Ref. Data,**1984**, *13*, 695-808.

Chapter 5

Reactions of Ni^+ and NiL^+ with aromatic compounds

Aromatic compounds show very interesting chemistry with metal ions. There are several reasons why aromatic compounds show good reactivity. The size of the molecules provides a large cross section for reaction. The aromatic ring for the most part does not participate in the reaction. The chemistry is simpler, with usually only one product being formed. In addition to these practical considerations, the chemistry of aromatic compounds in these reactions had been largely unexplored, except for a few isolated experiments. For these reasons we thought that aromatic compounds would be a good class of compounds to explore the role of ligands on the reactivity of metal ions.

Our observations on these reactions follow this introduction, in the form of a paper which has been submitted to the *Journal of the American Chemical Society*. The complete set of data compiled follows the copy of the paper, listed in Table 5-7. In addition to the reactions of aromatic compounds, the reactions of cyclopentanone, cyclohexanone, and dimethyl sulfoxide were also studied. These reactions are listed in Table 5-8. The results of these experiments will not be discussed.

While studying the reactions of different NiL^+, we observed that Ni^+ ions, produced by 70 eV electron ionization on the organometallic compounds $Ni(CO)_4$, $Ni(PF_3)_4$, and NiCpNO, have somewhat different reactivity. For example, Ni^+ produced from NiCpNO reacts with iodobenzene to form only the adduct $NiC_6H_5I^+$,

while Ni^+ produced from EI $Ni(CO)_4$ and $Ni(PF_3)_4$ reacts according to:

$$Ni^+ + C_6H_5I \rightarrow NiC_6H_4^+ + HI \quad (1)$$
$$\rightarrow NiC_6H_5^+ + I \quad (2)$$

The ratio of reaction 1 to 2 is 1:1 for Ni^+ produced from $Ni(CO)_4$ and 1:2 for Ni^+ produced from $Ni(PF_3)_4$.

In studies of half of the aromatic compounds (11 out of 22 cases studied) the Ni^+ ions from all three sources react identically. In general, the Ni^+ ions produced from $Ni(CO)_4$ and $Ni(PF_3)_4$ react very similarly, with slight differences in the branching ratios. However, Ni^+ from NiCpNO tends to form adducts more often than Ni^+ formed from the other two compounds. For example, Ni^+ made from NiCpNO forms the adduct with benzene, toluene, and aniline while Ni^+ from the other sources is unreactive. For nitrobenzene, ethylbenzene, benzylamine, acetophenone, and methyl benzoate, Ni^+ made from NiCpNO forms the adduct as well as the products that are formed from the other two Ni^+ ions. With benzyl alcohol, Ni^+ from NiCpNO forms one product, while Ni^+ from the other sources forms two. As stated above, Ni^+ made from NiCpNO forms only the adduct with iodobenzene, while the other Ni^+ ions form other products. In these reactions it seems that Ni^+ from NiCpNO is somewhat less reactive than the other two nickel ions. The one exception to this trend is phenol, in which Ni^+ from NiCpNO is unreactive, while the other two ions form the adduct.

For the reactions in Table 5-8 (reactions of DMSO, cyclopenatone, and cyclohexanone), the distinction between the different metal ions is not as clear. Comparison of the reactivity of Ni^+ from $Ni(CO)_4$ and $Ni(PF_3)_4$ with alkanes show that these ions can

at times exhibit different reactivity.

It seems possible that the Ni^+ ions formed by electron ionization are in different excited states. It has previously been reported that some portion of the Ni^+ ions produced from $Ni(CO)_4$ is in the excited state.[1] This was based on the observation of charge transfer between Ni^+ and $Ni(CO)_4$.

$$Ni^+ + Ni(CO)_4 \rightarrow Ni + Ni(CO)_4^+ \qquad (3)$$

The ionization potential of Ni is 7.63 eV, from spectroscopic experiments.[2] The ionization potential of $Ni(CO)_4$ is 8.35 eV. For reaction 3 to occur, Ni^+ must have 0.72 eV, or ~16 kcal/mol excess energy above the ground state.

Recently, Bowers has shown direct evidence for the existence of excited Ni^+ ions produced by EI on $Ni(CO)_4$.[3] In an experimental technique called high-resolution translational energy loss spectroscopy, mass selected ions are collided with a inert collision gas. Ions that are in the ground states can undergo inelastic collisions, and convert translational energy into electronic energy. Ions that are in excited states can undergo superelastic collisions, converting electronic energy into translational energy. In this experiment, Bowers was able to identify a peak 1.6 eV above the main peak for Ni^+. This was assigned as the ^2F excited state of Ni^+, derived from the $4s^1 3d^8$ configuration.

Unfortunately, data for ions produced from $Ni(PF_3)_4$ and NiCpNO have not been published at this time. Few labs are equipped to perform these experiments, due to the high resolution necessary. Another experimental technique that may be able to directly show the presence of excited states is electron ionization fluorescence (EIF). Very few labs are equipped to do this relatively simple

experiment, in which the visible spectrum produced by the electron ionization of molecules is recorded.

Excited states of the metal ion may play an important role in the reactions observed here, and this area will continue to be one of interest.

The Gas Phase Organometallic Chemistry of Ni^+, $NiCO^+$, $NiPF3^+$ and $NiC_5H_5^+$ With Aromatic Compounds: Chemical Consequences Due to the Presence of A Phenyl Group in the Organic Molecule, and Due to the Presence of a Ligand on the Metal

ABSTRACT

The gas phase chemistry of Ni^+ and the monoligated nickel cations $NiCO^+$, $NiPF_3^+$ and $NiC_5H_5^+$ with a series of aromatic compounds is reported here. The phenyl group is largely unreactive, and does not appear to prohibit the metal ion from interacting with other parts of these molecules. For some phenyl compounds, C_6H_5X, no reaction is observed for Ni^+. When Ni^+ does react, products such as $NiC_6H_4^+$ and $NiC_5H_5^+$ are formed - depending on the chemical composition of the attached functional group (-X). Ni^+ reacts with benzyl compounds by insertion into the $C_6H_5CH_2$–X bond, frequently followed by charge transfer to form $C_7H_7^+$ as a product. The Ni^+ ion is observed to decarbonylate aromatic carbonyl compounds. When a single ligand is attached to the Ni^+, changes in the chemistry are observed. In many cases, the reactivity decreases as the size of the ligand increases, suggesting the importance of steric interactions even for these monoligated species. There are some exceptions, where $NiC_5H_5^+$ is most reactive, even though the cyclopentadienyl ligand is the largest. It is suggested that some charge transfer may occur in $NiC_5H_5^+$, resulting in increased positive charge on the metal, leading to increased reactivity.

Introduction

The gas phase chemistry of transition metal ions with organic molecules has been extensively studied in recent years, using ion cyclotron resonance (ICR) and ion beam techniques. The reactions of metal and metal-containing ions have yielded fundamental insights into systems that activate bonds in organic molecules.[1] The organic molecules that have been studied include alkanes, as well as molecules that contain the basic structural features (straight chain, cyclic, branched) and functional groups of organic chemistry (halogens, alcohols, acids, esters, ketones, ethers, amines, nitro-compounds and nitriles). Some multifunctional compounds have also been studied.[2,3] The major reaction mechanisms have been discussed and reviewed.[1]

For small compounds such as alkyl halides (RX),[4] reaction products appear to be formed via a series of elementary steps. First, a transition metal ion such as Fe^+ inserts into the C-X bond to yield the intermediate R-Fe^+-X. If the R- group is an ethyl group or larger, a ß-H shifts to yield a complex of the form $(C_nH_{2n})Fe^+(HX)$. The complex dissociates in a competitive ligand loss step.[3] For more complex functional groups (e.g., carboxylic acids), insertion into bonds within the functional group can also be important.[5,6]

The role of the alkyl group in such reactions has been studied. The extent of <u>branching</u> can affect the overall reactivity. For example, ions such as Co^+ do not appear to insert into the C_3H_7-CN bond in n-propyl cyanide, but the insertion does occur for iso-propyl cyanide.[7] For straight chain polar organic compounds, the <u>length of the chain</u> is an important factor in determining the number and

types of products. For example, Co^+ reacts with ethanol by inserting into the C-OH bond, which leads to the ultimate products CoH_2O^+ and $CoC_2H_4^+$. Insertion into C-C or C-H bonds does not appear to occur.[4] However, the reaction products of the reaction of Co^+ with heptanol[8] suggest that insertion into the C-OH bond is a very minor pathway, compared to attack of C-C and C-H bonds in the alkyl group. Apparently, the metal may initially interact with the functional group, however parts of the alkyl group that are "remote" to the functional group may be brought into close proximity to the metal ion via cyclic intermediates - making a variety of C-C and C-H bonds candidates for insertion by the metal.

While extensive work has been performed on a variety of organic compounds, very little has been reported for aromatic molecules. The ϕ- group (cyclo-C_6H_5-) may behave much differently than other R- groups. Presented here is a survey of the reactions of Ni^+ with a variety of polar compounds that contain a phenyl group.

Several examples of the reactions of aromatic compounds with gas phase transition metal ions have been published. Corderman and Beauchamp[9] reported that $NiCp^+$ (Cp = cyclo-C_5H_5) decarbonylates a variety of carbonyl-containing compounds, reactions (1) and (2).

$$NiCp^+ + RCHO \rightarrow NiCpCO^+ + RH \quad (1)$$

$$\rightarrow NiCpRH^+ + CO \quad (2)$$

Decarbonylation was observed for a variety of aldehydes including benzaldehyde, to form benzene and CO.

In 1979, Dietz, Chatellier and Ridge[10] reported that Fe^+ can induce the dehydrohalogenation of halobenzenes, reaction (3).

$$Fe^+ + C_6H_5X \rightarrow FeC_6H_4^+ + HX \quad X = F,Cl,Br \qquad (3)$$

In the case of iodobenzene, the reactions (4) and (5) were observed:

$$Fe^+ + C_6H_5I \rightarrow FeC_6H_5^+ + I \ (85\%) \qquad (4)$$

$$\rightarrow FeI^+ + C_6H_5\cdot \ (15\%) \qquad (5)$$

Reactions (4) and (5) are analogous to those reported for Fe^+ with methyl iodide. Consideration of the reaction thermodynamics lead to the following proposed bond dissociation energies: $D(Fe^+\text{-}C_6H_4) > 66$ kcal/mol; $D(Fe^+\text{-}C_6H_5) > 64$ kcal/mol. The $FeC_6H_4^+$ may be an Fe^+-benzyne complex,[10] or may take the form of structure (I):

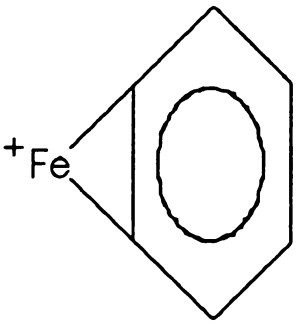

(I)

Recently, Chowdhury and Wilkins[11] reported the gas phase chemistry of Au^+ with benzene, toluene and ethylbenzene. Most of the products were due to hydride abstraction. (Note: the Au-H bond energy, 71 +/- 3 kcal/mol,[11] is greater than the Ni-H bond energy,[12] 60 kcal/mol). For example, Au^+ reacts with toluene by (6):

$$\phi\text{-}CH_3 + Au^+ \rightarrow C_7H_7^+ + AuH \quad (6)$$

It was determined that 90% of the ionic product was in the form of the benzyl cation, with the remaining 10% having a tropylium structure. In reactions such as (6), hydride stripping need not require insertion into a bond. This contrasts with reactions such as (7), which presumably proceeds[4] via an insertion intermediate, $C_3H_7\text{-}Ni^+\text{-}Cl$:

$$Ni^+ + C_3H_7Cl \rightarrow C_3H_7^+ + NiCl \quad (7)$$

Charge transfer following insertion may occur in (7). While the ionization energy of the isopropyl radical[13] (7.55 eV) is comparable to that for Ni (7.64 eV), the NiCl moiety has a much higher ionization energy, 11.4 eV[14]. Analogous processes may then be expected for compounds of the type ϕCH_2X, since the ionization energy of $\phi CH_2\cdot$ is 7.3 eV.

Based on our present understanding of gas phase organometallic ion/molecule reactions, would we expect aromatic compounds to react as their saturated alkyl analogs, or would we expect the phenyl group to dominate the initial interactions? Gas phase basicity data may provide some insights into this question. It has been noted that relative metal ion (M^+)-ligand interaction energies correlate with the ligand's proton affinity (P.A.).[15] Larger gas phase basicities indicate larger M^+-L interactions for simple π- and n-donor bases. Table 5-1 lists some relevant proton affinity data.[16] The basicities of functional groups, as indicated by small compounds such as acetaldehyde, ethanol, etc., are larger than that of benzene, suggesting that the presence of a phenyl group need not prohibit M^+ interactions with other parts of an aromatic molecule.

Table 5-1.

Some Relevant Proton Affinities[a]

Molecule	Proton Affinity (kcal/mol)
C_6H_6	181.3
CH_3CHO	186.6
C_2H_5OH	188.3
CH_3COOH	190.2
$(CH_3)_2O$	192.1
CH_3NO_2	192.5
$(CH_3)_2CO$	196.7
CH_3NH_2	214.1
ϕCH_3	189.3
ϕNO_2	193.4
ϕCHO	200.2
ϕOCH_3	200.3
ϕNH_2	209.5
ϕCH_2NH_2	216.8

a. Data obtained from ref. 16.

Reported here is the observed chemistry of Ni^+ with a series of aromatic compounds (phenyl- and benzyl- compounds) containing a variety of functional groups. These results provide a framework with which the behavior of the phenyl group may be put into perspective, relative to other C_nH_m- groups such as alkyl groups. In most cases, the phenyl group is unreactive, but affects the thermochemistry of the system through inductive effects, as will be discussed.

Also, the reactions of three ligated nickel ions, $NiCO^+$, $NiPF_3^+$ and $NiCp^+$ with the same aromatic compounds are presented. Changes in reactivity due to the presence of the various ligands reflect a number of chemical aspects of the ligands; the most important feature appears to be size (steric effects).

Experimental Section

All experiments were performed on an ion cyclotron resonance (ICR) mass spectrometer of conventional design which was constructed at Michigan State University and has been described elsewhere.[17] The ICR cell has been modified from a square to rectangluar cross-section (0.5 in. x 0.75 in.). All experiments were performed in drift mode. Mass spectra were obtained with a frequency-swept detector that was designed, built, and installed by Dr. John Wronka, and has been described elsewhere.[18] Data were obtained by scanning the frequency swept detector over the range of frequencies necessary to produce a spectrum, with the magnetic field of the Varian V-7800 electromagnet held constant at 16 kG. The aromatic compound and organometallic compound were admitted to the cell in approximately a 1:1 ratio, to a total pressure of 6×10^{-6}

torr. Typically, eleven mass spectra were signal averaged to improve the signal-to-noise ratio. Data were collected with a MacADIOS® data acquisition system (GW Instruments, Cambridge, MA) using a MacIntosh Plus® computer. The data acquisition program was written in Microsoft® BASIC. After a single resonance mass spectrum was acquired, a second, fixed frequency oscillator (tuned to the frequency of a reactant ion) is turned on. The irradiated ion is thus ejected from the source region of the cell, and another mass spectrum of the reaction mixture is acquired. Any ions in the spectrum that were products resulting from the reaction of the irradiated ion would not appear in the second spectrum. The spectrum acquired with the double resonance oscillator on is then subtracted from that obtained with the double resonance oscillator off. This difference spectrum consists of all ion/molecule reaction products of the irradiated ion. Double resonance spectra were obtained for all ions of interest in this way.

All chemicals used in this work were high purity commercial samples which were used as supplied, except for the liquid samples which were subjected to multiple freeze-pump-thaw cycles to remove non-condensable gases. Butylbenzene, benzyl bromide, benzyl chloride, benzylamine, and phenylacetaldehyde were obtained from Aldrich Chemical Co. Benzonitrile, acetophenone, phenol, and benzoyl chloride were obtained from Baker Chemical Co. Bromobenzene, chlorobenzene, nitrobenzene, benzaldehyde, benzoic acid, and benzyl alcohol were obtained from Fisher Scientific. Benzene and benzophenone were obtained from E. M. Science. Methyl benzyl alcohol was obtained from Eastman Organic Chemicals. Iodobenzene was obtained from Chem Service. Toluene, aniline, anisole, and ethylbenzene was obtained from Matheson, Coleman, and Bell. Nickel tetracarbonyl and tetrakis (trifluorophosphine)

nickel were obtained from Alfa Inorganics. Cyclopentadienyl nickel nitrosyl was obtained from Strem Chemicals.

Results and Discussion

The compounds that have been studied are divided up into three groups. The reactions of Ni^+ with the phenyl compounds are listed in Table 5-2. The reactions of Ni^+ with the phenyl compounds are listed in Table 5-3. Table 5-4 contains the results for aromatic carbonyl compounds. These tables contain a variety of thermochemical data[19] that are useful in understanding the observed chemistry.

We will first consider the reactant molecules in Table 5-2, the simple ϕ-X molecules. Similar to the reactions reported[10] for Fe^+, we do observe the formation of an $M^+C_6H_4$ product in some cases:

$$Ni^+ + C_6H_5X \rightarrow NiC_6H_4^+ + HX, \quad X = Br, I \qquad (8)$$

To form the HX product, a C-X and a C-H bond must be cleaved. Presumably the reaction proceeds by initial insertion into the C-X bond, rather than into the C-H bond, since the former is weaker. The reaction is not observed when X = H, Cl, CN, OH, NH_2, OCH_3 and NO_2. The $X=OCH_3$ and NO_2 cases will be discussed separately. In general, the reaction analogous to (8) is not observed when the ϕ-X bond is strong, and when $\Delta H_{rxn.}(\phi X \rightarrow C_6H_4 + HX)$ is relatively high. When this reaction product is not observed, it may be because the initial insertion is thermodynamically prohibited, or that the overall reaction is endothermic. In the case of ϕNH_2 the barrier may be in the insertion step, since Ni^+ has not been observed to insert into the C-N bond of primary amines.[17] Since the overall reaction for X=Cl would be exothermic (based on the energetics of the process for X = Br), we may conclude that the initial insertion does not occur.

Table 5-2

Reactions of Ni^+ with Phenyl Compounds

X =	PRODUCTS	D(ϕ-X)[a]	D(ϕCH$_2$-R)[a]	Relevant Thermochemistry, ΔH[a]		
H	No Reaction Observed	104	--	ϕH	→ $C_6H_4 + H_2$	80
Cl	No Reaction Observed	88	--	ϕCl	→ $C_6H_4 + HCl$	65
Br	$NiC_6H_4^+ + HBr$	75	--	ϕBr	→ $C_6H_4 + HBr$	67
I	$NiC_6H_4^+ + HI$ (45%)	61	--	ϕI	→ $C_6H_4 + HI$	57
	$NiC_6H_5^+ + I$ (55%)					
CN	No Reaction Observed	119	--	ϕCN	→ $C_6H_4 + HCN$	79
OH	No Reaction Observed	104	b	ϕOH	→ $C_6H_4 + H_2O$	65
OCH_3	$Ni\phi H^+ + CH_2O$	88	c	ϕOCH_3	→ $\phi H + CH_2O$	8
					→ $C_6H_4 + CH_3OH$	69
NH_2	No Reaction Observed	88	d	ϕNH_2	→ $C_6H_4 + NH_3$	64
NO_2	$NiC_5H_5^+ + CO + NO$ (84%)	65	--	ϕNO_2	→ $C_5H_5 + CO + NO$	41
	$NiC_6H_5O^+ + NO$ (16%)				→ $C_6H_5O + NO$	18

a. all thermochemical information in kcal/mol. b. D(ϕO-H) = 87 kcal/mol

c. D(ϕO-CH_3) = 60 kcal/mol d. D(ϕNH-H) = 82 kcal/mol

We note that, in the context of typical gas phase organometallic ion/molecule reactions that have been observed, reaction (8) is certainly unusual. In reaction (9), 19 kcal/mol is required to convert ethyl bromide to ethylene and HBr,

$$Ni^+ + C_2H_5Br \rightarrow NiC_2H_4^+ + HBr \qquad (9)$$

thus the reaction will be exothermic if the Ni^+-ethylene bond is stronger than 19 kcal/mol, which it surely is. In contrast, 67 kcal/mol are required to convert ϕBr to benzyne (C_6H_4) and HBr. The reaction is observed only because the binding energy in the $NiC_6H_4^+$ product is greater than 67 kcal/mol. This substantial bond energy may reflect sigma (M-C) bond formation in the product.

Very different reactions are observed for ϕOCH_3 and ϕNO_2. In the case of ϕOCH_3, insertion into the ϕ-O bond appears to occur, to give the ϕ-Ni^+-OCH_3 intermediate. This is the first case where both groups on the metal have ß-H atoms that can shift. Since the products {benzene and formaldehyde} are more stable than {benzyne and methanol} by 61 kcal/mol, the lower energy pathway available here is selected, and the shift of a H atom <u>from</u> the methoxy group dominates the chemistry.

The reactions of ϕNO_2 are very different from the other reactions reported, however nitroalkanes also exhibit chemistry with transition metal ions that is much different than that observed for alcohols and alkyl halides. In 1984, Cassady, Freiser, McElvany and Allison reported the reactions of Co^+ with as series of nitroalkanes.[6] In addition to reactions that proceed via insertion into the C-NO_2, C-H

and C-C bonds, additional intermediates were apparently formed such as RO-Co^+-NO. Mechanisms were suggested that would allow for access of such an intermediate.[6] In light of this, it is not surprising that NO elimination from ϕNO_2 was observed. However the major product is $C_5H_5Ni^+$, with loss of NO and CO. We propose that the products are formed in the sequence shown in reaction (10).

$$Ni^+ + \phi NO_2 \rightarrow \phi O\text{-}Ni^+\text{-}NO \xrightarrow{-NO} \phi O\text{-}Ni^+ \xrightarrow{-CO} C_5H_5Ni^+ \qquad (10)$$

We note that the C_6H_5O group has the same skeletal structure as a cyclic ketone, similar to cyclohexanone. The energy required to convert $C_6H_5O\cdot$ to $C_5H_5\cdot$ and CO, 23.2 kcal/mol, is similar to that required to decarbonylate cyclohexanone to 1-pentene and CO, 22.7 kcal/mol.

Finally we note that, for X = OH, OCH_3 and NH_2, the possibility exists for insertion into bonds in the functional group (as we see in ϕNO_2). While an insertion process such as reaction (11) for phenol

$$\phi OH + Ni^+ \rightarrow \quad \phi O\text{-}Ni^+\text{-}H \qquad (11)$$

may occur, there is no ß-H available to shift, and the only option for this intermediate may be to convert back into reactants.

The discussion will now move to the molecules in Table 5-3, the benzyl-compounds. In the chemistry with these molecules, insertion into the ϕ-X bond is not observed, but rather insertion into the ϕCH_2-R bond dominates, reflecting the relative weakness of this bond. This is graphically seen in variations of the C-C bond energies in n-butyl benzene. The ϕ-C bond is more than 30 kcal/mol stronger than the ϕCH_2-C bond!

Table 5-3

Reactions of Benzyl Compounds

X =	PRODUCTS	D(ϕ-X)[a]	D(ϕCH$_2$-R)[a]	Relevant Thermochemistry, ΔH[a]		
CH_3	No Reaction Observed	93	78	ϕCH_3	$\rightarrow C_6H_4 + CH_4$	70
CH_2Cl	$C_7H_7^+ + NiCl$	94	60	implication: D(Ni-Cl) > 56		
CH_2Br	$C_7H_7^+ + NiBr$	99	45	ϕCH_2Br	$\rightarrow C_6H_4 + CH_3Br$	73
				implication: D(Ni-Br) > 42		
CH_2OH	$C_7H_7^+ + NiOH$ (75%)	91	72	implication: D(Ni-OH) > 72		
	$Ni\phi CHO^+ + H_2$ (25%)			ϕCH_2OH	$\rightarrow \phi CHO + H_2$	15
					$\rightarrow \phi H + CH_2O$	17
CH_2NH_2	$Ni\phi CHNH^+ + H_2$	89	59			
CH_2CH_3	$Ni\phi CHCH_2^+ + H_2$	90	63	ϕC_2H_5	$\rightarrow \phi CHCH_2 + H_2$	30
					$\rightarrow C_6H_4 + C_2H_6$	73
$CH(OH)CH_3$	$Ni\phi CH_3^+ + CH_2O$ (69%)	88	81	$\phi CHOHCH_3$	$\rightarrow \phi CH_3 + CH_2O$	18
	$Ni\phi CHCH_2^+ + H_2O$ (31%)				$\rightarrow \phi C_2H_3 + H_2O$	13

Table 5-3, continued

X =	PRODUCTS	D(ϕ-X)[a]	D(ϕCH$_2$-R)[a]	Relevant Thermochemistry, ΔH[a]		
$(CH_2)_3CH_3$	$Ni\phi CH_3^+ + C_3H_6$	94	63	ϕbu	$\rightarrow \phi CH_3 + C_3H_6$	20
					$\rightarrow \phi H + C_4H_8$	23
					$\rightarrow \phi C_2H_5 + C_2H_4$	23
c-C_6H_5	No Reaction Observed	105	--	ϕϕ	$\rightarrow C_6H_4 + \phi H$	80

This correlates with the observation that only loss of propene is observed, although when Ni^+ reacts with n-butane, ethane loss and H_2 loss is observed. For benzyl chloride, bromide and benzyl alcohol, the only or major product is $C_7H_7^+$. (Thermodynamic discussions[19] will assume that the product is the benzyl cation). As indicated in the Introduction, such reactions are reasonable since the relative ionization energies predict charge transfer to the C_7H_7 moiety, and the strength of the bond in the neutral that is formed is substantial. Listed in Table 5-2 are the lower limits on various Ni-X bonds that are implied by assuming that the observed reactions are exothermic or thermoneutral. These are consistent with reported bond energies[21]: D(Ni-Cl) = 88 kcal/mol, D(Ni-Br) = 85 kcal/mol . Also, the relatively weak Ni-H bond,[12] 60 kcal/mol, would make the analogous reaction endothermic for toluene.

When X- in ϕ-X has at least 2 skeletal atoms, and both have one or more H atoms on them, H_2 elimination is observed. This suggests that a site of unsaturation is formed in the -X group - i.e., ethyl benzene is converted to styrene, benzyl alcohol becomes benzaldehyde, etc. Presumably, the benzyl C-H bond is the initial site of insertion in these cases.

Unexpected products are observed in the case of methyl benzyl alcohol. Water loss is observed, as is typical for aliphatic alcohols, indicative of insertion into the C-OH bond. An unexpected process is elimination of formaldehyde. One could conceive of elimination of CH_2O via either an initial insertion into the ϕ-C bond or the C-CH_3 bond, as shown in Scheme 5-1:

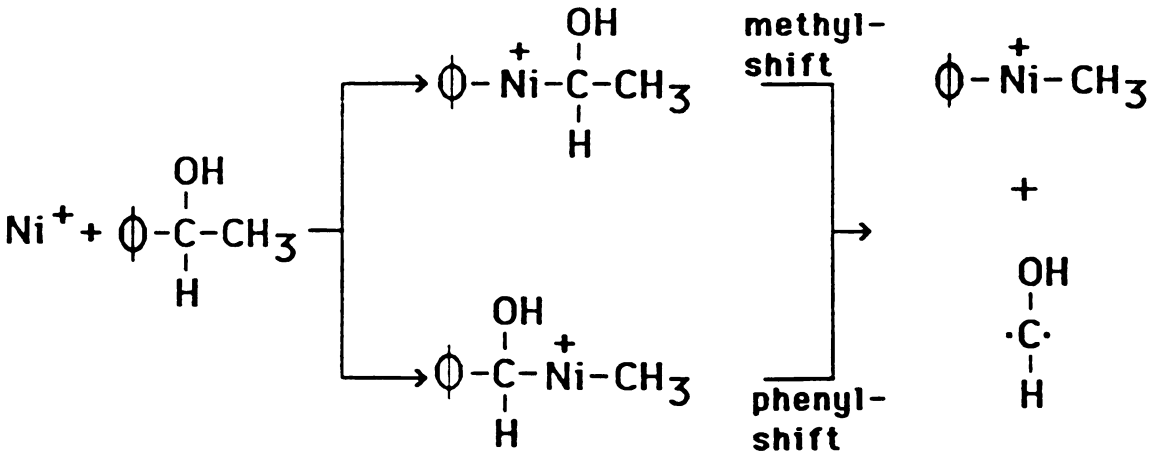

Scheme 5-1

Unfortunately, the possible insertions, followed by a methyl or phenyl shift, yields a diradical, not formaldehyde. An alternative mechanism would involve loss of H_2 first, followed by loss of CO. It has been reported that Ni^+ will induce the elimination of H_2 from alcohols, presumably via insertion into the O-H bond.[4] More importantly, we report it here for benzyl alcohol. Elimination of H_2 yields the corresponding carbonyl-compound as $Ni(\phi(CO)CH_3)^+$. As will be discussed shortly (Table 5-4), Ni^+ does decarbonylate acetophenone - thus we suggest a two step pathway, with the neutral product(s) being $\{H_2 + CO\}$, not CH_2O. This is also supported by the NiL^+ reactions that will be discussed in following sections.

The reactions of Ni^+ with a series of aromatic carbonyl compounds are listed in Table 5-4. For all of the compounds except benzoyl chloride, decarbonylation is observed. A number of reports have appeared concerning the chemistry of transition metal ions with carbonyl compounds.[5,22,23] The 1976 Corderman and Beauchamp publication was cited earlier.[9] It is interesting to note that, while $CpNi^+$ was observed to decarbonylate molecules such as CH_3CHO, the analogous reaction was not observed for acetyl chloride and bromide.[9] Freiser et al.[22,24] have studied the chemistry of Cu^+ and Fe^+ with ketones. Also, cyclic ketones were used in a number of publications since Fe^+ appears to form a metallacycle upon decarbonylation.[22,23,25,26] In 1984, Halle, Crowe, Armentrout and Beauchamp[23] reported the chemistry of M^+ with several ketones and aldehydes. They suggest that, in ketones, $R_1(CO)R_2$, transition metal ions appear to insert into both R_i-C bonds. However, in molecules such as aldehydes, insertion into the C-CO bond is favored over insertion into the C-H bond as an initial mechanistic step.

We note that reactions similar to reaction (8) for carbonyl compounds, such as reaction (12),

$$Ni^+ + \phi\text{-}C(O)H \quad \rightarrow \quad NiC_6H_4^+ + CH_2O \qquad (12)$$

are <u>not</u> observed. Relatively large amounts of energy are required. For the above reaction to be exothermic, the Ni^+-C_6H_4 bond energy would have to be greater than 82 kcal/mol. Thus, such pathways are thermodynamically prohibited in these compounds. In comparison, decarbonylation requires little energy. We also note that, for benzoic acid and methyl benzoate, CO_2 elimination is a thermodynamically favored process, but does not occur. For aliphatic organic acids, CO_2

Table 5-4

Reactions of Ni^+ with Aromatic Carbonyl Compounds

X ≡	PRODUCTS	D(ϕ-X)	D(ϕ(CO)-R)	Relevant Thermochemistry, ΔH		
(CO)H	$Ni\phi H^+ + CO$	78	89	ϕCHO	$\rightarrow \phi H + CO$	4
					$\rightarrow C_6H_4 + CH_2O$	82
$(CO)CH_3$	$Ni\phi CH_3^+ + CO$	91	82	$\phi COCH_3$	$\rightarrow \phi CH_3 + CO$	9
(CO)OH	$Ni\phi OH^+ + CO$	105	108	ϕCOOH	$\rightarrow \phi OH + CO$	23
					$\rightarrow \phi H + CO_2$	- 2
$(CO)OCH_3$	$Ni\phi OCH_3^+ + CO$	103	97	ϕCO_2CH_3	$\rightarrow \phi OCH_3 + CO$	29
					$\rightarrow \phi CH_3 + CO_2$	-10
(CO)ϕ	$Ni(\phi)_2^+ + CO$	86	86	ϕCOϕ	$\rightarrow \phi\phi + CO$	1
					$\rightarrow C_6H_4 + \phi CHO$	77
(CO)Cl	No Reaction Observed	91	84	ϕCOCl	$\rightarrow \phi Cl + CO$	15
$CH_2(CO)H$	$Ni\phi CH_3^+ + CO$	89	a	ϕCH_2CHO	$\rightarrow \phi CH_3 + CO$	2

a. $D(\phi CH_2\text{-}CHO)$ = 50 kcal/mol; $D(\phi CH_2C(O)\text{-}H)$ = 86 kcal/mol.

elimination is not observed,[5] so failure to observe the reaction is not related to the presence of the aromatic group here. Consider the case of benzoic acid. The decarbonylation may occur via the $\phi(CO)$-Ni^+-OH intermediate, and would require a ϕ-shift. If insertion lead to an intermediate of the form ϕ-Ni^+-COOH, the geometry about the acid group, due to the sp^2 hybridization of the carbonyl C may place the H too far from the metal for a H shift to occur. However, an OH shift may occur, again leading to decarbonylation.

In decarbonylation reactions, when both bonds to the carbonyl group are cleaved, it would be difficult to suggest whether one bond is attacked preferentially in the initial step. The bond energies in Table 5-3 suggest that either would be possible. In the case of benzoic acid, insertion into the C-OH bond may be favored, due to preferred initial interactions such as those shown in structure (II):

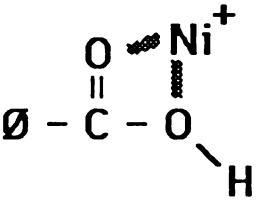

(II)

In the case of $\phi CH_2(CO)H$, the very weak ϕCH_2-C bond is presumably the site of attack to form ϕCH_2-Ni^+-(CO)H; a H shift leads to decarbonylation.

The results presented in Tables 5-2, 5-3, and 5-4 provide a good understanding of how a phenyl group behaves in these gas phase ion/molecule reactions. In most cases, it behaves as an unreactive "terminal" group such as H- or CH_3-. Actually the bond energies

place it between the two, e.g., $D(H\text{-}CH_3) > D(\phi\text{-}CH_3) > D(CH_3\text{-}CH_3)$.

While an H can be removed from a ϕ- group such as in the ϕ-I reaction, this certainly does not suggest that ϕ- behaves as an alkyl group such as an ethyl group. In fact the energy required to eliminate HI from methyl iodide is closer to that for ϕ-I than it is for C_2H_5I. What we have seen as the major influence of the phenyl group is in its inductive effects, substantially weakening neighboring bonds - as seen in the benzyl compounds. We suggest that this effect may be very useful. Since the phenyl ring does not hamper access of the metal ion to other parts of the molecule, one may be able to add a phenyl group to various positions on an alkyl chain, create "unusually" weak bonds, and determine how such thermodynamic variations of the molecule affect the chemical reactivity.

The gas phase chemistry of NiL^+ (L = CO, PF_3, Cp) with aromatic compounds: The observed chemistry of $NiCO^+$, $NiPF_3^+$ and $NiCp^+$ with the aromatic compounds that are the focus of this work, is summarized in Table 5-5. First, a few comments are in order on these ligands, and how their presence may affect the chemistry of the metal ion in these gas phase reactions.

$NiCO^+$: Of the ligands studied in such gas phase ion/molecule reactions to date, CO has been among the most popular, since volatile transition metal carbonyl compounds are readily accessible for mass spectrometric studies.[1,4,15,27] Recent theoretical calculations suggest that, while the bonding in neutral MCO species (where M is a first row transition metal) may be described by a Dewar-Chatt type interaction, this is not the case for the analogous cation. In MCO^+ the metal-ligand bonding is essentially electrostatic in nature.[28,29]

Table 5-5

Reactions of mono-ligated Ni^+ with aromatic compounds

	PRODUCTS		
NiL^+ =	$NiCO^+$	$NiPF_3^+$	$NiCp^+$
P Phenyl-X			
ϕ-H	$NiP^+ + L$	$NiP^+ + L$	$NiLP^+$
ϕ-Cl	$NiP^+ + L$	$NiP^+ + L$	$NiLC_6H_4^+ + HCl$
ϕ-Br	$NiP^+ + L$	$NiP^+ + L$	$NiLC_6H_4^+ + HBr$
ϕ-I	$NiP^+ + L$	No Reaction	$NiLC_6H_4^+ + HI$
ϕ-CN	$NiP^+ + L$	$NiP^+ + L$	No Reaction
ϕ-OH	$NiP^+ + L$	$NiP^+ + L$	No Reaction
ϕ-OCH_3	$Ni\phi H^+ + CH_2O + L$ (17%) $NiP^+ + L$ (60%) $NiLP^+$ (23%)	$NiP^+ + L$	$NiLP^+$
ϕ-NH_2	$NiP^+ + L$	$NiP^+ + L$	No Reaction
ϕ-NO_2	$NiP^+ + L$ (72%) $NiLP^+$ (28%)	$NiP^+ + L$	$NiLP^+$

Table 5-5 , continued

NiL^+ =	PRODUCTS $NiCO^+$	$NiPF_3^+$	$NiCp^+$
Benzyl-X			
ϕ-CH_3	$NiP^+ + L$	$NiP^+ + L$	$NiLP^+$
ϕ-CH_2Cl	No Reaction	$C_7H_7^+ + NiCl(L)$	$C_7H_7^+ + NiCl(L)$
ϕ-CH_2Br	$C_7H_7^+ + NiBr(L)$	$C_7H_7^+ + NiBr(L)$ (80%)	No Reaction
		$NiP^+ + L$ (20%)	
ϕ-CH_2OH	$Ni\phi CHO^+ + H_2 + L$ (37%)	$Ni\phi CHO^+ + H_2 + L$ (22%)	No Reaction
	$NiP^+ + L$ (63%)	$NiP^+ + L$ (78%)	
ϕ-CH_2NH_2	$Ni\phi CHNH^+ + H_2 + L$ (68%)	$Ni\phi CHNH^+ + H_2 + L$ (31%)	$NiL\phi CHNH^+ + H_2$ (58%)
	$NiP^+ + L$ (32%)	$NiP^+ + L$ (69%)	$NiL\phi CN^+ + 2\ H_2$ (42%)
ϕ-CH_2CH_3	$Ni\phi CHCH_2^+ + H_2 + L$ (41%)	$NiP^+ + L$	No Reaction
	$NiP^+ + L$ (59%)		
ϕ-$CH(OH)CH_3$	$Ni\phi COCH_3^+ + H_2 + L$	$Ni\phi CHCH_2^+ + H_2O + L$ (70%)	$NiL\phi CHCH_2^+ + H_2O$
		$Ni\phi COCH_3^+ + H_2 + L$ (30%)	
ϕ-$(CH_2)_3CH_3$	$Ni\phi CH_3^+ + C_3H_6 + L$ (44%)	$NiP^+ + L$	No Reaction
	$NiP^+ + L$ (56%)		

Table 5-5 , continued

	PRODUCTS		
NiL^+ =	$NiCO^+$	$NiPF_3^+$	$NiCp^+$
Aromatic Carbonyls			
$\phi(CO)H$	$Ni\phi H^+ + CO + L$ (29%) $NiP^+ + L$ (71%)	$NiP^+ + L$	$NiL\phi H^+ + CO$
$\phi(CO)CH_3$	$Ni\phi CH_3^+ + CO + L$ (42%) $NiP^+ + CO$ (58%)	$Ni\phi CH_3^+ + CO + L$ (20%) $NiP^+ + L$ (80%)	$NiLP^+$
$\phi(CO)OH$	$Ni\phi OH^+ + CO + L$ (32%) $NiP^+ + L$ (68%)	$NiP^+ + L$	No Reaction
$\phi(CO)OCH_3$	$Ni\phi OCH_3^+ + CO + L$ (45%) $NiP^+ + L$ (55%)	$NiP^+ + L$	$NiLP^+$
$\phi(CO)\phi$	$NiP^+ + L$	$NiP^+ + L$	No Reaction
$\phi(CO)Cl$	No Reaction	No Reaction	No Reaction
$\phi CH_2(CO)H$	$Ni\phi CH_3^+ + CO + L$ (32%) $NiP^+ + L$ (68%)	$NiP^+ + L$	No Reaction

Thus, the electronic structure of the metal in MCO^+ is essentially the same as that in the bare metal ion. We have recently discussed the chemistry of MCO^+ ions;[28] in general they react very similarly to M^+. There are some cases in which the CO can become involved in the chemistry; that is, MCO^+ can react with a molecule AB via intermediates such as A-M^+-(CO)-B. However, the CO is usually simply a spectator, having little effect on the chemistry. Recent work suggests that D(Ni^+-CO) is approximately 25-30 kcal/mol.[29] While CO has an appreciable electron affinity[30] (E.A. (CO) = 31.6 kcal/mol), little charge transfer occurs, i.e., the charge on the nickel atom is +1.

$NiPF_3^+$: Little has been done to date in the gas phase with the PF_3 ligand. Reaction (13) has been observed,[15c] which

$$CoCO^+ + PH_3 \rightarrow CoPH_3^+ + CO \qquad (13)$$

indicates that PH_3 is more strongly bound than CO to Co^+. If, as has been suggested, the proton affinity of simple ligands reflect their relative binding energies to transition metal ions, PF_3 would be more weakly bound than PH_3 (PA(PF_3), 166.5 kcal/mol < PA(PH_3), 188.6 kcal/mol)[16]. PF_3 has a negative electron affinity, so charge transfer would lead to dissociation. Ligand substitution processes such as reaction (14)

$$NiPF_3^+ + \phi X \rightarrow Ni\phi X^+ + PF_3 \qquad (14)$$

suggest that PF_3 exists as an intact ligand, as opposed to a structure such as F-Ni^+-PF_2. From appearance potential measurements[31] on the ions derived from electron ionization of $Ni(PF_3)_4$, it has been suggested that $\Delta H_f(NiPF_3^+)$ = 35 kcal/mol. Based on $\Delta H_f(Ni^+)$= 279 kcal/mol,[14] and $\Delta H_f(PF_3)$ = -219.6 kcal/mol,[14] this would lead to a

bond strength of $D(Ni^+-PF_3)$ = 24.6 kcal/mol. Based on this information it is difficult to decide whether PF_3 would be expected to be more or less strongly bound to Ni^+ than is CO. To order the relative metal-ligand binding energies, we studied the ion/molecule reactions in a mixture of $Ni(CO)_4$ and PF_3. Reaction (15)

$$NiCO^+ + PF_3 \rightarrow NiPF_3^+ + CO \qquad (15)$$

was observed. We suggest that the two bond energies are similar, with $D(Ni^+-PF_3) > D(Ni^+-CO)$ by a few kcal/mol.

$NiCp^+$: The cyclopentadienyl ligand appears to be much different concerning its effects on the chemistry of a metal than the other two ligands studied here. Jacobson and Freiser[32a] studied the chemistry of $CoCp^+$, and report some bond energies that suggest that $CoCp^+$ forms stronger bonds than does Co^+ (for example, $D(Co^+-C_4H_6) < D(CpCo^+-C_4H_6)$, $D(Co^+-Cp) < D(CpCo^+-Cp)$). They report that $D(Co^+-Cp)$ = 85 +/- 10 kcal/mol, which is larger than $D(Co^+-C_6H_6)$, 70 +/- 4 kcal/mol. This suggests that a bonding mechanism other than a simple electrostatic one may be operative for the Cp group. It has been suggested that the Cp group can be actively involved in the chemistry of the attached metal - molecular fragments can be "stored" on the Cp ring,[32] as well as on the metal ion. For example, reaction (16)

$$CoCp^+ + C_4H_8 \rightarrow CoCp(CH_2)^+ + C_3H_6 \qquad (16)$$

has been discussed[32a] by suggesting that the CH_2 may not be bound to the metal, but may be incorporated into the ring to yield a Co(methyl-cyclopentadienyl)$^+$ product.

The Cp ligand appears to be strongly bound to Ni^+. In Table 5-5, this ligand is never displaced by an aromatic compound, while CO and PF_3 are. Also, the molecular ion of CpNiNO reacts with all of the aromatic compounds studied here in a ligand displacement reaction, reaction (17),

$$CpNiNO^+ + \phi X \rightarrow CpNi\phi X^+ + NO \qquad (17)$$

with the Cp never being displaced. It is possible that some charge transfer takes place between the metal ion and the Cp group to yield a structure of the type $Ni^{+\{1+\delta\}}Cp^{-\delta}$. Charge transfer of this type has been observed for ligands such as the chlorine atom.[33] The electron affinity of C_5H_5 has been reported to be $\leq$ 42.3 kcal/mol.[34] If additional positive charge is generated on the metal with this ligand, it may explain the strength of the Ni^+-Cp bond, as well as the increased bond energies to Co^+ when the Cp ligand is present, relative to those for Co^+ alone. The reaction of ϕNO_2 with Ni^+ in Table 5-2 to form $NiC_5H_5^+$ suggests that $D(Ni^+\text{-}C_5H_5) > 41$ kcal/mol, <u>if the C_5H_5 exists as an intact ligand in the reaction product</u>. We note that in organometallic chemistry[35], the Cp ligand is frequently considered to take the form Cp^-; charge transfer from the metal to Cp would yield an aromatic ligand (6 π-electrons).

Expected Trends in the reactions of NiL^+: Based on what is known about these three ligands, some reaction trends may be proposed. However, first a comment should be made on the "pitfalls" of over-interpreting the data[7] in Table 5-5. Consider the two reactions:

$$Ni^+ + ABC \rightarrow NiB^+ + AC \quad (18)$$

$$NiCO^+ + ABC \rightarrow NiABC^+ + CO \quad (19)$$

One may be attempted to suggest that, while Ni^+ reacts with ABC, $NiCO^+$ only undergoes a ligand substitution reaction (i.e., does not insert into bonds, etc.). However, this may not be the case. If $NiCO^+$ induces the rearrangement of ABC to AC and B, the species that dissociates to the final products is $Ni^+(AC)(B)(CO)$. The order in which ligands are lost appear to reflect their relative bond energies to the metal ion. Thus, if AC = H_2, it would be preferentially lost relative to CO, and, if a reaction occurred, it would be apparent. However, if the products AC and B are the more strongly bound ligands, reaction (19) will be observed. Thus reaction (19) provides no information (in the latter case) as to whether rearrangement of ABC to AC and B has occurred. Thus, it is important, when comparing the chemistry of Ni^+ and NiL^+, to consider the possible reaction products and their proton affinities.[7] In this way, one may be able to conclude whether or not the presence of the ligand affects the chemistry, or whether such information cannot be obtained from the experimental results presented.

We interpret reactions such as

$$NiCO^+ + \phi Cl \rightarrow Ni\phi Cl^+ + CO$$

as ligand displacement reactions. If chlorobenzene reacted on the metal center to form C_6H_4 and HCl, HCl is more weakly bound than CO and would be lost. That is, if the HCl elimination occurred, we would expect to see either $NiC_6H_4^+$ or $NiCOC_6H_4^+$ as a $NiCO^+$ product. Note that $NiCp^+$ does not participate in ligand substitution reactions,

presumably reflecting the strong Ni^+-Cp bond energy.

Changes in the chemistry of NiL^+ as L varies would be expected to parallel the relative bond energies, which we expect to be:

$$D(Ni^+\text{-}CO) < D(Ni^+\text{-}PF_3) < D(Ni^+\text{-}Cp)$$

Also, the relative sizes of the three ligands may introduce steric effects. We have found the "cone angle" concept[36] to be useful in this regard; it suggests that the Cp ligand is the largest, occupying a "cone" from the origin (metal center) with an angle of 136^o, with PF_3 next at 104^o, and CO the smallest, 95^o. These steric effects may favor the formation of intermediates in which at least one of the groups attached to the metal is small such as -H. Steric effects may hinder the insertion process in which two bulky groups are bound to the metal (in addition to the ligand). In addition to steric effects, differences in the chemistry of the Ni^+ when Cp is attached may reflect either an increased positive charge on the metal, or reactions which involve storage of some molecular fragment on the ring.

The trends in reactivity that will be highlighted from the data in Table 5-5 fall into a few simple categories. There are some reactions in which $NiCp^+$ appears to be more reactive than the other NiL^+, and even Ni^+, which may be due to the increased positive charge on the metal. We suggest that most of the trends can be related to steric effects.

<u>Increased Reactivity of $NiCp^+$</u>: This is observed in the reactions of the halobenzenes in Table 5-5. Ni^+ reacts with bromo- and iodobenzene to eliminate HX, but not with chlorobenzene. Only

ligand substitution reactions appear to be occurring with these compounds for $NiCO^+$ and $NiPF_3^+$. In contrast, $NiCp^+$ eliminates HX from all three ϕX compounds. The thermochemical data[19] in Table 5-1 suggests that the failure of Ni^+ to react with ϕCl may be due to the relatively strong ϕ-Cl bond (rather than the overall reaction enthalpy). If the Ni in $NiCp^+$ has a charge of greater than +1.0, polarization effects may lead to the formation of stronger bonds. That is, $NiCp^+$ may react with ϕCl because

$$[D(CpNi^+\text{-}Cl) + D(Cp(Cl)Ni^+\text{-}\phi)] > [D(Ni^+\text{-}Cl) + D(ClNi^+\text{-}\phi)].$$

With the Cp ligand, there are, of course, many other possibilities such as coupling of the C_6H_4 group to the Cp ring.

<u>Trends reflecting steric effects:</u> We propose two types of steric effects. In the first case, a reaction may be "turned off" due to the presence of a bulky ligand. That is, while Ni^+ may react with ABCH via the intermediate A-Ni^+-BCH, the steric interactions may prevent access of the analogous intermediate when a bulky ligand is present. A second steric effect can be seen when the products of Ni^+ reflect attack of several bonds. For the molecule ABCH, the product distributions for Ni^+ may suggest that the intermediate (III) is formed to a greater extent than intermediate (IV):

A-Ni^+-BCH	ABC-Ni^+-H
(III)	(IV)

However, with a bulky ligand on the metal, steric interactions would be less if the C-H bond was attacked, making intermediate (VI) more stable than (V).

(V) (VI)

Consider, for example, the reactions of ϕCH_2X, X = Cl and Br. Ni^+ reacts by halide abstraction with both compounds. $NiPF_3^+$ so does as well. $NiCO^+$ only reacts with ϕCH_2Br. This may suggest that the ionization energies (I.E.) may vary, with I.E. (NiCO) < I.E. $(NiPF_3)$[37], thus the presence of the CO may hinder the charge transfer step that leads to the formation of the $C_7H_7^+$ product. However, $NiCp^+$ <u>only</u> reacts with the chloride. This may be a case where the energetically more facile reaction (for the ϕCH_2Br) does not occur because the Br atom is too large, preventing access of the $\phi CH_2\text{-}Ni^+(Cp)\text{-}Br$ intermediate. This further suggests that the formation of $C_7H_7^+$ occurs via an insertion intermediate, not a stripping process.

The decrease in reactivity with increasing ligand size is more apparent in the data for the aromatic carbonyl compounds in Table 5-4. Here reactivity (i.e., ability to induce decarbonylation) follows the order

$$NiCO^+ > NiPF_3^+ > NiCp^+$$

decreasing as the size of the ligand increases. Consider first $\phi(CO)CH_3$. If decarbonylation proceeds via intermediates of the type

ϕ-Ni^+(L)-$(CO)CH_3$, we would expect decreasing reactivity as the size of L increases. We note that the cone angles[36] of C_6H_5- and $(CO)CH_3$ are both estimated to be 100^o. Thus, 42% of the products correspond to decarbonylation for $NiCO^+$, 20% for $NiPF_3^+$ and 0% for $NiCp^+$. The ability of the metal in $NiCp^+$ to form stronger bonds apparently cannot compensate for the steric energies involved. However, this may not be the case for $\phi(CO)H$. $NiCp^+$ does decarbonylate benzaldehyde, suggesting that the reaction proceeds by insertion into the C-H bond; this will minimize steric interactions since one molecular fragment on the metal is an -H, with a cone angle[36] of only 75^o. Why then doesn't $NiCp^+$ decarbonylate $\phi CH_2(CO)H$? This may reflect the fact that the weak benzyl-C bond favors insertion at that point - that is, that decarbonylation of $\phi(CH_2)(CO)H$ proceeds through intermediate (VII), not (VIII).

ϕCH_2-Ni^+-$(CO)H$ (VII)

$\phi CH_2(CO)$-Ni^+-H (VIII)

The increased probability that NiL^+ will favor intermediates of the type ABC-$Ni(L)^+$-H is seen in a number of instances. Consider benzyl alcohol, ϕCH_2OH. Ni^+ reacts with this compound to form $C_7H_7^+$, and to eliminate H_2, presumably via intermediates (IX) and (X), respectively.

$\phi(CH_2)$-Ni^+-OH (IX)

ϕCH_2O-Ni^+-H (X)

In contrast, $NiCO^+$ and $NiPF_3^+$ only appear to react via an intermediate analogous to (X); again the extent of reaction decreases

as the size of the ligand increases. In fact, many of the cases where $NiPF_3^+$ and $NiCp^+$ react correspond to those mechanisms in which insertion into a C-H, O-H, or N-H bond occurs. Also note that there is only one case where $NiCO^+$ does <u>not</u> induce a decarbonylation of an aromatic carbonyl when Ni^+ does. The exception is $\phi(CO)\phi$, in which the two groups that would be on the metal upon insertion are the largest. Thus, in this case, even the smallest ligand, CO, appears to exert steric influences.

In the experiments performed to yield the data in Tables 5-2, 5-3, and 5-4, the reactions of the multi-ligated ions such as $Ni(CO)_{2,3,4}^+$ were also studied. These are not reported here since they are generally uninteresting. Typically, only ligand displacement reactions are observed. There were only two cases in which NiL_2^+ ions were observed to react:

$$Ni(PF_3)_2^+ + \phi CH_2OH \rightarrow Ni\phi CHO^+ + H_2 + 2\,PF_3 \qquad (20)$$

and

$$Ni(CO)_2^+ + \phi CH(OH)CH_3 \rightarrow Ni\phi COCH_3^+ + H_2 + 2CO \qquad (21)$$

When two ligands are present, steric effects would certainly be increased, which would be consistent with decreased "reactivity". These two cases in which NiL_2^+ ions react are both systems in which hydrogen elimination occurs. That is, they proceed via intermediates with minimal steric energy in the insertion intermediate, since they place a -H on the metal as one of the two fragments of the molecule.

It was suggested that, in the case of $\phi CH(OH)CH_3$, the loss of CH_2O was actually a two step process - elimination of H_2 followed by

elimination of CO. This is supported by the reactions of the ligated species, where H_2 elimination is observed. Following H_2 elimination, cleavage of the Ni^+-L bond appears to occur rather than decarbonylation of the ketone that is formed as a result of dehydrogenation.

Finally, we note only one case in which the presence of a ligand actually leads to new products. All three NiL^+ ions react with benzyl amine, ϕCH_2NH_2, to eliminate H_2, consistent with our suggestion that reactions that proceed by insertion into C-H, O-H or N-H bonds are least affected by steric interactions. However, $NiCp^+$ alone induces the elimination of a second dihydrogen

$$NiCp^+ + \phi CH_2NH_2 \rightarrow \quad CpNi\phi CN^+ + 2H_2 \qquad (22)$$

If H_2 elimination occurs, sufficient energy may be released when the resulting ϕCHNH interacts with the $Ni^{+\{1+\delta\}}$center to overcome the barrier that leads to the elimination of a second H_2. Reaction (23)

$$\phi CH_2NH_2 \rightarrow \quad \phi CN + 2\ H_2 \qquad (23)$$

requires 33 kcal/mol, thus the metal-ϕCN binding energy must be greater than this value. In the discussion of the chemistry of ML^+ cations, we suggest that steric interaction energies in some insertion intermediates may make them energetically less favorable, when L is large. One may not be able to distinguish between steric effects at this point in the mechanism, from those in it's immediate precursor - the initially formed ion/molecule complex. That is, the presence of L may affect the ability of the metal to get close to some bonds (structure (XI)) more so than others (structure (XII)), increasing the stability of XII over XI when L is present:

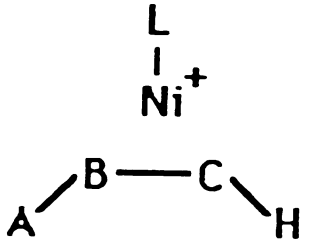

(XI)

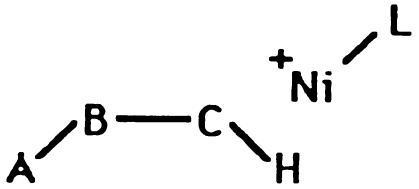

(XII)

We have pointed out that there appears to be a number of correlations in the chemistry of ML^+ with the size of L, with cone angles increasing in the order CO < PF_3 < Cp. However, one must ask whether the reactivity trends reflect steric interactions or some other feature of the chemistry. Would the steric interactions with three groups about the metal (as in the insertion intermediate or in some activated complex that immediately preceeds insertion) be sufficient to prohibit many reactions? We also noted that $D(Ni^+\text{-}CO) < D(Ni^+\text{-}PF_3) << D(Ni^+\text{-}Cp)$. Could the bond energies be the important factor instead? Many of the trends could be explained as well by

assuming that the initial interaction energy upon ion/molecule complexation is an important factor --required for subsequent chemistry to occur. Suppose, when Ni^+ complexes with some ϕX compound, 35 kcal/mol is generated, and assists in accessing, in fact is required for accessing, the insertion intermediate structure. Now consider the reaction of NiL^+. When it forms the initial complex, 35 kcal/mol is released, and 30 kcal/mol is consumed in rapid cleavage of the Ni^+-L bond. The resulting complex, $Ni\phi X^+$ now has only 5 kcal/mol which may be insufficient for further reaction to occur (a relatively "cold" $Ni\phi X^+$ complex), the result being only ligand displacement. These considerations would predict that the reactivity of NiL^+ would decrease as $D(Ni^+\text{-}L)$ increases - for those cases in which ligand displacement reactions occur. We note that Schilling and Beauchamp[37] recently proposed a similar argument to explain the unreactive behavior of Pr^+ and Eu^+ with small alkanes - citing the possible importance of the "chemical activation" that occurs upon complexation and its relationship to barriers early in the reaction. This energetic argument has some attractive features, and may seem more reasonable than the steric argument. However the energetic argument does not explain the observation that facile reactions occur for ML^+ ions when the initial insertion step involves attack of a C-H, O-H or N-H bond. These questions are providing a framework for future studies of ligand effects in gas phase organometallic chemistry. Similar studies on a larger variety of ML^+ ions in which small, relatively strongly bound ligands are used, will allow the relative importance of various energetic and steric interactions to be determined.

Conclusions

In these gas phase organometallic ion/molecule reactions the phenyl group behaves chemically, in some ways, intermediate to the methyl and ethyl groups. H transfer from the phenyl group is a high energy process, much closer in energy to that required for H transfer from a methyl group than an ethyl group. The formation of the strong benzyne-Ni^+ bond makes H-abstraction from C_6H_5- possible in a few cases. When other pathways are open, such as the elimination of a small neutral molecule from the functional group, this latter pathway is preferred.

For comparison, the results of reactions of Ni^+ with several different small alkyl compounds are listed in Table 5-6. In cases where no data for Ni^+ are available, data for Co^+ are listed instead. In comparision to reactions with aromatic compounds, the results are very interesting. In general, the alkyl compounds form more products than aromatic compounds. For example, Co^+ with propanoic acid forms 5 different products, decarbonylation products representing only 25% of the total reaction products.[5] Decarbonylation accounts for 100% of the reactions of Ni^+ and benzoic acid.

The reactions of sec-butyl amine are interesting because a major product in the reaction with Ni^+ is hydride abstraction with charge transfer:[38]

$$s\text{-}C_4H_9NH_2 + Ni^+ \rightarrow C_4H_{10}N^+ + NiH \quad (60\%)$$

Hydride abstraction is also an important pathway for the reactions of Co^+ and amines.[17] This reaction is not observed for aniline or benzylamine.

The results in this table show that even relatively simple alkyl

molecules can react in many different ways. Aromatic compounds are much more selective in their reactions.

A major effect of the the presence of a phenyl group in an organic molecule is its inductive effects. This can be seen in reactions of substituted benzyl compounds. The weak $C_6H_5CH_2$-X bond plays an important role in the observed chemistry. This bond is the only bond attacked for most of the benzyl compounds studied. Charge transfer to the $C_6H_5CH_2$ moiety following insertion into this bond occurs due to the low ionization potential of this group.

The effect of ligands on metal centers is of major importance in the understanding of transition metal chemistry in condensed phases. The reactions of $NiPF_3^+$ follow closely the reactions of $NiCO^+$, with slightly less reactivity observed for the $NiPF_3^+$ ion. The metal-ligand bonding in $NiCO^+$ and $NiPF_3^+$ is probably very similar, so this result is not suprising. The slightly less reactivity of $NiPF_3^+$ reflects the steric crowding involved upon insertion produced by this larger ligand. Much of the chemistry of the NiL^+ ions can be explained by considering the formation of intermediates which would exhibit low steric interactions. The reactivity of $NiCp^+$ with the halobenzenes indicate that this ligand affects the metal ion much differently than either CO or PF_3. Charge transfer to the cyclopentadienyl group to increase its aromatic character may explain why $NiCp^+$ is more reactive than the other NiL^+ species in these examples. In other cases the steric hindrance of the bulky Cp group appears to block reaction pathways.

Acknowledgements

The National Science Foundation (grant #CHE 8722111) is acknowledged for partial support of this work. Also the authors wish to thank Professor John Wronka for assistance in implementation of the frequency-swept detector for the MSU ICR, and Professor James F. Harrison, for helpful discussions and collaborations concerning the nature of transition metal ion-ligand bonding.

Table 5-6

Reactions of small alkyl molecules with metal ions

C_3H_7CN +	$Co^+ \rightarrow$	$CoC_2H_4^+ + CH_3CN$ (.05)
		$CoCH_3CN^+ + C_2H_4$ (.60)
		$CoC_3H_7CN^+$ (.35)
C_2H_5I[a] +	$Co^+ \rightarrow$	$CoC_2H_4^+ + HI$ (.78)
		$CoI^+ + C_2H_5$ (.11)
		$CoHI^+ + C_2H_4$ (.11)
C_3H_7Cl[a] +	$Co^+ \rightarrow$	$C_3H_7^+ + CoCl$ (.72)
		$CoC_3H_6^+ + HCl$ (.23)
		$CoHCl^+ + C_3H_6$ (.05)
C_2H_5OH[a] +	$Ni^+ \rightarrow$	$CoC_2H_4^+ + H_2O$ (.79)
		$CoH_2O^+ + C_2H_4$ (.16)
		$CoC_2H_4O^+ + H_2$ (.05)
CH_3OCH_3[b] +	$Ni^+ \rightarrow$	$NiCH_2O^+ + CH_4$ (.61)
		$NiC_2H_6O^+$ (.39)
C_2H_5CHO +	$Ni^+ \rightarrow$	$NiCO^+ + C_2H_6$ (.43)
		$NiC_3H_4O^+ + H_2$ (.12)
		$NiC_3H_6O^+$ (.45)

Table 5-6, continued

$C_3H_7NO_2$[c] +	$Ni^+ \rightarrow$	$C_3H_7^+ + NiNO_2$ (.35)
		$NiHN_2O^+ + C_3H_6$ (.20)
		$NiC_3H_5^+ + H_2 + NO_2$ (.08)
		$NiOH^+ + C_3H_6NO_2$ (.06)
		$NiNO^+ + C_3H_7O$ (.06)
		(plus six minor (<5%) products)
s-$C_4H_9NH_2$[b] +	$Ni^+ \rightarrow$	$C_4H_{10}N^+ + NiH$ (.60)
		$NiC_2H_7N^+ + C_2H_4$ (.07)
		$NiC_3H_7N^+ + CH_4$ (.19)
		$NiC_4H_7N^+ + 2\ H_2$ (.07)
		$NiC_4H_9N^+ + H_2$ (.06)
$C_2H_5COCH_3$[c] +	$Co^+ \rightarrow$	$CoC_2H_4^+ + C_2H_4O$ (.24)
		$CoC_2H_4O^+ + C_2H_4$ (.52)
		$CoC_3H_4O^+ + CH_4$ (.11)
		$CoC_4H_6O^+ + H_2$ (.05)
C_2H_5COOH[d] +	$Co^+ \rightarrow$	$CoH_2O^+ + C_3H_4O$ (.40)
		$CoC_3H_4O^+ + H_2O$ (.06)
		$CoC_2H_4^+ + C_2H_2O_2$ (.10)
		$CoC_2H_2O_2^+ + C_2H_4$ (.19)
		$CoCO^+ + C_2H_6O$ (.25)

a. ref. 4 b. ref 38 c. ref 6 d. ref. 5

Table 5-7

Reactions of aromatic compounds with Ni^+ and NiL^+

C_6H_6 +	Ni^+ (a) →	N. R.
	Ni^+ (b)	N. R.
	Ni^+ (c)	NiP^+
	$NiCO^+$	$NiP^+ + CO$
	$Ni(CO)_2^+$	$NiP^+ + CO$
		$NiCOP^+ + CO$
	$NiPF_3^+$	$NiP^+ + PF_3$
	$Ni(PF_3)_2^+$	$NiLP^+ + PF_3$
	$NiCp^+$	$NiCpP^+$
	$NiCpNO^+$	$NiCpP^+ + NO$
$C_6H_5CH_3$ +	Ni^+ (a) →	N. R.
	Ni^+ (b)	N. R.
	Ni^+ (c)	NiP^+
	$NiCO^+$	$NiP^+ + CO$
	$Ni(CO)_2^+$	N. R.
	$NiPF_3^+$	$NiP^+ + PF_3$
	$Ni(PF_3)_2^+$	N. R.
	$NiCp^+$	$NiCpP^+$
	$NiCpNO^+$	$NiCpP^+ + NO$

N. R. = No Reaction

Ni^+ (a) = Ni^+ produced from $Ni(CO)_4$

Ni^+ (b) = Ni^+ produced from $Ni(PF_3)_4$

Ni^+ (c) = Ni^+ produced from NiCpNO

Table 5-7, continued

C_6H_5OH +	Ni^+ (a) →	NiP^+
	Ni^+ (b)	NiP^+
	Ni^+ (c)	N. R.
	$NiCO^+$	$NiP^+ + CO$
	$Ni(CO)_2^+$	N. R.
	$NiPF_3^+$	$NiP^+ + PF_3$
	$Ni(PF_3)_2^+$	$NiLP^+ + PF_3$
	$NiCp^+$	N. R.
	$NiCpNO^+$	$NiCpP^+ + NO$
$C_6H_5NH_2$ +	Ni^+ (a) →	N. R.
	Ni^+ (b)	N. R.
	Ni^+ (c)	NiP^+
	$NiCO^+$	$NiP^+ + CO$
	$Ni(CO)_2^+$	N. R.
	$NiPF_3^+$	$NiP^+ + PF_3$
	$Ni(PF_3)_2^+$	$NiP^+ + 2\ PF_3$
	$NiCp^+$	N. R.
	$NiCPNO^+$	N. R.
C_6H_5COCl +	Ni^+(a) →	N. R.
	Ni^+(b)	N. R.
	Ni^+(c)	N. R.
	$NiCO^+$	N. R.
	$Ni(CO)_2^+$	N. R.
	$NiPF_3^+$	N. R.
	$Ni(PF_3)_2^+$	N. R.
	$NiCp^+$	N. R.
	$NiCpNO^+$	$NiCpP^+ + NO$

Table 5-7, continued

C_6H_5CN +	Ni^+ (a) →	NiP^+
	Ni^+ (b)	NiP^+
	Ni^+ (c)	NiP^+
	$NiCO^+$	$NiP^+ + CO$
	$Ni(CO)_2^+$	$NiCOP^+ + CO$
	$NiPF_3^+$	$NiP^+ + PF_3$
	$Ni(PF_3)_2^+$	$NiLP^+ + PF_3$
	$NiCp^+$	N. R.
	$NiCpNO^+$	$NiCpP^+ + NO$
C_6H_5CHO +	Ni^+ (a) →	$NiC_6H_6^+ + CO$
	Ni^+ (b)	$NiC_6H_6^+ + CO$
	Ni^+ (c)	$NiC_6H_6^+ + CO$
	$NiCO^+$	$NiC_6H_6^+ + 2\ CO$ (.29)
		$NiP^+ + L$ (.71)
	$Ni(CO)_2^+$	$NiLP^+ + L$
	$NiPF_3^+$	$NiP^+ + L$
	$Ni(PF_3)_2^+$	$NiP^+ + L$ (.87)
		$NiLP^+ + L$ (.13)
	$NiCp^+$	$NiCpC_6H_6^+ + CO$
	$NiCpNO^+$	$NiCpP^+ + NO$
C_6H_5Cl +	Ni^+ (a) →	NiP^+
	Ni^+ (b)	NiP^+
	Ni^+ (c)	NiP^+
	$NiCO^+$	$NiP^+ + CO$
	$Ni(CO)_2^+$	$NiLP^+ + L$
	$NiPF_3^+$	$NiP^+ + L$

Table 5-7, continued

	$Ni(PF_3)_2^+$	N.R.
	$NiCp^+$	$NiCpC_6H_4^+ + HCl$
	$NiCpNO^+$	N.R.
C_6H_5Br +	Ni^+ (a) →	$NiC_6H_4^+ + HBr$
	Ni^+ (b)	$NiC_6H_4^+ + HBr$
	Ni^+ (c)	$NiC_6H_4^+ + HBr$
	$NiCO^+$	$NiP^+ + CO$
	$Ni(CO)_2^+$	$NiP^+ + 2\ L$
	$NiPF_3^+$	$NiP^+ + L$
	$Ni(PF_3)_2^+$	$NiPL^+ + L$
	$NiCp^+$	$NiCpC_6H_4^+ + HBr$
	$NiCpNO^+$	$NiCpP^+ + NO$
C_6H_5I +	Ni^+ (a) →	$NiC_6H_4^+ + HI$ (.45)
		$NiC_6H_5^+ + I$ (.55)
	Ni^+ (b)	$NiC_6H_4^+ + HI$ (.37)
		$NiC_6H_5^+ + I$ (.63)
	Ni^+ (c)	NiP^+
	$NiCO^+$	$NiP^+ + CO$
	$Ni(CO)_2^+$	N.R.
	$NiPF_3^+$	N.R.
	$Ni(PF_3)_2^+$	$NiPL^+ + L$
	$NiCp^+$	$NiCpC_6H_4^+ + HI$
	$NiCpNO^+$	N.R.

Table 5-7, continued

$C_6H_5NO_2$ +	Ni^+ (a) →	$NiC_5H_5^+$ + CO + NO (.84)
		$NiC_6H_5O^+$ + NO (.16)
	Ni^+ (b)	$NiC_5H_5^+$ + CO + NO (.86)
		$NiC_6H_5CO^+$ + NO (.14)
	Ni^+ (c)	$NiC_5H_5^+$ + CO + NO (.52)
		$NiC_6H_5O^+$ + NO (.26)
		NiP^+ (.21)
	$NiCO^+$	$NiCOP^+$ (.28)
		NiP^+ + CO (.72)
	$Ni(CO)_2^+$	$NiCOP^+$ + CO
	$NiPF_3^+$	NiP^+ + L
	$Ni(PF_3)_2^+$	NiP^+ + 2 L (.24)
		$NiPL^+$ + L (.76)
	$NiCp^+$	$NiCpP^+$
	$NiCpNO^+$	$NiCpP^+$ + NO
$C_6H_5OCH_3$ +	Ni^+ (a) →	$NiC_6H_6^+$ + CH_2O
	Ni^+ (b)	$NiC_6H_6^+$ + CH_2O
	Ni^+ (c)	$NiC_6H_6^+$ + CH_2O (.31)
		NiP^+ (.69)
	$NiCO^+$	$NiC_6H_6^+$ + CH_2O + CO (.17)
		NiP^+ + CO (.60)
		$NiCOP^+$ (.23)
	$Ni(CO)_2^+$	NiP^+ + 2 CO
	$NiPF_3^+$	NiP^+ + L
	$Ni(PF_3)_2^+$	$NiPL^+$ + L
	$NiCp^+$	$NiCpP^+$
	$NiCpNO^+$	$NiCpP^+$ + NO

Table 5-7, continued

$C_6H_5C_4H_9$ +	Ni^+ (a) →	$NiC_6H_5CH_3^+ + C_3H_6$
	Ni^+ (b)	$NiC_6H_5CH_3^+ + C_3H_6$
	Ni^+ (c)	$NiC_6H_5CH_3^+ + C_3H_6$
	$NiCO^+$	$NiC_6H_5CH_3^+ + C_3H_6 + CO$
		$NiP^+ + CO$ (.56)
	$Ni(CO)_2^+$	$NiP^+ + 2\ L$
	$NiPF_3^+$	$NiP^+ + L$
	$Ni(PF_3)_2^+$	$NiP^+ + 2\ L$
	$NiCp^+$	N.R.
	$NiCpNO^+$	$NiCpP^+ + NO$
$C_6H_5C_2H_5$ +	Ni^+ (a) →	$NiC_6H_5CHCH_2^+ + H_2$
	Ni^+ (b)	$NiC_6H_5CHCH_2^+ + H_2$
	Ni^+ (c)	$NiC_6H_5CHCH_2^+ + H_2$ (.63)
		NiP^+ (.37)
	$NiCO^+$	$NiC_6H_5CHCH_2^+ + H_2 + CO$ (.41)
		$NiP^+ + CO$ (.59)
	$Ni(CO)_2^+$	$NiP^+ + CO$ (.37)
		$NiCOP^+ + CO$ (.63)
	$NiPF_3^+$	$NiP^+ + L$
	$Ni(PF_3)_2^+$	$NiLP^+ + L$ (.47)
		$NiP^+ + 2\ L$ (.53)
	$NiCp^+$	N.R.
	$NiCpNO^+$	$NiCpP^+ + NO$

Table 5-7, continued

$C_6H_5CH_2NH_2$ +	Ni^+ (a) →	$NiC_6H_5CHNH^+ + H_2$
	Ni^+ (b)	$NiC_6H_5CHNH^+ + H_2$
	Ni^+ (c)	$NiC_6H_5CHNH^+ + H_2$ (.66)
		NiP^+ (.37)
	$NiCO^+$	$NiC_6H_5CHNH^+ + H_2 + CO$
	$Ni(CO)2^+$	$NiP^+ + 2\ CO$ (.67)
		$NiCOP^+ + CO$ (.32)
	$NiPF_3^+$	$NiC_6H_5CHNH^+ + H_2 + PF_3$ (.31)
		$NiP^+ + L$ (.69)
	$Ni(PF_3)_2^+$	$NiP^+ + 2\ L$
	$NiCp^+$	$NiCpC_6H_5CHNH^+ + H_2$ (.58)
		$NiCpC_6H_5CN^+ + 2\ H_2$ (.42)
	$NiCpNO^+$	$NiCpP^+ + NO$
$C_6H_5CH_2CHO^+$	Ni^+ (a) →	$NiC_6H_5CH_3^+ + CO$
	Ni^+ (b)	$NiC_6H_5CH_3^+ + CO$
	Ni^+ (c)	$NiC_6H_5CH_3^+ + CO$
	$NiCO^+$	$NiC_6H_5CH_3^+ + 2\ CO$ (.32)
		$NiP^+ + CO$ (.68)
	$Ni(CO)_2^+$	$NiP^+ + 2\ CO$
	$NiPF3^+$	$NiC_6H_5CH_3^+ + CO + PF3$ (.17)
		$NiP^+ + L$ (.83)
	$Ni(PF3)2^+$	$NiP^+ + 2\ L$
	$NiCp^+$	N.R.
	$NiCpNO^+$	$NiCpP^+ + NO$

Table 5-7, continued

$C_6H_5CH_2OH$ +	Ni^+ (a)	→	$C_7H_7^+$ + Ni + OH (.75)
			$NiC_6H_5CHO^+ + H_2$ (.25)
	Ni^+ (b)		$C_7H_7^+$ + Ni + OH (.85)
			$NiC_6H_5CHO^+ + H_2$ (.15)
	Ni^+ (c)		$NiC_6H_5CHO^+ + H_2$
	$NiCO^+$		$NiC_6H_5CHO^+ + H_2$ + CO (.37)
			NiP^+ + CO (.63)
	$Ni(CO)_2^+$		NiP^+ + 2 CO
	$NiPF_3^+$		$NiC_6H_5CHO^+ + H_2 + PF_3$ (.22)
			NiP^+ + L (.78)
	$Ni(PF_3)_2^+$		$NiC_6H_5CHO^+ + H_2$ + 2 L
	$NiCp^+$		N.R.
	$NiCpNO^+$		$NiCpP^+$ + NO
$C_6H_5CH_2Cl$ +	Ni^+ (a)	→	$C_7H_7^+$ + Ni + Cl
	Ni^+ (b)		$C_7H_7^+$ + Ni + Cl
	Ni^+ (c)		$C_7H_7^+$ + Ni + Cl
	$NiCO^+$		N.R.
	$Ni(CO)2^+$		N.R.
	$NiPF3^+$		$C_7H_7^+$ + Ni + Cl + PF_3
	$Ni(PF_3)_2^+$		N.R.
	$NiCp^+$		$C_7H_7^+$ + Ni + Cp + Cl
	$NiCpNO^+$		N.R.

Table 5-7, continued

$C_6H_5CH_2Br$ +	Ni^+ (a) →	$C_7H_7^+$ + Ni + Br
	Ni^+ (b)	$C_7H_7^+$ + Ni + Br
	Ni^+ (c)	$C_7H_7^+$ + Ni + Br
	$NiCO^+$	$C_7H_7^+$ + Ni + CO + Br
	$Ni(CO)_2^+$	NiP^+ + 2 CO (.63)
		$NiCOP^+$ + CO (.37)
	$NiPF_3^+$	$C_7H_7^+$ + Ni + Br + PF_3 (.80)
		NiP^+ + PF_3 (.20)
	$Ni(PF_3)_2^+$	NiP^+ + 2 PF_3
	$NiCp^+$	N.R.
	$NiCpNO^+$	$NiCpP^+$ + NO
$C_6H_5CHOHCH_3$ +	Ni^+ (a) →	$NiC_6H_5CH_3^+$ + CH_2O (.69)
		$NiC_6H_5CHCH_2^+$ + H_2O (.31)
	Ni^+ (b)	$NiC_6H_5CH_3^+$ + CH_2O (.52)
		$NiC_6H_5CHCH_2^+$ + H_2O (.48)
	Ni^+ (c)	$NiC_6H_5CH_3^+$ + CH_2O (.24)
		$NiC_6H_5CHCH_2^+$ + H_2O (.76)
	$NiCO^+$	$NiC_6H_5COCH_3^+$ + H_2 + CO
	$Ni(CO)_2^+$	$NiC_6H_5COCH_3^+$ + H_2 + 2 CO (.64)
		NiP^+ + 2 CO (.36)
	$NiPF_3^+$	$NiC_6H_5CHCH_2^+$ + H_2O + PF_3(.70)
		$NiC_6H_5COCH_3^+$ + H_2 + PF_3 (.30)
	$Ni(PF_3)_2^+$	NiP^+ + 2 L (.38)
		$NiPL^+$ + L (.62)

Table 5-7, continued

	$NiCp^+$	$NiCpC_6H_5CHCH_2^+ + H_2O$ (.28)
		$NiCpP^+$ (.72)
	$NiCpNO^+$	$NiCpP^+ + NO$
$C_6H_5COCH_3$ +	Ni^+ (a) →	$NiC_6H_5CH_3^+ + CO$
	Ni^+ (b)	$NiC_6H_5CH_3^+ + CO$
	Ni^+ (c)	$NiC_6H_5CH_3^+ + CO$ (.88)
		NiP^+ (.12)
	$NiCO^+$	$NiC_6H_5CH_3^+ + 2\ CO$ (.42)
		$NiP^+ + CO$ (.58)
	$Ni(CO)_2^+$	N.R.
	$Ni(PF_3)^+$	$NiC_6H_5CH_3^+ + CO + PF_3$ (.20)
		$NiP^+ + L$ (.80)
	$Ni(PF_3)_2^+$	$NiPL^+ + L$
	$NiCp^+$	$NiCpP^+$
	$NiCpNO^+$	$NiCpP^+ + NO$
$C_6H_5COOCH_3$ +	Ni^+ (a) →	$NiC_6H_5OCH_3^+ + CO$
	Ni^+ (b)	$NiC_6H_5OCH_3^+ + CO$
	Ni^+ (c)	$NiC_6H_5CH_3^+ + CO$ (.88)
		NiP^+ (.12)
	$NiCO^+$	$NiC_6H_5OCH_3^+ + 2\ CO$ (.45)
		$NiP^+ + CO$ (.55)
	$Ni(CO)_2^+$	N.R.
	$NiPF_3^+$	$NiP^+ + L$
	$Ni(PF_3)_2^+$	$NiPL^+ + L$
	$NiCp^+$	$NiCpP^+$
	$NiCpNO^+$	$NiCpP^+ + NO$

Table 5-7, continued

C_6H_5COOH +	Ni^+(a) →	$NiC_6H_5OH^+ + CO$
	Ni^+(b)	$NiC_6H_5OH^+ + CO$
	Ni^+(c)	$NiC_6H_5OH^+ + CO$
	$NiCO^+$	$NiC_6H_5OH^+ + 2\ CO$ (.32)
		$NiP^+ + CO$ (.68)
	$Ni(CO)2^+$	$NiCOP^+ + CO$
	$NiPF3^+$	$NiP^+ + PF3$
	$Ni(PF3)2^+$	N.R.
	$NiCp^+$	N.R.
	$NiCpNO^+$	$NiCpP^+ + NO$
$(C_6H_5)_2CO$ +	Ni^+ (a) →	$Ni(C_6H_5)2^+ + CO$
	Ni^+ (b)	$Ni(C_6H_5)2^+ + CO$
	Ni^+ (c)	$Ni(C_6H_5)2^+ + CO$
	$NiCO^+$	$NiP^+ + CO$
	$Ni(CO)2^+$	$NiP^+ + 2\ CO$
	$NiPF3^+$	$NiP^+ + L$
	$Ni(PF3)2^+$	N.R.
	$NiCp^+$	N.R.
	$NiCpNO^+$	$NiCpP^+ + NO$

Table 5-8

Reactions of dimethyl sulfoxide, cyclopentanone and cyclohexanone with Ni^+ and NiL^+

	Ni^+	Ni^+	Ni^+	$NiCO^+$	$Ni(CO)_2^+$	$NiPF_3^+$	$Ni(PF_3)_2^+$	$NiCp^+$	$NiCpNO^+$
Dimethyl Sulfoxide	(a)	(b)	(c)						
$NiSO^+ + C_2H_6$	.04	.10	.24						
$NiCH_2SO^+ + CH_4$	.05	.13	.41	.10					
$NiCH_3SO^+ + CH_3$	.43	.47	.18						
$NiC_2H_6SO^+$ (+ L)	.47	.29	.16	.90		.74			
$NiPL^+ + L$					1.0	.26	1.0		
$NiCpCH_3SO^+ + NO + CH_3$								.46	
$NiCpP^+$ (+ NO)								.54	1.0
Cyclopentanone									
$NiCO^+ + C_4H_8$	.55	.18	.30						
$NiC_4H_6^+ + CH_2O$	.45	.30	.16						
$NiC_4H_8^+ + CO$		.12	.35						
NiP^+ (+ L)		.45	.35	1.0	N. R.	1.0			
$NiPL^+ + L$							1.0		
$NiCpC_5H_6O^+ + H_2 + NO$								.61	
$NiCpC_4H_6^+ + CH_2O + NO$								.18	
$NiCpP^+$ (+ NO)								.21	1.0

N. R. = No Reaction

Ni^+ (a) = Ni^+ produced from $Ni(CO)_4$

Ni^+ (b) = Ni^+ produced from $Ni(PF_3)_4$

Ni^+ (c) = Ni^+ produced from NiCpNO

Table 5-8, continued

Cyclohexanone	Ni^+ (a)	Ni^+ (b)	Ni^+ (c)	$NiCO^+$	$Ni(CO)_2^+$	$NiPF_3^+$	$Ni(PF_3)_2^+$	$NiCp^+$	$NiCpNO^+$
$NiCO^+ + C_5H_{10}$		.17							
$NiC_3H_6^+ + C_2H_4CO$	.56	.28	.23						
$NiC_5H_6^+ + CH_3OH$	.24	.19	.15						
$NiC_5H_8^+ + CH_2O$		.06	.09						
$NiC_5H_{10}^+ + CO$	.20		.08						
NiP^+ (+ L)		.30	.45	1.0		.73			
$NiPL^+$ (+ L)					1.0	.27	1.0		
$NiCpC_6H_8O^+ + H_2 + NO$								.48	
$NiCpC_6H_6O^+ + 2\,H_2 + NO$								.52	
$NiCpP^+ + NO$									1.0

References

1. Allison, J. *Prog. Inorg. Chem.* **1986,** *34,* 627.
2. Lombarski, M.; Allison, J. *Int. J. Mass Spec. Ion Phys.***1983,** *49,* 281.
3. Tsarbopoulos, A.; Allison, J. *Organometallics***1984,** *3,* 86.
4. Allison, J.; Ridge, D. P. *J. Am. Chem. Soc.***1979,** *101,* 4998.
5. Lombarski, M.; Allison, J. *Int. J. Mass Spec. Ion Proc.***1985,** *65,*31.
6. Cassidy, C. J.; Freiser, B.S.; McElvany, S. W.; Allison, J.; *J. Am. Chem. Soc.***1984,** *106,* 6125
7. Stepnowski, R. M.; Allison, J. *Organometallics*in press
8. Tsarboploulos, A.; Allison, J. *J. Am. Chem. Soc.***1985,** *107,* 5085.
9. Corderman, R. R.; Beauchamp, J. L. *J. Am. Chem. Soc.***1976,** *98,* 5700
10. Dietz, T. G.; Chatellier, D. S.; Ridge, D. P. *J. Am. Chem.Soc.***1978,***100,*4905.
11. Chowdhury, A. K.; Wilkins, C. L. *J. Am. Chem. Soc.***1987,** *109,* 5336.
12. Squires, R. R. *J. Am. Chem. Soc.***1985,** *107,* 4385.
13. Rosenstock H. M.; Draxl, K.; Steiner, B.W.; Herron, J.T. *J. Phys. Chem. Ref. Data***1977,** *6,* suppl. 1.
14. Franklin J. L.; Dillard, J. G.; Rosenstock H. M.; Herron, H. T.; Draxl, K.; Field F. H. Nat. Stand. Ref. Data Ser., Nat. Bur. Stand. **1969,**26

15a. Foster; M. S.; Beauchamp, J. L.; *J. Am. Chem. Soc.***1971,** *93,* 4924.

b. Foster; M. S.; Beauchamp, J. L.; *J. Am. Chem. Soc.***1975,** *97,* 4808.

c. Weddle, G.H.; Allison, J.; Ridge, D. P. *J. Am. Chem. Soc.***1977,** *99,* 105.

16. Lias, S. G.; Liebman, J. F.; Levin, R. D. *J. Phys. Chem. Ref. Data***1984,***13,* 695.
17. Radecki, B. D.; Allison, J. *J. Am. Chem. Soc.***1984,** *106,* 946.
18. Wronka, J.; Ridge, D. P. *Rev. Sci. Inst.***1982,** *53,* 491.
19. Thermodynamic data were taken and derived from the following

sources. **a**. ref 14 **b**. ref 13 **c.** Weast, R.C.; Astle, M. J. Handbook of Chemistry and Physics, CRC Publishing Co. 1983. **d.** Rosenstock, H.M.; Larkins, J. T.; Walker, J.A. *Int. J. Mass Spec. Ion Phys.***1973,** *11,* 309.
In cases where no data were available, heats of formation were estimated from group equivalent tables given in ref 14.

20. Gaydon, A. G. "Dissociation Energies and Spectra of Diatomic Molecules" Chapman and Hall, London, 1968
21. Burnier, R. C.; Byrd, G. D.; Freiser, B. S. *J. Am. Chem. Soc.***1981,** *103*,4360.
22. Halle, L. F.; Crowe, W. E.; Armentrout, P. B.; Beauchamp, J. L. *Organometallics* **1984,** *3,* 1694.
23. Burnier, R. C.; Byrd, G. D.; Freiser, B. S. *Anal. Chem.* **1980,** *52*,1641.
24. Jacobson, D. B.; Freiser, B. S. *J. Am. Chem. Soc.***1983,** *105*,7492.
25. Jacobson, D. B.; Freiser, B. S. *Organomet.***1984,** *3,* 513.
26. a. Dunbar, R.C.; Ennever, J. F.; Fackler, J.P. *Inorg. Chem.* **1973** *12* 2735.
    b. Meckstroth, W. K.; Ridge, D. P. *Int. J. Mass Spec. Ion Proc.***1984,***61*,149
    c. Wronka, J.; Ridge, D. P. *J. Am. Chem. Soc.***1984,** *106*,67.
27. Allison, J.; Mavridis, A.; Harrison, J. F. *Polyhedron,* in press
28. Blomberg, M.; Brandemark, U.; Johansson, J.; Siegbahn, P.; Wennerberg, J. *J. Chem. Phys.***1988,** *88,* 4324.
29. Refeay, K.M. A.; Franklin, J.L. *Int. J. Mass Spec. Ion Phys.***1976,** *20*,19
30. Kiser, R. W.; Krassoi, M. A.; Clark, R. J*J. Am. Chem. Soc.***1967,** *89,* 3653.
31 a. Jacobson, D. B.; Freiser, B. S. *J. Am. Chem. Soc.***1985,** *107,* 7399.
    b. Corderman, R. R.; Beauchamp, J. L. *Inorg. Chem.* **1978** *17,* 68.
32. Alvarado-Swaisgood, A. E.; Harrison, J. F. *J. Phys. Chem.* in press
33. Richardson, J. H.; Stephenson, L. M.; Brauman, J.I. *J. Chem. Phys.***1973,** *59,* 5068.
34. Cotton, F. A.; Wilkinson G. Advanced Inorganic Chemistry, John Wiley & Sons, New York, 1980
35. Tolman, T. A. *Chem. Rev.* **1977,** *77*,313.
36. Would we expect IP(NiCO) to be < IP($NiPF_3$)? We can look at what happens when Ni is surrounded by 4 ligands:

$IP(Ni(CO)_4)$ = 8.28 eV,[14] $IP(Ni(PF_3)_4)$ =9.6 eV,[30] so it is not unreasonable!

37. Schilling,J. B.; Beauchamp, J. L. *J. Am. Chem. Soc.***1988,***110*,15.
38. Huang, S. K., Ph.D Thesis, Michigan State University, **1983**

Chapter 6

Conclusions

Many areas of gas phase metal ion/molecule reactions have been studied in recent years. The projects described in this dissertation add to our knowledge of this field. The reactions of nitriles and aldehydes show how the functional group influences the reaction.

In a previous study, the reactions of long alkyl chain chloroalkanes and alcohols were compared.[1] The formation of cyclic intermediates, allowing metal ion insertion into sites in the alkyl chain remote from the functional group, dramatically shows that the alkyl chain can have an active role in the reaction. The alcohols were observed to form cyclic intermediates to a greater extent than the chloroalkanes, because the initial interaction between the molecule and the metal ion is greater for alcohols than chloroalkanes. With chloroalkanes, Co^+ complexes with the Cl, and inserts into the R-Cl bond, favored by the strong Co^+-Cl bond energy.

In the same way that -Cl and -OH have a major role in directing where bond insertion will occur in the molecule, the -CN and -CHO groups also have unique directing ability. Fewer products are formed for aldehydes than the corresponding alcohol, indicating that the presence of the carbonyl may lead to intermediates that are more rigid, making fewer C-C bonds susceptible to attack.

Several factors make the reactions of alkyl nitriles interesting. The strong R-CN bond energy makes this bond inaccessible for metal ion insertion. The initial interaction between the metal ion and nitrile appears to lead to an "end-on" complex. The large size of the end-on complex results in larger cyclic intermediates being formed.

Insertion into bonds farther from the functional group (relative to the alcohols) occurs, with up to eight members in the ring of the cyclic intermediate.

The addition of a CO ligand to Co^+ had an dramatic effect on the reactions observed. Very little insertion products were observed for the $CoCO^+$ ion, and only in the cases of hexyl and octyl cyanide. Two possibilities are suggested as to why this occurs, both related to steric effects. The first possibility is that the CO ligand interferes with insertion into interior C-C bonds due to steric hindrance. The second possibility is that the ligand does not interfere with insertion, but the intermediate formed, such as C_3H_7-Co^+(CO)-C_3H_6CN, may be less stable due to the steric interactions between the three ligands on the metal. This implies that insertion intermediates that have relatively small groups on the metal, i.e., -H or -CH_3, will have higher stability and lead to product formation. These observations concerning reactions of nitriles with $CoCO^+$ are similar to those made for metal-ligand reactions with alkanes.[2]

Aromatic compounds have also been an interesting class of compounds to study because of the wide variety of reactions observed. Many were unreactive, such as C_6H_5Cl and $C_6H_5NH_2$. However, some compounds reacted by H transfer from the phenyl ring: C_6H_5Br and C_6H_5I. One example of phenyl ring cleavage was observed was in the reactions of $C_6H_5NO_2$.

The inductive effect of the phenyl ring is the most important factor in the reactions of the substituted benzyl compounds. The weak $C_6H_5CH_2$-X bond is the only bond attacked for the majority of benzyl compounds. In some cases, charge transfer to $C_6H_5CH_2$ follows due to the low ionization potential of this group which is lower than the ionization potential of the metal.

The effect of different ligands on the metal ion can be observed

in the reactions of $NiCO^+$, $NiPF_3^+$, and $NiCp^+$ with aromatic compounds. The reactions of $NiPF_3^+$ follow closely the reactions of $NiCO^+$, with slightly less reactivity for the $NiPF_3^+$ ion. The bonding of $NiCO^+$ and $NiPF_3^+$ is probably very similar, so this result is not surprising. The slightly less reactivity of $NiPF_3^+$ reflects the steric crowding involved for insertion produced by this larger ligand. Much of the chemistry of the NiL^+ ions can be explained by the formation of intermediates with low steric interactions. It is important to remember that for these three ligands, the Ni^+-L bond strength increases $NiCp^+ > NiPF_3^+ > NiCO^+$. The size of the ligands, as measured by their cone angle, also increases in this order. Both factors should be considered in mechanisms explaining the reactions of M^+-L species.

The reactivity of $NiCp^+$ with the halobenzenes indicate that this ligand affects the metal ion much differently than either CO or PF_3. Charge transfer to the . cyclopentadienyl group to increase its aromatic character may explain why this ion is more reactive than the other NiL^+ species in these examples. In other cases the steric hindrance of the bulky Cp group appears to block reactions.

The study of substituted aromatic compounds with Ni^+ and NiL^+ has produced many interesting reactions that perhaps would not be predicted based on comparison with similar substituted alkyl compounds. These reactions provide valuable insight into the question of how transition metal ions react with organic molecules.

Several questions remain unanswered in the reactions of NiL^+ with aromatic compounds. In several cases, it was observed that the NiL_2^+ (L = CO or PF_3) did not undergo ligand substitution reactions:

$$NiL_2^+ + P \rightarrow NiLP^+ + L$$

However, when three ligands were present, the reaction:

$$NiL_3^+ + P \rightarrow NiLP^+ + 2\,L$$

was observed. Unfortunately, the reactions of the NiL_3^+ ions were studied only in a few isolated cases. The reactions of these ions may be useful to determine why ligand substitution reactions sometimes do not occur.

Another unsettled question is whether Ni^+ ions are formed in different electronic states, depending on the molecule from which they are formed. Determining the states of the ions may help in explaining the observed chemistry.

In conclusion, aromatic compounds have provided an interesting view of the reaction of metal ions with organic molecules. The small number of products formed in the typical reaction, combined with the amount of product formed, made these compounds very easy to study. Because of the variety of reactions observed, these compounds should prove useful in developing new ideas about the reactions of metal ions. This, in turn, can lead to a better understanding of fundamental questions of how organo-metallic compounds react.

References

1. Tsarboploulos, A.; Allison, J. *J. Am. Chem. Soc.* **1985,** *107,* 5085.
2. Radeki, B. D. Ph.D. Thesis, Michigan State University, 1985

APPENDIX

APPENDIX

ICR Operating Manual

The following is a short description of the electronic components that make up the ICR at MSU. The typical operating parameters are given. The procedure used for obtaining a spectrum using a frequency swept detector (FSD) is described. The operation of the instrument has been automated by the use of a MacIntosh computer; the program used to obtain data with the computer is also listed.

Magnet The Varian Fieldial magnet control is usually operated at a constant field of 16 kGauss. Maximum field strength is 23 kGauss. The magnet and power supply is cooled with distilled water that circulates from a Haskris heat exchanger that is itself cooled with tap water.

Emission Current Controller This home-built unit (designed and constructed by Marty Rabb) controls the amount of current that passes through the ionizing filament. On "EM" mode, the actual amount of current that makes up the ionizing beam is monitored and held constant. A voltage proportional to this current is generated from a Keithley picoammeter (see below), and is input into the back of this unit. The amount of current is set with the current knob. On "FIL" mode, the feedback circuit is bypassed. Filament bias voltage is input on the front panel of this unit via a BNC connector.

The filament should only be switched on when the magnetic field is on. The filament on/off switch is on the "little box".

filament current, converts it to a voltage, and passes this signal to the emission current controller. It is used with the "1μA" button depressed. When the filament is first switched on, the current through the filament will rise rapidly to about one amp, and the picoammeter will read .003. If the filament current rises to about 1.5 amps with no emitted current, this indicates that the filament is not positioned over the filament hole on the cell, the bias voltage has not been applied, or there is some problem in detecting the emitted current. If the current through the filament remains zero, this indicates that the filament is burned out.

"The little box" Many different electronic signals and voltages must be interfaced to the cell through a high vacuum feedthrough. This box sits on top of the high vacuum feedthrough, and provides a way to apply the voltages necessary to operate the cell. It also provides the interface for the filament current input and emission current measurement.

Tektronix PG 505 Pulse Generator Used in the "locked on" mode, the pulse generator is used to provide -70 volts to the emission current control bias input.

Tektronix FG 504 Function Generator (FG) Provides the rf power that is used to detect ions. It can sweep a frequency range by setting the stop and start frequencies on the frequency dial, setting the sweep duration, and having the "free run" button in the out position. If the free run button is pressed in, the FG will stay at the start frequency (TRIG SWP mode). A frequency scan can also be created externally, by applying voltages in the range of -10 to +10 volts to the "VCF input." This voltage is usually provided by the MacADIOS. The rf output is sent to the rf attenuator and also to the 503 counter. When on "free run mode",

attenuator and also to the 503 counter. When on "free run mode", the "lin sweep output" is sent to channel X of the oscilloscope. The "trig output", the 0-5 Volt square wave 90° shifted to the rf signal, is sent to reference input of the phase sensitive detector.

Tektronix DC 503 Universal Counter Measures the frequency of the rf signal from the 504 Function Generator.

RF attenuator Reduces the voltage of the rf signal from the 504 FG. Usually about -40 dB is used. The amount of attenuation should be set to maximize the signal size. The rf signal is then sent to the signal summer.

Signal Summer This module splits the rf signal into two 180° phase-shifted signals. Half of the rf is sent to the excitation plate of ICR cell, the other half is sent to the balance capacitor. There is a second signal input, which can be used to add a second rf signal to the first. The two gate inputs allow both signals to be gated on or off. The "drift top analyzer" dc bias voltage is input from the "little box"; the bias voltage is added to the rf signal.

Balance capacitor The balance capacitor is mounted on a BNC "T" to the vacuum flange along with the preamplifier. The vacuum end of the "T" is attached to the drift bottom analyzer plate. The balance capacitor is made of three high quality air capacitors. They should be adjusted until their capacitance equals exactly the capacitance of the ICR analyzer plates. The procedure is given in the FSD instruction manual. Basically they are adjusted until a flat baseline is reached. This capacitance is very small, about a picofarad, and cannot be measured with typical capacitance meters.

Preamplifier This is mounted on the BNC "T" and provides a 101 x gain to the ion signal. The drift bottom analyzer dc bias voltage is input from the little box and is sent to that plate.

Phase sensitve detector (PSD) Receives the ion signal from the preamplifier and compares the signal with the reference signal. Signals not in phase with the reference signal are rejected. The reference signal from the 504 FG must be phase shifted to account for the phase shifts in the components of the bridge detector. This is done with the digital delay located in the bottom part of the PSD. The reference signal from the 504 FG has 50Ω output impedance, so the reference impedance switch should be set to 50Ω and not TTL.

Keithley electrometer This electrometer is used as a voltage amplifier. The main dial should be set to "volts", and 0.1 on the gain dial. Typically, the unit is operated with power on, but meter off. This is to prevent damage to the meter needle. The dc level of the signal baseline can be adjusted with the zero knob.

Oscilloscope The oscilloscope can be used to monitor the signal as it is detected. When taking fast sweeps, the spectrum can be seen using the linear sweep output of the 504 FG as the X channel, using the oscilloscope in XY mode. The ion signal should be input into the Y channel.

Buffer A LF 356 op amp is used as a buffer between the amplifier and the MacADIOS. This is necessary to prevent feedback from the MacADIOS that occurs when data are analyzed. The signal buffer is located in the control panel.

Filter A low pass RC filter eliminates most of the high frequency noise produced by the amplifiers. It processes the signal immediately before the AIN0 input of the MacADIOS. The resistor, R, is 100 kΩ, and the capacitor, C, is 10^4 picofarads.

Wavetek 144 Function Generator This FG is used when doing a double resonance experiment. The rf is sent to the source of the ICR cell. The rf can be gated by the MacADIOS at the "TRIG IN." The Wavetek FG can also be scanned with an external voltage, here labeled "VCG IN." This is used in a parent scan double resonance experiment, with the 504 FG set at a constant frequency.

Control panel The control panel is a homebuilt panel used to adjust the bias voltages that go to the 8 adjustable plates of the ICR cell. The control panel also has timing controls to perform trapped ICR experiments, but these have never been used. The "computer" module provides a convenient way to monitor the cell voltages. Also, a voltage divider is provided to reduce the magnitude of the frequency controlling voltage ramp from the MacADIOS.

Obtaining a spectrum: To obtain a spectrum, be sure that all the components listed above are operational, set to the appropriate parameters, and connected according to the block diagram Figure 2-5. Set up the Tektronix FG to sweep an appropriate range (100-900 kHz) with about 0.1 sec sweep time (FREE RUN mode). This sweep should be seen on the oscilloscope (XY mode). with a sample on an inlet line, open a leak valve slowly until pressure in the cell is about 5×10^{-6} torr as read by the ion gauge. Turn on the filament and adjust the current until

about 30 nAmps of current are emitted. Peaks should now appear on the oscilloscope. If no peaks appear, the cell probably has to be "tuned up". Adjust the voltages on the cell plates until peaks appear. Generally, the trap plates should be ~1 V, the drift bottom plates ~0 V, and the drift top plates ~-0.5 V. These voltages should be adjusted so that peak heights are optimized, and may be quite different than those suggested.

At this point, one must be careful to avoid trapping the ions. When the ions are trapped, the intensities of low mass ions decreases as the intensity of the high mass product ions increases markedly. To test if trapping is occurring, turn off the filament. The ion peaks should instantly disappear. If the peaks slowly decreases, then trapping is occurring. The trapping voltages are probably too high and should be decreased. Increasing the drift voltages may help, too.

Other parameters that can be adjusted are the sweep time, irradiating voltage, and filament current. Sweep time and irradiating voltage both relate to how much energy is absorbed by the ions. As sweep time is decreased, the peak intensity decreases as the ions are absorbing less energy. Also with fast sweep times, "ringing" occurs. The ion signal is still detected after the irradiation time, because the ions are in motion for a short period of time. This ringing is not noticeable at slow scan speeds. The irradiating voltage can be adjusted with the attenuator. The voltage should be increased until the height of the highest peak no longer increases. At the point when the signal no longer increases, the cell is saturated. Filament current can also be changed to increase the number of the ions in the cell.

Once a spectrum has been obtained, the next step is to set up for a double resonance experiment. Turn on the Wavetek FG and set the frequency to match the frequency of the ion that is to

be ejected. The signal from the Wavetek will appear as a "squiggle" on the oscilloscope trace. The double resonance rf should be about 0.5 V peak-to-peak. Carefully adjust the double resonance frequency until the signal from the Wavetek FG is positioned exactly over the peak of the ion that is to be ejected. Now set the Wavetek to gated mode; the signal should disappear. Set the Tektronix FG to TRIG SWP mode; the scan will stop. At this point, data is ready to be collected by the computer.

Data collection: Data can be collected from the FSD using the MacADIOS data acquisition system. Data is stored and manipulated in arrays called "waves". The program used to collect double resonance data, "Scanner", is listed below, written in Microsoft BASIC. The purpose of this program is to collect two complete spectra. The first spectrum, "irrad", is taken with the double resonance irradiation on; the other spectrum, "noirrad", is taken with the same conditions except that the double resonance irradiation is off. The two spectra are then subtracted so that any differences can be seen. This result is stored in the subtraction spectrum, "back".

The MacADIOS has 12 bit analog inputs and outputs and a +10 V to -10 V range. This means a 20 volt range is divided by 4096 discrete increments; thus the resolution is 20 V/4096 = 4.88mV. Programs must take this into account. Here is the program followed with line-by-line remarks:

SCANNER

```
1    DIM  irrad%(3150),noirrad%(3150),irrado%(3150),noirrado%
       (3150),spec%(20),smooth%(5):x!=0:er%=0:smooth%(0)=1:
        smooth%(1)=1:smooth%(2)=1:smooth% (3)=1:smooth%(4)=1
2 LIBRARY "MacADIOS Calls":  CALL mainit
10 FOR i%=-1101 TO 2047
20 CALL ainx(0,0,11,VARPTR(er%),VARPTR(spec%(0)),0,0,0,0,0,0,0)
30 j%=i%*4.88:CALL aout(j%,5000,0,0):k%=i%+1101
40 CALL integ(VARPTR(spec%(0)),1,11,VARPTR(x!),-2)
50 irrad%(k%)=x!
60 NEXT i%
70   CALL plot(0,20,220,60,VARPTR(irrad%(0)),1000,0,3150,10,2,1,)
110 FOR i%=-1101 TO 2047
120 CALL ainx(0,0,11,VARPTR(er%),VARPTR(spec%(0)),0,0,0,0,00)
130 j%=i%*4.88: CALL aout(j%,0,0,0):k%=i%+1101
140 CALL integ(VARPTR(spec%(0)),1,11,VARPTR(x!),-2)
150 noirrad%(k%)=x!
160 NEXT i%
200  CALL convolve(VARPTR(irrad%(0)),VARPTR(smooth%(0)),
       VARPTR(irrado%(0)),3130,3,0)
210   CALL convolve(VARPTR(noirrad%(0)),VARPTR(smooth%(0)),
         VARPTR(noirrado%(0)),3130,3,0)
220  CALL scale(VARPTR(irrado%(0)),3130,0,1,4,2):CALLscale
         (VARPTR(noirrado%(0)),3130,0,1,4,2)
230  CALL bsave("ICDR","irrad",VARPTR(irrado%(0)),2,6280):
     CALL bsave("ICDR","noirrad",VARPTR(noirrado%(0)),2,6280)
240  CALL subi(VARPTR(irrado%(0)),
       VARPTR(noirrado%(0)),0,6280,0)
250  CALL bsave("ICDR","back",VARPTR(irrado%(0)),2,6280)
260  BEEP
270  CALL aout(-5372,0,0,0)
```

Remarks:

1 Dimensions all necessary variables,

2 Opens the file holding the MacADIOS routines ("calls"). Starts communication between the MacADIOS and the Macintosh.

10 Starts the first loop which will collect 3150 data points. The ramp starts at negative value so that a more of the allowable output range is used.

20 At each step, 12 points are input into the array "spec%".

30 The counter value i% is multiplied by 4.88, so that the ramp is incremented by 1 step. This value for j% is output through aout0. The ramp is incremented as soon as possible after collecting data. This allows the maximum time for the ion signal to stabilize before data is collected. The aout command also sends a 5 volt signal out aout1, which is used to gate the Wavetek FG signal on. Then, 1101 is added to the counter value; k% will be used to label points in the array irrad%, which must have positive values.

40 The points in array spec%, are added together (integrated) and saved as x!, a single precision variable.

50 The current point of the array irrad% is loaded with x!.

60 Returns the loop to line 10.

70 Displays the first collected spectrum so that the user can see if things are working correctly.

100-160 Repeats the loop 10-60 exactly, with two exceptions. In line 130, the gate signal to the Wavetek is zero, so no double resonance rf voltage goes to the cell. Since the ions are not receiving double resonance, this spectrum is saved as noirrad%.

200-210 The two collected waves are convoluted by a step

function, smooth%. This removes much of the undesired noise.

220 The convolution step also multiples the signal, so this scaling step reduces the wave's values to the original, preconvoluted, values.

230 The waves are saved as irrado% and noirrado%. This allows the information to be examined using the Macintosh Manager.

240 Noirrado% is subtracted from the wave irrado% and the result is stored in the array irrado%.

250 The subtracted spectrum is saved as the array "back".

260 The beep alerts the user that the program is finished (almost).

270 This resets the ramp to the starting voltage and thus the Tektronix FG to the starting frequency.

To use this program, the first step is to RUN the program. If the "tsfr" (transfer) light on the MacADIOS is flashing, and the frequency read on the Tektronix 503 Counter is increasing, then the program is successfully running. Halfway through the program, the computer will display a spectrum, so the user can see if data is being collected correctly.When it is completed, a beep will sound. TRANSFER from Microsoft BASIC to MacADIOS Manager. Once in MacADIOS Manager, then LOAD CONFIGURATION "plotto". Using the command LOAD FROM BASIC, load "wave" with irrado, "rave" with noirrado, and "backer" with back. Open the window View Four and drag "wave" and "back" to this window to display them. "Wave" should look like the expected mass spectrum. The baseline may not be flat. "Backer" should be a flat line. Ions that are the products of the irradiated ion will be seen

as a negative dip in "backer".(See Figure 2-9)

This program has also been translated to MacADIOS Manager language. Although it was not used to gather anybof the data in this dissertation, it will be listed here, because it should be more convenient for future experimenters than the BASIC program. The main convenience is that the experimenter can look at new data immediately without having to transfer into MacADIOS Manager to use the display windows there. The program will not be described because it is essentially the same program as the BASIC program but with slightly different syntax.

```
For cycle = 0 to 1
For index = -1101 to 2047
      ainx(0,0,11,spec,0,0,0,0,0,0,0)
      aout0= (4.88*index)
      let rave[index+1101]= integ(spec,1,11,-2)
next index
      aout0=-5372
      update[rave]
      if cycle = 0 then aout1 = 5000
      if cycle = 0 then copywave(rave,wave)
      if cycle = 1 then aout1 = 0
      if cycle = 1 then convolve(rave,step,ravo,3145,3)
      if cycle = 1 then convolve(rave,step,ravo,3145,3)
      if cycle = 1 then copywave(ravo,subtracto)
      if cycle = 1 then sub(subtracto,wavo,0,3149)
next cycle
```

A minor inconvenience is that the displayed spectra have no

scale telling the viewer what the masses of the ions are. The experiment produces a frequency scan which is linear. Because of the inversely proportional relationship between frequency and mass-to-charge, the spacing between mass peaks is not constant across a spectrum. But if two of the ions can be identified, the other masses can be identified by using the following equation, which uses the mass of the two ions (m_1 and m_2) and their data point numbers (n_1 and n_2, the point at which the center of the peak occurs.)

$$m(n)= \{(n-n_1)[(m_2^{-1} - m_1^{-1}) / (n_2- n_1)] + m_1\}^{-1}$$

The equation finds the range of mass between two data point numbers. It is convenient to use a calculator to calculate the masses of the ions. A program for a Hewlett-Packard calculator to do this calculation is:

RCL2 - RCL3 1/x RCL1 1/x STO5 - RCL4 RCL2 - / x RCL5 + 1/x

To use this program, first enter the program into the calculator. Then enter the mass of the first ion in memory 1, its data point number in memory 2, the second ion mass in memory 3, and its data point number in memory 4. With the program entered, then enter the data point number an unknown peak, n, and press R/S. The mass of the unknown ion will be calculated. The data point number for the center of the peaks can be found by using the cursor in the View Four window.